D.O. CONTROL AND O.U.R. ESTIMATION IN THE ACTIVATED SLUDGE PROCESS

by

Stephan Bocken
B.Sc.(Eng) (Cape Town)

Submitted to the University of Cape Town in
partial fulfillment of the requirements for
the degree of Master of Science in Engineering

August 1987

DECLARATION BY CANDIDATE

I hereby declare that this thesis is my own work and has not been submitted for a degree at any other University.

S.M. Bocken

August 1987

SYNOPSIS

The objective of this investigation was to evaluate Holmberg's method for simultaneous dissolved oxygen control and parameter estimation in a completely mixed diffused air activated sludge reactor.

Holmberg's method is based on an adaptive controller which estimates parameters in a model of the process. A dissolved oxygen (DO) mass balance on the liquid phase in the CFSTR gives:

$$\frac{dC_{OUT}}{dt} = \frac{Q}{V} \cdot (C_{IN} - C_{OUT}) + K_L a \cdot (C^S - C_{OUT}) - R$$

where

C_{OUT}	=	dissolved oxygen concentration in the reactor and the stream leaving the completely mixed reactor
C_{IN}	=	dissolved oxygen concentration in stream entering the reactor
C^S	=	dissolved oxygen saturation concentration
Q	=	flow rate of stream entering/leaving reactor
V	=	CFSTR volume
R	=	oxygen utilisation rate (= Respiration rate)
$K_L a$	=	oxygen transfer coefficient
t	=	time

Holmberg (1986) proposed two simplifications of the actual process model. Firstly, it was assumed that the mass transfer coefficient for oxygen input is a linear function of the air flow rate, i.e.:

$$K_L a = \alpha \cdot F_{AIR}$$

The second assumption was that the contribution of the flow term in the mass balance in negligible compared to the oxygen transfer and oxygen utilisation rate terms. These assumptions lead to the simplified process model:

$$\frac{dC_{OUT}}{dt} = \alpha \cdot F_{AIR} \cdot (C^{S} - C_{OUT}) - R \qquad \ldots\ldots\ldots(3.4)$$

Holmberg proposed that the two terms α (relating to K_La) and the oxygen utilisation rate R could be estimated on-line without any measurements additional to F_{AIR} and C_{OUT} and without introducing major disturbances in the process.

In the development of the deadbeat estimator, Holmberg assumed that the input F_{AIR} oscillated and changed at every sampling instant. However the requirement of continuous excitation contradicts the objective of the controller the aim of which is to reduce all errors to a minimum. This leads to the concept of dual control, where a compromise is made between DO-regulation and on-line estimation of α and R.

Holmberg's dual DO controller cum OUR/K_La estimator was evaluated through simulations of controlled process behaviour. The following conclusions were apparent from the results :

(i) The simulation program was shown to predict the results presented by Holmberg (1986) very closely.

(ii) Simulations were conducted in which the α and OUR parameters of the real process were held constant. These conditions are encountered at the end of an aeration train. Results indicated that under such conditions Holmberg's estimator converged rapidly and without offset to the true parameter values. The dissolved oxygen (DO) control was also effective.

(iii) Simulations were conducted in which the α and OUR parameters of the real process were assumed to vary in a sinusoidal fashion: the amplitude of the OUR fluctuation was similar to that encountered in practice at the head of an aeration train. Under these circumstances the parameter estimates converged rapidly to the true values but the estimates now oscillated about the true values. The magnitude of the estimate oscillations were shown to

be dependent on a parameter, S, that Holmberg had defined. The DO control was effective.

(iv) Two methods for parameter estimation were proposed by Holmberg. The first method, termed the "zero order" method assumes the α and OUR parameters to be constant over each sampling interval. The second method, termed the "first order" method assumes the α and OUR parameters to vary linearly over the sampling interval. Simulations in which the sampling interval ranged from 1 to 10 minutes demonstrated that the two methods yield virtually indistinguishable parameter estimates and DO control. This is at variance with Holmberg's observation that the first order method yields "greatly improved" estimates.

(v) Holmberg's estimator assumes the flow terms of the real process DO mass balance to be negligible. If the flow terms are included in simulation of the real process, but excluded from the estimator model, offsets occur in the values of the parameter estimates. Nevertheless, the dissolved oxygen control is effective.

(vi) In Holmberg's simulations it was assumed that in the real process, the oxygen transfer coefficient, K_La, is directly proportional to the air flow rate and that the relation passes through the origin. However, Goto (1985) found that a linear relationship, but not passing through the origin, best described the K_La/air flow rate relationship. If the real process K_La/air flow rate relationship was modelled in the form proposed by Goto (1985), Holmberg's estimator was shown to yield large offsets in the estimated values of the parameters, especially the OUR. DO control was still satisfactory.

(vii) An incorrect saturation dissolved oxygen concentration, C^s, was shown to cause offsets in the estimates of the OUR and α. The offset in the OUR estimates was small whereas the offset in the α estimate was large.

(viii) Holmberg's observation that the objectives of the DO controller and the parameter estimator are contradictory was shown to be correct. At given conditions, improving the DO control resulted in worse parameter estimates. Similarly, improving the parameter estimates resulted in worse DO control.

(ix) An extension to Holmberg's method was proposed to overcome the small parameter estimate offsets resulting from excluding the flow terms in the estimator model of the real process.

(x) A further extension to Holmberg's method was proposed to overcome the significant offsets (particularly in OUR) resulting from an incorrectly assumed K_La/F_{AIR} relationship. This proposed extension was shown to eliminate the offsets in the parameter estimates.

(xi) The effect of dead-time on parameter esimation was investigated. It was found that:

- for a given dead-time, the greater the sampling interval, the smaller the parameter estimate offsets.
- for a given sampling interval, the greater the dead-time, the greater the parameter estimate offsets.

ACKNOWLEDGEMENTS

I would like to express my sincere appreciation to Associate Professors P.L. Dold and M. Braae for their guidance and assistance throughout the duration of this project.

Many thanks to all staff and postgraduate students of the Chemical Engineering Department, in particular Mr E.W. Randall for his assistance with the software development.

The Council for Scientific and Industrial Research is thanked for its financial support.

And finally, a very special thanks to Bridgitte for her companionship and encouragement over the years.

CONTENTS

LIST OF FIGURES

Chapter Two

Chapter Three

Chapter Four

Chapter Five

LIST OF TABLES

NOMENCLATURE

a_1	-	Occasionally used synonomously to α.
a_2	-	Constant in expression: $K_L a = \alpha . F_{AIR} + a_2$ (Eq 3.2)
a_c	-	Controller gain
ASP	-	Activated Sludge Process
C_{IN}	-	Dissolved oxygen concentration in stream entering the reactor
C_{OUT}	-	Dissolved oxygen concentration in the reactor and the stream leaving the completely mixed reactor
COD	-	Chemical Oxygen Demand
CFSTR	-	Continuous Flow Stirred Tank Reactor
C^*	-	Dissolved oxygen saturation concentration
d	-	Controller constant (see Eq 3.48)
DO	-	Dissolved Oxygen
e	-	Error about the setpoint = $y_{SP} - y$
e_k	-	Error used in linear regression (Appendix B)
F_{AIR}	-	Air flow rate
h	-	Sampling interval
h^*	-	Generalised sampling interval (see Eq 3.13)
K	-	Plant specific oxygen transfer coefficient.
k_d	-	Controller constant (see Eq 3.49)
$k_L a$	-	Oxygen transfer coefficient
$K_1 -> K_4$	-	Runge-Kutta variables
$O(h^4)$	-	Other terms of order four
OUR	-	Oxygen Utilisation Rate (Respiration rate)
Q	-	Flow rate of stream entering/leaving reactor
R	-	Respiration rate = OUR (used in formulae)
s, S	-	Dummy variable used in various integrals
S	-	Sum of errors squared, e_k^2 (Appendix B)
T	-	Parameter used in A. Holmberg's method of DO dynamics.
STC	-	Self Tuning Control/Controller
t	-	Time
TKN	-	Total Kjeldhal Nitrogen.
TOC	-	Total Organic Carbon
TOD	-	Total Oxygen Demand

u	-	Process input or manipulated variable (In this thesis usually F_{AIR})
V	-	CFSTR volume
y	-	Process output (In this thesis usually C_{OUT})

GREEK ALPHABET

α	-	Proportionality constant between $K_L a$ and F_{AIR} (Eq 3.2)
	-	Parameter estimated through least squares in A Holmberg's second method of estimating the OUR.
β	-	Parameter estimated through least squares in A Holmberg's second method of estimating the OUR.
Δ	-	Difference of values at successive sampling intervals.
Γ	-	Sampled linear differential equation term (see Eq 3.12)
ξ	-	Sampled linear differential equation term (see Eq 3.11)
θ	-	Parameter vector = $\lvert \alpha \; R \rvert^T$ (Eq 3.25)
φ	-	Measured variables vector = $\lvert u*(C^S - y) - 1 \rvert^T$ (Eq 3.24)

SUPERSCRIPTS

^{0}	-	Starting/initial value
$^{-1}$	-	Matrix inverse
^{T}	-	Matrix transpose
$\cdot$	-	The derivative of that variable
$\hat{}$	-	The estimated value of that variable

SUBCRIPTS

$_{1,2,\ldots n}$	-	The n'th occurance/value
$_{OLD}$	-	Value at previous sampling interval
$_{SP}$	-	Setpoint value

CHAPTER ONE

INTRODUCTION

The objective of this investigation is to evaluate the Holmberg/Olsson method for simultaneous dissolved oxygen control and and oxygen utilisation rate estimation in the activated sludge process. (Holmberg and Olsson, 1985; Holmberg, 1986).

The activated sludge process (ASP) is established as the most widely used large scale wastewater treatment process for domestic and organic-bearing industrial wastewaters. In the process, wastewater is treated while passing through a series of one or more mixed reactors containing a dilute slurry of biological organisms. The essence of the treatment step lies in the biological reactions of the heterogeneous organisms present in the reactors. These micro-organisms utilize the organic material present in the wastewater (the pollutant) as a food source. In utilizing the organic matter, a portion of the carbon is directed into the formation of new cellular mass. The remaining portion is oxidized by the organisms to provide the energy required in the formation of the new cellular mass. Molecular oxygen is the primary final electron acceptor in the biological oxidation process. Thus oxygen must be supplied to the reactors in order to sustain the micro-organisms. The amount of oxygen required, termed the "oxygen demand", is related to the organic load on the process[1].

The influent to a wastewater treatment plant generally exhibits wide diurnal variations in both flow and concentration of organic pollutants (and ammonia). These variations usually follow a characteristic cyclic pattern repeated closely from day to day, the cyclic input reflecting the water utilisation patterns of the community being served. Because the influent flow rate and concentration vary, the loading rate (the product of flow rate and concentration) also varies. A consequence of the variation in the load on the process is a variation in the process oxygen demand over the cycle. The oxygen input to the system

[1] Under certain conditions oxygen is also consumed in the biological oxidation of ammonia to nitrate. This process, termed nitrification, will add to the carbonaceous oxygen requirement.

thus needs to be controlled so as to ensure that the dissolved oxygen level is maintained above some minimum which guarantees the continuous growth of the aerobic micro-organisms. A dissolved oxygen (DO) content of approximately 2 mgO/l generally is satisfactory; this concentration corresponds to roughly 20 percent of the saturation dissolved oxygen level.

A further incentive for controlling the dissolved oxygen concentration is the possible savings in operating costs. The energy requirement for aeration is the major operating cost in the ASP. Therefore, by exercising control over the oxygen input, over-aeration can be avoided through supplying only sufficient oxygen to match the time-varying demand. In this way operating costs are minimised. The implementation of effective automatic control strategies has resulted in reductions in energy inputs in the range of 10 to 40 percent relative to processes where the oxygen input is regulated by plant operators (Flanagan, 1977).

The method employed for the implementation of dissolved oxygen control traditionally has been of the linear feedback type. In this approach the dissolved oxygen concentration in the process is measured, providing a feedback signal for a controller. The controller, in turn, manipulates the aeration rate with the objective of adjusting the measured dissolved oxygen concentration to some desired setpoint value. Linear feedback control systems have been utilised with a fair degree of success. However, in recent years microprocessor-based adaptive controllers (particularly the self-tuning regulator) have received increasing attention as these can offer certain improvements in dissolved oxygen control over the simpler feedback type. One reason is that conventional linear controllers cannot function optimally at all operating levels as a result of the inherent non-linearities in the system. Adaptive controllers on the other hand are able to adjust the controller parameters according to the operating conditions, thus 'adapting' controller response on-line to suit process conditions.

A further reason for the interest in the approach of adaptive control of the dissolved oxygen concentration relates to the computations which form a part of the controller parameter adjustment mechanism, or which can be carried out in parallel. In the case of the self-tuning regulator

(STR) one of the steps in updating controller constants is the estimation of parameters in a mathematical model which represents (identifies) the process. If the model is suitably defined the estimated parameters can be used to calculate information which reflects process operating conditions. One possible application that has been suggested for diffused air wastewater treatment systems is the on-line estimation of oxygen utilisation rate (OUR) (e.g. Olsson, Rundqwist, Eriksson and Hall, 1985).

The rate of oxygen consumption in the activated sludge process is linked directly to the biological activity and therefore is a parameter reflective of process operation. Knowledge of the OUR would be very useful to plant operating personnel as a basis for deciding on operating strategies. Alternatively the OUR could be used as an input variable in other on-line process control procedures. In either case knowledge of the OUR should be useful in regulating plant performance.

The objective of this investigation has been to evaluate one of the methods proposed for adaptive DO control with simultaneous estimation of OUR. This method, proposed by Holmberg and Olsson (1986), appears particularly suitable because it only requires measurement of the DO concentration. The means for evaluating the scheme is through simulating the controlled process behaviour on a micro-computer. The simulations of plant behaviour have been restricted to diffused air ASP systems. That is, the oxygen input to the system is varied by varying the air flow rate from a compressor. However, the technique for DO control and simultaneous OUR estimation could also be applied to systems with surface aeration.

The dissertation starts by briefly reviewing the various approaches to OUR measurement. This places the Holmberg/Olsson method in the context of the current work in the field, justifying the selection of this method. This is followed by a more in-depth analysis of the method. The results of computer simulations using the method are then presented and discussed. Suggested modifications to the method are evaluated.

CHAPTER TWO

OXYGEN UTILISATION RATE ESTIMATION METHODS

2.1 INTRODUCTION

In the Activated Sludge Process (ASP) treating municipal wastewater, the total oxygen demand can be divided into four components associated with phenomena taking place in the system. The biodegradable organic material in the influent may be regarded as being comprised of a soluble readily biodegradable portion and a slowly biodegradable particulate fraction. In removal of the two fractions a rapid utilisation of oxygen can be associated with the readily biodegradable fraction and a slower rate of consumption with the particulate material. In addition to the two growth processes, a third component is the oxygen consumption associated with endogenous respiration. These three components relate to growth and maintenance of heterotrophic organisms and have been termed the carbonaceous OUR (Dold and Marais, 1985). A fourth component is encountered in nitrifying activated sludge processes. In such systems, ammonia nitrogen is converted to nitrate by autotrophic organisms; oxygen is also required for this biological oxidation.

Because oxygen consumption is linked directly to the biological processes within a system, oxygen utilisation rate (OUR) is reflective of process behaviour. For this reason knowledge of the OUR can be a useful indicator of process status and perhaps can be used as a measured variable in control strategies. The OUR has long been recognized as one of the most meaningful parameters in control. Because of the value of the information gathered in knowing the OUR, extensive research has been conducted into methods for measuring or estimating the OUR. This chapter will present the most common measurement methods and the most important proposals for estimating the OUR using identification.

2.2 DIRECT METHODS FOR MEASURING OUR

2.2.1 Laboratory measurement of OUR

Measurement of OUR in a laboratory-scale activated sludge system is a simple procedure. To illustrate the method, consider a single completely mixed reactor through which a stream is passing. The technique for measuring OUR in this reactor is as follows : The dissolved oxygen (DO) concentration is increased by increasing the rate of oxygen input. In the laboratory unit this would typically involve increasing the air flow rate to the reactor. Oxygen input is terminated when the DO concentration has been raised to near the saturation value; for example, to 7 or 8 mgO/l in a unit operated at 20°C. The DO concentration then decreases with time as no air is being bubbled through the reactor to balance the oxygen demand arising from the activity of the biological organisms. The OUR is obtained by monitoring the rate of decrease of DO with time. This is achieved very simply by recording the DO concentration change on an X-time plotter as shown in Fig 2.1. The slope of the straight line gives the OUR.

In the laboratory measurement method an important factor to note is that any flow to the reactor must be maintained during the test. Spurious results will be obtained if the feed is stopped at any time. This is particularly true for reactors receiving the influent flow. The error is associated principally with the OUR component for readily biodegradable substrate removal. The readily biodegradable material in the influent is utilized rapidly on entering the reactor. Therefore by terminating the feed to the reactor there will virtually be a step change in OUR. This is demonstrated in Fig 2.2 which shows the OUR response in a single aerobic ASP reactor receiving a cyclic square-wave input of municipal wastewater (i.e. 12 hours feed/12 hours no feed). The step change in OUR on feed termination is readily apparent (Ekama, Dold and Marais, 1985).

2.2.2 Grab sample method for measuring the OUR

A grab sample method for OUR measurement in full-scale plants has developed out of the laboratory method. This method has been reported as being the simplest to apply at full-scale (Goto, 1985). A grab sample of an aeration reactor's mixed liquor is taken and air bubbled vigorously

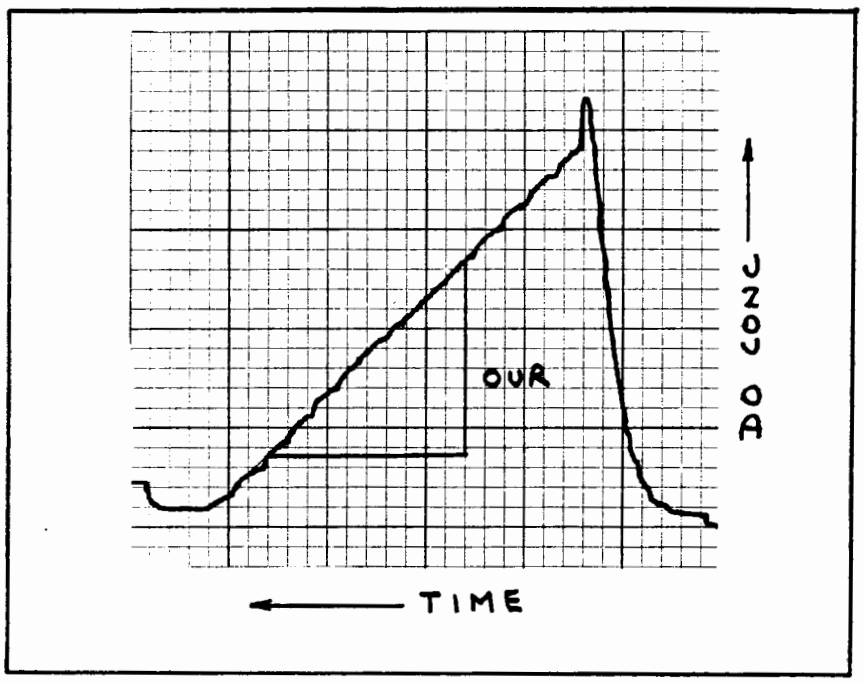

Fig 2.1 Example of a DO concentration time plot used to estimate the OUR in a laboratory reactor.

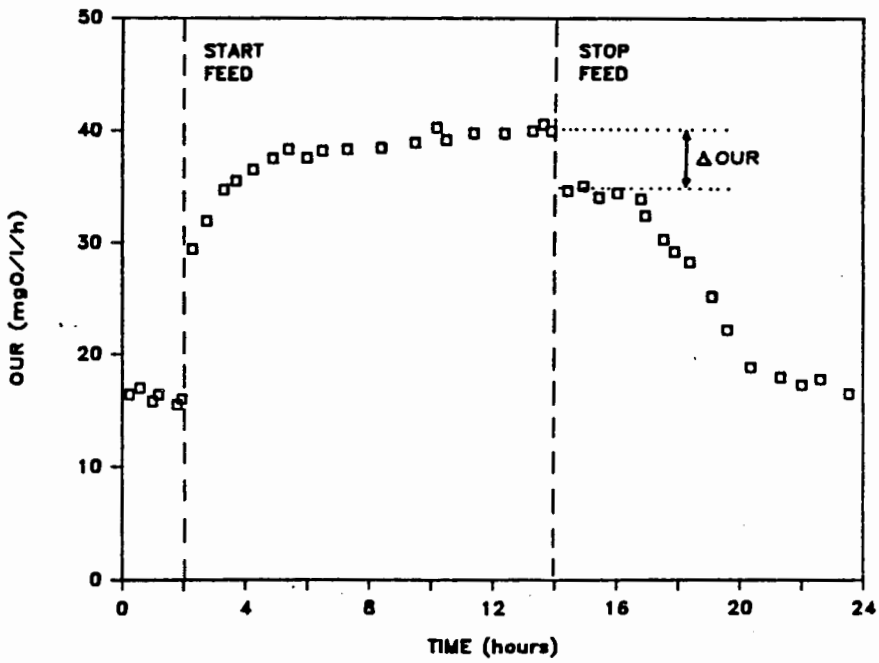

Fig 2.2 Oxygen utilisation rate (OUR) response observed over one cycle in an aerobic activated sludge unit subjected to daily cyclic square wave loading (12 hours feed / 12 hours no feed) with municipal wastewater as influent.

through the sample bottle until the DO concentration has increased to close to the saturation concentration. This procedure may require aeration for several minutes. The air supply is then turned off, and thereafter DO concentration is measured continuously over the next few minutes. As was the case in the laboratory measurement method, the OUR is given by the rate of decrease of the DO concentration.

One disadvantage of this method is its manual nature which makes it unsuitable for frequent daily use. Furthermore the grab-sample method generates values that are only as good as the representativeness of the grab sample. As non-ideal flows are present in all aeration basins, large variations frequently exist over small distances within a reactor. Indeed, it is quite possible that two grab samples taken from the same area at the same time yield different OUR's as a result of a non-ideal flow regime present in the reactor. However, other sources of error are more important in critisising the method.

In the method, a sample is taken from the continuous flow reactor and thereafter oxygen utilisation is measured in a batch test. In the batch test, concentrations of various compounds will change with time. Therefore the OUR also will change with time and the measured value may differ from the OUR in the continuous flow reactor. This problem is compounded by the fact that during the period in which the DO concentration is raised before the OUR measurement is commenced, it is likely that any readily biodegradable COD will be removed and nitrification also may be completed. Therefore these components will be excluded from the OUR measurement, and the OUR will be underpredicted. An additional problem with the batch mode of measurement is that the grab-sample method is tantamount to measuring the OUR in the continuous flow reactor but with the feed switched off. Therefore major errors can be incurred in the OUR measurement for the reasons outlined in Section 2.2.1. One possible approach to overcome problems with the grab-sample method is to use a small-scale reactor or 'respirometer' alongside the full-scale plant.

2.2.3 Respirometers for measurement of OUR

In recent years, a number of automatic respirometers (OUR monitors) have been developed and installed for continuous use (Goto, 1985). Respirometers consist of small-scale reactors usually placed alongside the full-scale plant. A continuous stream is diverted from the full-scale plant into the respirometer and, after passing through the respirometer, is returned to the aerator. The OUR is measured in the respirometer, and this measurement is taken as the OUR in the full-scale plant.

A number of methods for measuring the OUR in the respirometer have been proposed. One approach is to raise the DO within the respirometer and then terminate the air supply; thereafter the OUR is measured as in the laboratory scale method. An alternative approach is to adjust the air flow rate in the respirometer so as to maintain the DO concentration at some setpoint. The OUR is then estimated through solving the mass balance for DO concentration in the respirometer. A drawback of this approach is that some estimate of the mass transfer coefficient, K_La, is required. A third approach for measuring OUR in the respirometer is based on measurement of the pressure change in a closed vessel.

A disadvantage with the respirometer method is that close attention must be given to the experimental system and to the test procedures. To obtain reliable results requires considerable experience. The experimental difficulties with the respirometer itself are compounded by the difficulties in transferring a representative sample from the full-scale plant to the respirometer.

2.3 INDIRECT METHODS FOR ESTIMATION OF OUR

2.3.1 Estimating OUR via prior K_La estimates

Goto and Andrews (1985) developed a technique for the on-line estimation of OUR on a full-scale diffused air ASP plant. The method is based on readily available sensors and a process control computer. A dissolved oxygen balance on a well-mixed tank reactor gives:

$$\frac{dC_{OUT}}{dt} = \frac{Q}{V} \cdot (C_{IN} - C_{OUT}) + K \cdot (C^S - C_{OUT}) - OUR \quad \ldots\ldots\ldots (2.1)$$

where
- OUR = oxygen utilisation rate
- Q = aerator volumetric outflow
- V = aerator volume
- C_{IN} = DO concentration in aerator influent stream
- C_{OUT} = DO concentration in aerator and its effluent stream
- K = plant specific oxygen transfer coefficient
- C^S = saturation dissolved oxygen (DO) concentration

Goto (1985) noted that K, the plant specific oxygen transfer coefficient, was primarily a function of air flow rate, F_{AIR} i.e.

$$K = K(F_{AIR}) \quad \ldots\ldots\ldots (2.2)$$

Substituting Eq 2.2 into Eq 2.1 and re-arranging :

$$OUR = Q/V \cdot (C_{IN} - C_{OUT}) + K(F_{AIR}) \cdot (C^S - C_{OUT}) - dC_{OUT}/dt \quad \ldots\ldots (2.3)$$

Goto (1985) proposed that in order to estimate the OUR, all that remained was to find the relationship between K, the plant specific oxygen transfer coefficient, and the air flow rate, F_{AIR}, by a series of off-line experiments. An experiment was conducted in each of the aeration basins of a full-scale plant by introducing step changes in the air flow rate and following the DO with time. The empirical relationship between K and F_{AIR} was found using least squares curve fitting techniques. Based on this information, the estimated OUR values showed reasonable agreement with the measured values over a 24 hour period.

A major disadvantage of the Goto/Andrews method is its non-portability. A series of off-line tests are first required on every reactor in order to determine that aerator's specific empirical relationship between F_{AIR} and K. Furthermore these relationships need to be updated as changes occur with time.

Holmberg[2] and Ranta (1982) compared three estimation algorithms for determining the OUR and the oxygen transfer coefficient, K_La, of the ASP of a functional wastewater plant. The first of these is similar to the Goto/Andrews method. The method assumes that the DO concentration is strictly controlled. That is, it was assumed that $dC_{OUT}/dt=0$. By completing a DO mass balance in the form of Eq 2.1 and ignoring the flow terms, an equation very similar to that of Goto's (Eq 2.3) was derived :

$$OUR = K_La(F_{AIR})\cdot(C^S-C_{OUT}) \qquad .....(2.4)$$

To estimate the OUR, the relation between K_La and F_{AIR} was determined through a number of experiments in which the response of dissolved oxygen was recorded after a step change in the air flow rate. A graphical method, as opposed to Goto's least squares method, was used to determine the relation between K_La and F_{AIR}. Holmberg and Ranta concluded that the method for determining the K_La/F_{AIR} relationship graphically turned out to be poor. The method also occasionally failed when the assumption $dC_{OUT}/dt = 0$ was not valid.

2.3.2 OUR estimation via identification techniques

Holmberg and Ranta's second method for determining the OUR consisted of a recursive least squares estimation of OUR and K_La considering K_La to be an "unstructured parameter". The dissolved oxygen dynamics were approximated by a first order response, i.e. :

$$T\frac{dC_{OUT}}{dt} + C_{OUT} = K\cdot F_{AIR} \qquad .....(2.5)$$

where

$$T = 1/K_La \qquad .....(2.6)$$

$$K = C^S/F_{AIR} - OUR/[K_La\cdot F_{AIR}] \qquad .....(2.7)$$

Equation 2.5 was discretised giving :

$$C_{OUT}(k) = \alpha\cdot C_{OUT}(k-1) + \beta\cdot F_{AIR}(k-1) \qquad ....(2.8)$$

---

[2] This is the only reference to A. Holmberg (from Norway) who should not be confused with U. Holmberg (from Sweden) referred to regularly later.

in which

$$\alpha = 1-\Delta t/T \qquad .....(2.9)$$

$$\beta = (1-\alpha)\cdot K \qquad ....(2.10)$$

Δt = discretization step.

The parameters α and β were estimated through a recursive least squares algorithm. The values of α and β obtained through this algorithm allowed the OUR and K_La to be estimated through the rearrangement of Eqs 2.9, 2.10, 2.6 and 2.7. Simulations showed that under ideal conditions, the estimates of K_La and OUR converged to the correct values, but only when K_La and OUR were constant. An offset in the estimates was observed if K_La or OUR varied. The algorithm also experienced stability problems if the control was not constant for a long enough period to allow the parameter estimates to converge. When applied to a real process, the estimation of the parameters was not successful because the OUR varies.

Holmberg's third method was a recursive least squares estimation of OUR and K_La using a linear expression for K_La. ie :

$$K_La = a_1\cdot F_{AIR} + a_2 \qquad .....(2.11)$$

Ignoring the flow terms of the dissolved oxygen mass balance and substituting Eq 2.11 into the dissolved oxygen mass balance equation, Eq 2.1, gives :

$$\frac{dC_{OUT}}{dt} = a_1\cdot F_{AIR}\cdot[C^S-C_{OUT}] + a_2\cdot[C^S-C_{OUT}] - OUR \qquad ..... (2.12)$$

This equation can be discretized and expressed as :

$$y_1(k) = [1-a_2(k-1)\cdot\Delta t]\cdot y_1(k-1) - a_1(k-1)\cdot\Delta t\cdot y_2(k-1) + OUR(k-1)\cdot\Delta t\cdot y_3(k-1). \qquad .....(2.13)$$

in which

$$y_1(k) = C^S - C_{OUT}(k)$$

$$y_2(k) = y_1(k)\cdot F_{AIR}(k)$$

$$y_3(k) = 1$$

Δt = discretization step.

Equation 2.13 is linear in the parameters a_1, a_2 and OUR and therefore can be estimated recursively with a least squares algorithm. The estimates when applied to a real process were satisfactory, and were better than those obtained in the second method. For the estimation, a short sampling interval of one minute was used. The process was stimulated through small changes in the DO setpoint every 6 minutes. The general conclusion obtained for Holmberg and Ranta's second and third method was that although the estimates were good during transients with great dynamic changes, the process did not provide sufficient dynamics for successful estimation of all the parameters during normal controlled operation .

Holmberg[3] and Olsson (1985) also proposed a method for simultaneous K_La and OUR estimation. It was shown that both K_La and OUR can be estimated on-line simultaneously without any steady-state off-set even if both quantities are time varying. This was not possible with Holmberg and Ranta's second method. The ASP system was modelled on the simple DO mass balance of Eq 2.1. Two techniques for estimating the OUR and K_La were proposed. The first method used the Kalman filter parameter estimator with the Bayesian approach to account for the different rates of change in the OUR and K_La. The second approach was termed the deadbeat estimator and made use of singular excitations in the air flow rate. Holmberg and Olsson (1985) noted that extra air flow excitation is required to continuously ensure satisfactory identification. Both estimation techniques yielded very good results in simulation tests and feasible results were generated on an operational plant. The estimators were not directly linked to any form of DO control algorithm.

In the schemes of Holmberg and Ranta (1982) and Holmberg and Olsson (1985) the parameter identification is considered separately from DO control. The values of the parameter estimates obtained were not used to determine or influence the control action i.e. the controller parameters were held constant. In contrast, a number of researchers have considered OUR parameter identification together with dissolved oxygen control. In

[3] In this case, the researcher was U Holmberg not A Holmberg as with Holmberg and Ranta (1982)

these schemes the estimated values of the parameters are used to influence the control action, i.e. adaptive control.

Ko, McInnis and Goodwin (1982) demonstrated by simulation experiments the effectiveness of nonlinear adaptive control for the dissolved oxygen process. In addition to obtaining very effective control of the DO concentration level they showed that it was possible to obtain on-line estimates of K_La and the OUR. The DO dynamics were represented by a bilinear model the parameters of which were identified by a least-squares procedure. The identified parameters implicitly defined the K_La and the OUR. In order to overcome the problem of low process dynamics, a square wave set-point, varying between 1.8 and 2.2 mgO/l and of period 100 minutes, was used. Unfortunately Ko et al (1982) only demonstrated the effectiveness of their parameter estimating algorithm and control strategy at constant OUR and K_La, conditions rarely found in practice.

Olsson, Rundqwist, Eriksson and Hall (1985) proposed a method that would simultaneously estimate the time varying OUR and K_La as well as providing DO control in ASP aerators. The ASP aerator model was based on the integrated form of the DO mass balance (Eq 2.1):

$$C(t) = a_s \cdot C(t-1) + b_s \cdot F_{AIR}(t-1) - r_s \cdot OUR(t-1) \qquad .....(2.14)$$

where
- C = DO concentration
- F_{AIR} = air flow rate
- OUR = oxygen utilisation rate
- $(t-1),(t)$ = previous and current sampling interval
- $a_s = \exp(-a \cdot h)$ .....(2.15)
- $a = a_0 + a_1 \cdot F_{AIR}$ .....(2.16)
- h = sampling interval
- a_1 = slope of K_La versus F line, ie $K_La = a_1 \cdot F$
- $a_0 = Q/V$ .....(2.17)
- Q = influent volumetric flow rate
- V = aerator volume
- $r_s = [1/a] \cdot [1-a_s]$ .....(2.18)
- $b_s = r_s \cdot a_1 \cdot C^s$ .....(2.19)
- C^s = saturation dissolved oxygen concentration

The parameters a_s, b_s and r_s are time-varying, but are assumed constant over the sampling interval. It should be noted that these three terms are all functions of a_1 and F_{AIR}. The self tuning controller used the process model

$$y(t)=a^{*}\cdot y(t-1) + b^{*}\cdot u(t-1) \qquad .....(2.20)$$

where

y = dissolved oxygen concentration = C_{OUT} of Eq 2.12

u = air flow = F_{AIR} of Eq 2.14

The parameters a^{*} and b^{*} are constants determined by some recursive least squares algorithm. Equation 2.20 differs from Eq 2.14 by the omission of the last term of the right hand side of Eq 2.14, i.e. the term $r_s \cdot OUR(t-1)$. Thus the process model considers the $r_s \cdot OUR(t-1)$ term an unknown disturbance. The method of estimating OUR(t-1) is as follows: By putting $a^{*} = a_s$, a_1 can be calculated from Eqs 2.15 and 2.16. The value of r_s and b_s can then be estimated using Eqs 2.18 and 2.19, respectively. Hence all the terms of Eq 2.14 are known except for OUR(t-1), thus allowing OUR(t-1) to be estimated. According to Olsson et al (1985) these estimates are sensitive to a_s and may have high variance. In the current investigation simulations showed that the estimates obtained using this method were poor.

Holmberg (1986) improved on his previous work with Olsson by expanding his deadbeat K_La and OUR parameter estimator system to include simultaneous on-line dissolved oxygen control. Simulations showed that in closed-loop the dissolved oxygen control and parameter estimates were excellent. The estimator structure utilised the DO mass balance of Eq 2.1. Methods of approximating the left hand side derivative term of Eq 2.1, dC_{OUT}/dt, were developed, and these estimates utilised to estimate the OUR and K_La.

The control objective was to use the estimated time-varying parameters in the controller in such a way that the closed loop system tended to become a linear time-invariant system. This objective required fast parameter tracking. The tracking objectives however, required high excitation of the system, contradicting the control objective. It was

apparent that a compromise had to be reached between parameter estimation and DO control. This compromise was made by introducing a limit cycle to the closed loop system. The amplitude of the limit cycle was made sufficiently large so as to provide sufficient information about the system to the parameter estimator but was small enough so as not to contradict the control objective.

As Holmberg's method seemed the most promising of all the recently proposed simultaneous parameter estimation and DO control techniques, it was decided that a more thorough investigation into the method was appropriate. Chapter 3 presents the development of Holmberg's method in detail.

CHAPTER THREE

HOLMBERG METHOD FOR D.O. CONTROL AND O.U.R. ESTIMATION

3.1 INTRODUCTION

The concept of self-tuning control, where the controller parameters are adjusted on-line, was first proposed in the early 1950's. This approach to control arose primarily out of a need to control non-linear processes in which one set of controller parameters is not appropriate over the entire range of operating conditions. The general strategy of such a control system is shown in the block diagram overleaf (Fig 3.1). In summary the system involves two separate aspects. Firstly, appropriate parameters for a dynamic process model are estimated on-line (parameter estimation); and secondly, these model parameters are utilised to select appropriate controller parameters on-line (controller design). In this way, by continually adjusting controller parameters, the control method is referred to as 'adaptive'.

The self-tuning control (STC) configuration of Fig 3.1 is flexible enough to accommodate a wide variety of parameter estimation techniques and controller design strategies. Typically the dynamic process model is assumed to be a linear difference equation with parameters that are constant for a given sampling interval. One of a number of possible parameter estimation techniques is used to identify and update these process model parameters at each interval. Given the model parameters, a variety of methods also can be used to estimate appropriate values for the controller constants. Typically the controller is designed either to minimise a quadratic cost function or to place the poles (and perhaps the zeros) of the closed loop system at desired locations. However, many other controller design techniques exist.

Adaptive control is normally employed when the actual process is nonlinear and/or time-varying. In the STC model of the process,

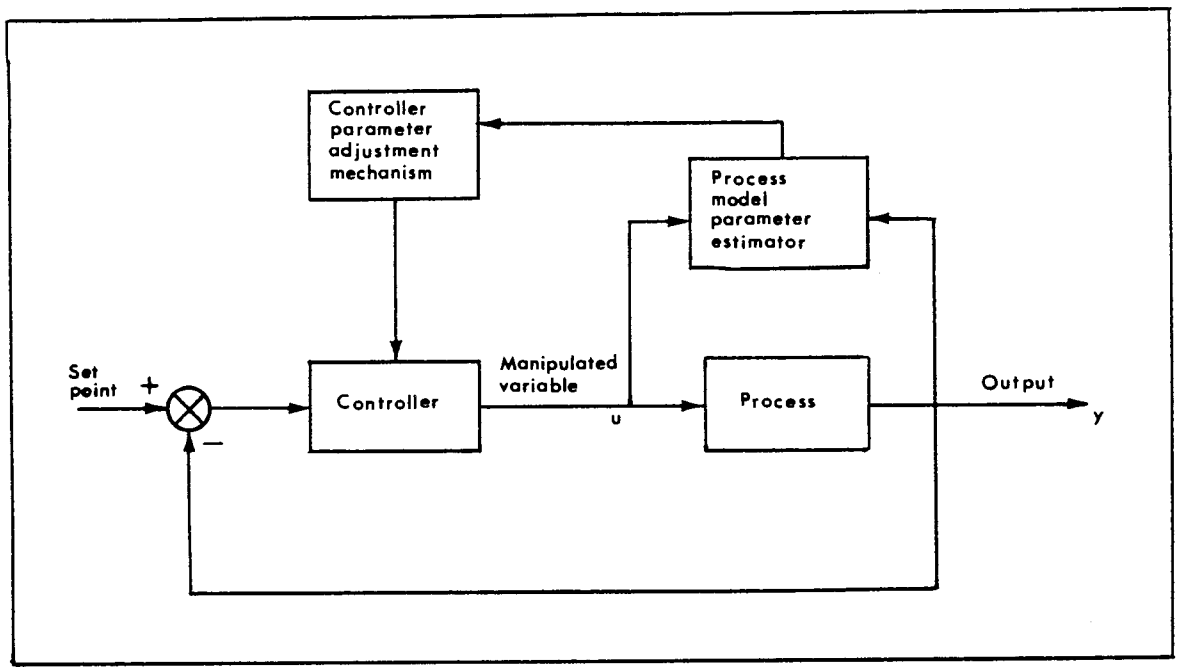

Fig 3.1 The structure of the Self Tuning Controller.

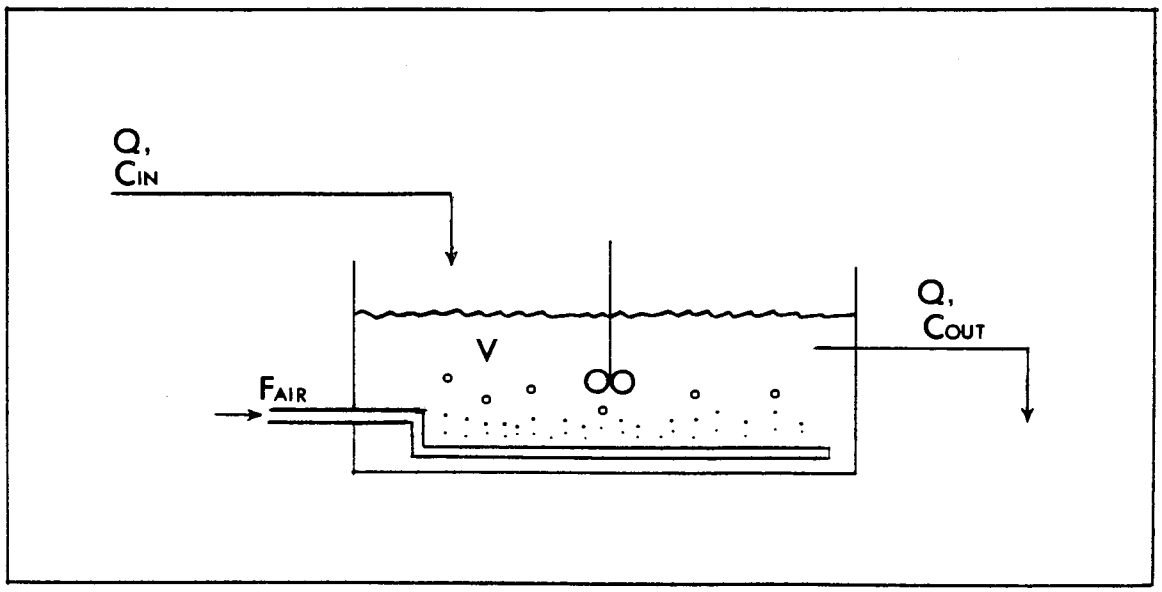

Fig 3.2 A CFSTR aerator of the Activated Sludge Process.

approximate models of the real process, usually linear and of low-order, are employed for purposes of simplifying the implementation. These simple models suffice even though they may not reflect the actual process dynamics accurately because deficiencies in the model are compensated for by the continual adjustments in the model parameters. In certain cases however, the process may in fact actually be of low order. When such a process is modelled by a corresponding low-order differential equation then some correspondence may exist between the STC model and the equation describing the actual process. Also some relationship between the estimated model parameters and the true process parameters may exist. In this instance it is sometimes possible to abstract estimates of certain process parameters from the on-line STC process model as opposed to making measurements of these variables in the actual process. This is the general basis of the Holmberg method for Oxygen Utilisation Rate (OUR) and Oxygen transfer coefficient (K_La) estimation through identification techniques.

In this chapter the method for simultaneous DO control OUR estimation proposed by Holmberg (1986) is analyzed and discussed. Modifications to Holmberg's method will be proposed later (Chapter 5). In this chapter, the original method is presented in three phases :

1) Selection of a model to mimic the real process;
2) Estimator structure and parameter estimation;
3) Control combined with parameter estimation;

The development of Holmberg's method is presented in what might initially appear unnecessary detail. This detail is provided for two reasons: Firstly, the method is presented very briefly by Holmberg, and a substantial effort was required to unravel the detail to enable simulation of the system. Secondly, modifications to the method can be presented clearly given the detailed presentation here. It should also be noted that in this presentation no attempt is made to place Holmberg's method in its control context; that is, the method is presented without any reference to the underlying control concepts.

3.2 SELECTION OF A PARAMETER ESTIMATION MODEL

Consider the single continuous flow stirred tank reactor (CFSTR) of an activated sludge process (ASP) shown in Fig 3.2. Oxygen input to the reactor is via a diffused air system. In the liquid phase the oxygen is consumed in the biological oxidation reactions; the oxygen utilisation rate (OUR) is an unknown function of, inter alia, dissolved oxygen, substrate and bacteria concentrations. A dissolved oxygen (DO) mass balance on the liquid phase in the CFSTR gives

$$\frac{dC_{OUT}}{dt} = \frac{Q}{V}\cdot(C_{IN}-C_{OUT}) + K_La\cdot(C^S-C_{OUT}) - R \qquad \ldots\ldots\ldots (3.1)$$

where

C_{OUT}	=	dissolved oxygen concentration in the reactor and the stream leaving the completely mixed reactor
C_{IN}	=	dissolved oxygen concentration in stream entering the reactor
C^S	=	dissolved oxygen saturation concentration
Q	=	flow rate of stream entering/leaving reactor
V	=	CFSTR volume
R	=	oxygen utilisation rate (= Respiration rate)
K_La	=	oxygen transfer coefficient
t	=	time

Holmberg (1986) proposed two simplifications of the actual process model of Eq 3.1. This was with the objective of formulating a simplified model of the process which nevertheless would predict the dynamic process behaviour with acceptable accuracy. By using this simplified model as the parameter estimation model it would then be possible, perhaps, to use the on-line parameter estimates to abstract information about the behaviour of the real process ie. about the parameters in Eq 3.1. The first simplification was to specify the oxygen transfer rate as a linear function of the air flow rate, F_{AIR} (Olsson et al, 1985):

$$K_La = \alpha\cdot F_{AIR} + a_2 \qquad \ldots\ldots\ldots (3.2)$$

The coefficient α is a function of aerator type, air production system, water depth, basin shape and even air flow rate itself and is not known in practice. Often a_2 is assumed to be zero (Olsson et al, 1985). With this assumption Eq 3.1 becomes:

$$\frac{dC_{OUT}}{dt} = \frac{Q}{V}\cdot(C_{IN}-C_{OUT}) + \alpha\cdot F_{AIR}\cdot(C^{S}-C_{OUT}) - R \qquad .....(3.3)$$

A second possibility for simplifying Eq 3.1 involves considering the magnitude of the different terms. The contribution of the flow term $[Q/V\cdot(C_{IN}-C_{OUT})]$ to the right hand side of Eq 3.3 typically is less than 1 percent of each of the other terms. Therefore this flow term can be ignored without incurring a large error to give :

$$\frac{dC_{OUT}}{dt} = \alpha\cdot F_{AIR}\cdot(C^{S}-C_{OUT}) - R \qquad .....(3.4)$$

In the process model of Eq 3.4 the terms F_{AIR} and C_{OUT} are readily obtained by measurement; C^{S} is a known function of temperature and pressure. The two remaining terms α (relating to K_La) and the oxygen utilisation rate R are unknowns. Holmberg proposed that these two terms could be estimated on-line without any measurements additional to F_{AIR} and C_{OUT} and without introducing major disturbances in the process.

3.3 ESTIMATOR STRUCTURE AND PARAMETER ESTIMATION

To estimate α (relating to K_La) and oxygen utilisation rate (R in Eq 3.4.) the process model in the parameter estimator should closely resemble Eq 3.4. The computer-based estimator structure operates in discrete time. Thus Eq 3.4 must be put in discrete form. A simple transform would be to approximate the derivative using Euler's method. That is

$$\frac{dC_{OUT}(kh)}{dt} = \frac{C_{OUT}(kh+h) - C_{OUT}(kh)}{h} \qquad .....(3.5)$$

where

h = sampling interval

k = integer counter representing the k'th sampling interval

C_{OUT} = measured DO concentration in the reactor and the stream leaving the continuous flow stirred tank reactor.

The Euler approximation of Eq 3.5 based on the measured C_{OUT} values is not appropriate, however, since experience has shown that such an estimator structure gives a bias in the estimates even if the parameters are constant over the sampling interval. Alternatively if the derivative approximation of Eq 3.5 uses estimated values of C_{OUT} as opposed to true measurements of C_{OUT}, there will be no bias in the estimates provided C_{OUT} and the other parameters are constant over the sampling interval. This corresponds to zero order hold sampling. However the problem is to track parameters α and R that are not constant over the sampling interval. The continuously varying α and R can be accounted for by assuming that α and R vary linearly over each sampling interval. This corresponds to first order hold sampling and should improve the parameter tracking.

Consider the nonlinear time varying system of Eq 3.4. Re-writing Eq 3.4 using a more standard nomenclature

$$\frac{dy}{dt} = \alpha \cdot u \cdot (C^s - y) - R \qquad \text{.....(3.6)}$$

where $y = C_{OUT}$ (process output)

$u = F_{AIR}$ (process input)

Putting $a = -\alpha \cdot u$ .....(3.7)

and $v = \alpha \cdot u \cdot C^s - R$ .....(3.8)

transforms the nonlinear equation to the linear equation:

$$\frac{dy}{dt} = a \cdot y + v \qquad \text{.....(3.9)}$$

It is convenient at this point to adopt the standard notation for sampled systems when deriving the estimator structure. Sampling this continuous time linear system of Eq 3.9 gives (see Appendix A.1)

$$y(kh+h) = \underline{\xi} \cdot y(kh) + \Gamma \qquad \text{.....(3.10)}$$

where

$$\underline{\xi} \equiv \underline{\xi}(h) \equiv \exp\left[\int_0^h a(kh + s)ds\right] \qquad \text{.....(3.11)}$$

$$\Gamma \equiv \Gamma(h) \equiv \int_0^h \underline{\xi}(s) \cdot v(kh+h-s)ds \qquad \text{.....(3.12)}$$

It will be apparent later that it is convenient to define

$$h^* = \int_0^h \underline{\xi}(s)ds \qquad \text{.....(3.13)}$$

3.3.1 Zero order extrapolation

Assume the parameters α and R and the air flow rate u to be constant over each sampling interval. It is clear from the definitions of a and v (Eq 3.7 and Eq 3.8), that constants α and R generate constants a and v. Thus the parameters a and v are also constant over the sampling interval. Equations 3.11 and 3.12 then integrate to give :

$$\underline{\xi} = \exp[a*h] \qquad \text{.....(3.14)}$$

$$\Gamma = h^* \cdot v(kh) \qquad \text{.....(3.15)}$$

Integrating Eq 3.13 gives:

$$h^* = \int_0^h \underline{\xi}(s)ds = (\exp[a*h] - 1)/a$$

$$= (\underline{\xi}-1)/a \qquad \text{.....(3.16)}$$

which re-arranges to

$$\underline{\xi} = 1 + h^* \cdot a \qquad \text{.....(3.17)}$$

Substituting Γ and $\underline{\xi}$ of Eq 3.15 and Eq 3.17 into Eq 3.10 gives

$$y(kh + h) = (1+h^{*}\cdot a)\cdot y(kh) + h^{*}v(kh) \quad \text{.....(3.18)}$$

$$\Rightarrow \frac{y(kh+h) - y(kh)}{h^{*}} = a\cdot y(kh) + v(kh) \quad \text{.....(3.19)}$$

$$= \dot{y}(kh) \quad \text{.....(3.20)}$$

If the parameter variation is not too rapid during the sampling interval a reasonable approximation of the derivative would be

$$\hat{\dot{y}}(kh) = \frac{y(kh+h) - y(kh)}{h^{*}} \quad \text{.....(3.21)}$$

Note the similarity between the above equation and the Euler approximation, Eq 3.5 where instead of the sampling interval h we have substituted for a 'generalised sampling interval' h^{*}. The relationship between the generalised sampling interval, h^{*}, and the sampling interval ,h, can be clarified by expanding the exponential term of Eq 3.16 to give:

$$h^{*} \approx h + \frac{a.h^{2}}{2!} + \frac{a^{2}.h^{3}}{3!} + \ldots \quad \text{.....(3.22)}$$

Having an approximation of $\hat{\dot{y}}$, the derivative of y, it makes sense to write the system in matrix format

$$\dot{y} = \left[\varphi^{T}\right]\cdot\left[\theta\right] \quad \text{.....(3.23)}$$

where

$$\varphi = \begin{bmatrix} u\cdot(C^{s} - y) \\ -1 \end{bmatrix} \quad \text{.....(3.24)}$$

and

$$\theta = \begin{bmatrix} \alpha \\ R \end{bmatrix} \qquad \text{.....(3.25)}$$

and to estimate the parameter vector θ from the linear regression model

$$\dot{y} = \left[\varphi^T\right] \cdot \left[\theta\right] \qquad \text{.....(3.23)}$$

The deadbeat estimator for zero order extrapolation

Consider the DO equation (Eq. 3.23) at two consecutive sampling instants (indexed $()_1$ and $()_2$). Assuming the parameters to be constant over the interval, i.e. $\theta_1 = \theta_2 = \theta$ we can write the two equations in matrix form

$$\begin{bmatrix} \varphi_1^T \\ \varphi_2^T \end{bmatrix} \cdot \theta = \begin{bmatrix} \dot{y}_1 \\ \dot{y}_2 \end{bmatrix} \qquad \text{.....(3.26)}$$

Let the input change at every sampling instant to make the linear equation well conditioned. The following estimator can then be used

$$\begin{bmatrix} \hat{\theta} \end{bmatrix} = \begin{bmatrix} \varphi_1^T \\ \varphi_2^T \end{bmatrix}^{-1} \cdot \begin{bmatrix} \dot{y}_1 \\ \dot{y}_2 \end{bmatrix} \qquad \text{.....(3.27)}$$

where the estimator is a direct solution of a set of linear algebraic equations. Since the estimates converge in finite steps the estimator was called a deadbeat estimator by Holmberg.

3.3.2 First order extrapolation

It has been noted earlier that assuming the parameters α and R to be constant during the sampling interval is not always valid. In this

situation a natural step of refinement is to use information about the parameter derivatives in the approximation of $\dot{y}$, ie.

$$\hat{\dot{y}} = \hat{\dot{y}}\left[\hat{\theta},\hat{\dot{\theta}}\right] \qquad \text{.....(3.28)}$$

The caret (or 'hat') indicates that the estimated value of a parameter is being used.

Assume the parameters to vary linearly over the sampling interval, ie.

$$\begin{bmatrix} a(kh+t) = a + \dot{a}*t \\ v(kh+t) = v + \dot{v}*t \end{bmatrix} \text{ where } \begin{bmatrix} a = a(kh) \;;\; \dot{a} = \dot{a}(kh) \\ v = v(kh) \;;\; \dot{v} = \dot{v}(kh) \end{bmatrix} \qquad \text{...(3.29)}$$

Using techniques analogous to the zero order method it is possible to show that :

$$\underline{\xi}(h) = \int_0^h a(kh+s).\underline{\xi}(s)ds = 1 + ah^* + \dot{a}.\int_0^h s.\underline{\xi}(s)ds$$

$$= 1 + ah^* + \dot{a}.I_1 \qquad \text{.....(3.30)}$$

where

$$I_1 = \int_0^h s.\underline{\xi}(s)ds \qquad \text{.....(3.31)}$$

and

$$r = \int_0^h \underline{\xi}(h-s).v(kh+s)ds = h^*.v + \dot{v}.\int_0^h s.\underline{\xi}(h-s)ds$$

$$= h^{*}.v + \dot{v}.I_2 \qquad \text{.....(3.32)}$$

where

$$I_2 = \int_0^h s.\underline{\xi}(h-s)ds \qquad \text{.....(3.33)}$$

Appendix A.2 provides detailed derivations of Eq 3.30 and Eq 3.32.

Substitution of ξ and Γ of Eq 3.30 and Eq 3.32 respectively into Eq 3.10 gives:

$$y(kh+h) = y(kh) + h^* \cdot (ay(kh) + v(kh) + \dot{a} \cdot I_1 \cdot y(kh) + \dot{v} \cdot I_2$$

$$\Rightarrow \frac{y(kh+h) - y(kh) - (\dot{a}.I_1.y(kh) + \dot{v}.I_2)}{h^*} = a\,y(kh) + v(kh)$$

$$= \dot{y}(kh) \quad .....(3.34)$$

If the parameter derivatives do not vary too rapidly during the sampling interval a reasonable approximation of $\dot{y}$ would be

$$\hat{\dot{y}}(kh) = \frac{y(kh+h) - y(kh) - (\hat{\dot{a}} \cdot I_1 \cdot y(kh) + \hat{\dot{v}} \cdot I_2)}{h^*} \quad .....(3.35)$$

In order to estimate $\dot{y}(kh)$ through the use of Eq 3.35 the following variables must be known :

$y(kh+h)$ and $y(kh)$;
I_1 and I_2;
h^*;
$\hat{\dot{a}}$ and $\hat{\dot{v}}$.

The DO concentrations at successive sampling intervals, $y(kh)$ and $y(kh+h)$, are known as these are measured. The integrands in I_1 and I_2 are very smooth functions and almost linear when a is small, making it possible to approximate these two functions with polynomials without incurring great errors. Taking one step with a Runge-Kutta integrator of 4th order gives :

$$I_1 = \int_0^h s \cdot \xi(s)ds = \frac{h^2}{6}(2\xi(\frac{h}{2}) + \xi(h)) + O(h^4) \quad .....(3.36)$$

and

$$I_2 = \int_0^h s \cdot \xi(h-s)ds = \frac{h^2}{6}(2\xi(\frac{h}{2}) + \xi(0)) + O(h^4) \quad .....(3.37)$$

The detailed derivation of Eq 3.36 and Eq 3.37 is given in Appendix A.3.

In order to calculate h^* the integral expression for h^* (Eq 3.13) does not need to be solved as in the zero order case but instead Eq 3.30 can be used once I_1 has been calculated:

$$\hat{h}^* = (1/\hat{a}_{o1d}).(\xi - 1 - \hat{a}_{o1d} \cdot I_1) \qquad \text{.....(3.30)}$$

The parameter derivatives $\dot{a}$ and $\dot{v}$ may then be estimated by taking the derivatives with respect to time of Eq 3.7 and Eq 3.8 ie.

$$\dot{a} = -\dot{\alpha} \cdot u \qquad \text{.....(3.38)}$$

$$\text{and} \qquad \dot{v} = \dot{\alpha} \cdot u \cdot C^s - \dot{R} \qquad \text{.....(3.39)}$$

Note that the airflow rate u and the saturation DO concentration C^s are assumed constant over the sampling interval. Estimation of the parameter derivatives $\dot{\alpha}$ and $\dot{R}$ can be done using the least squares method. If n is the number of estimates, the estimated derivative of α is

$$\hat{\dot{\alpha}} = \frac{n \cdot \sum_{k=1}^{n} ((kh).\hat{\alpha}_k) - \sum_{k=1}^{n} (kh) \cdot \sum_{k=1}^{n} \hat{\alpha}_k}{n \cdot \sum_{k=1}^{n} (kh)^2 - (\sum_{k=1}^{n} (kh))^2} \qquad \text{.....(3.40)}$$

Similarly $\dot{R}$ is estimated from :

$$\hat{\dot{R}} = \frac{n \cdot \sum_{k=1}^{n} (kh).\hat{R}_k - \sum_{k=1}^{n} (kh) \cdot \sum_{k=1}^{n} \hat{R}_k}{n \cdot \sum_{k=1}^{n} (kh)^2 - (\sum_{k=1}^{n} (kh))^2} \qquad \text{.....(3.41)}$$

See Appendix A.4 for the detailed derivation of Eq 3.40 and Eq 3.41 .

The deadbeat estimator for first order extrapolation

Again consider the DO equation at two consecutive sampling instants one and two steps before the current time (indexed $()_1$ and $()_2$). Assume the parameters to vary linearly over the intervals, i.e. $\theta = \theta_1 + \dot{\theta}_1 \cdot h = \theta_2 + \dot{\theta}_2 \cdot h$. Then the deadbeat estimator solves the following linear equation system with respect to $\hat{\theta}$:

$$\begin{bmatrix}\varphi_1^T\\ \varphi_2^T\end{bmatrix} \cdot \hat{\theta} = \begin{bmatrix}\hat{y}_1 + \varphi_1^T \cdot \hat{\theta}_1 \cdot h\\ \hat{y}_2 + \varphi_2^T \cdot \hat{\theta}_2 .2h\end{bmatrix} \qquad .....(3.42)$$

3.4 SIMULTANEOUS OUR ESTIMATION AND DISSOLVED OXYGEN CONTROL

The idea of the dual controller/parameter estimator is to use the estimated time-varying parameters in the controller in such a way that the closed loop system tends to become a linear time-invariant system. In order to track the parameters with good accuracy, the deadbeat estimator presented earlier is used.

Consider the process

$$\frac{dy}{dt} = \alpha \cdot u \cdot (C^s - y) - R \qquad .....(3.6a)$$

Let the setpoint be y_{sp} and the error $e = y_{sp} - y$. Choose the controller

$$u = \frac{\hat{R} + e}{\hat{\alpha} \cdot (C^s - y)} \qquad .....(3.43)$$

so that substituting for u of Eq 3.43 into Eq 3.6 results in the closed loop system:

$$\frac{dy}{dt} = \frac{\alpha \cdot (\hat{R}+e)}{\hat{\alpha}} - R \qquad .....(3.6b)$$

It is apparent that if the estimates of α and R are accurate (ie. $\hat{\alpha} \approx \alpha$ and $\hat{R} \approx R$) then the closed loop system becomes

$$\frac{dy}{dt} = \frac{-de}{dt} = e \qquad .....(3.44)$$

and we expect the error to go to zero exponentially.

In the development of the deadbeat estimator, Holmberg assumed that the input u oscillated and changed at every sampling instant. In order to be able to estimate the parameters continuously it is necessary that the

right hand side of Eq 3.6, $\alpha \cdot u \cdot (C^s - y) - R$, does not remain constant at successive sampling points. If the error is kept close to zero for a long time with constant input u, we cannot be sure the parameters are constant. They may drift along the line $\alpha \cdot K = R$, where $K = u.(C^s - y) =$ constant. Thus an estimator can give accurate estimates only at occasions when the parameters deviate from this line. That is, DO control and parameter estimation is greatly hindered unless the system is excited in some manner. However the requirement of continuous excitation contradicts the objective of the controller the aim of which is to reduce all errors to a minimum. This leads to the concept of dual control, where a compromise is made between DO-regulation and on-line estimation of α and R.

A minor modification of the above control scheme provides the deadbeat estimator with the necessary excitation and thus ensures a nonsingular linear equation system even when the error is small. Modifying the control signal with the term sign(e) yields:

$$u = \frac{\hat{R} + e + \text{sign}(e)}{\hat{\alpha} \cdot (C^s - y)} \qquad \text{.....(3.45)}$$

where sign(e) is the function

$$\text{sign}(e) = \begin{cases} -1 & \text{for } e < 0 \\ 1 & \text{for } e \geq 0 \end{cases}$$

yielding for $\hat{\alpha} = \alpha$ and $\hat{R} = R$:

$$\frac{dy}{dt} = \frac{-de}{dt} = e + \text{sign}(e) \qquad \text{.....(3.46)}$$

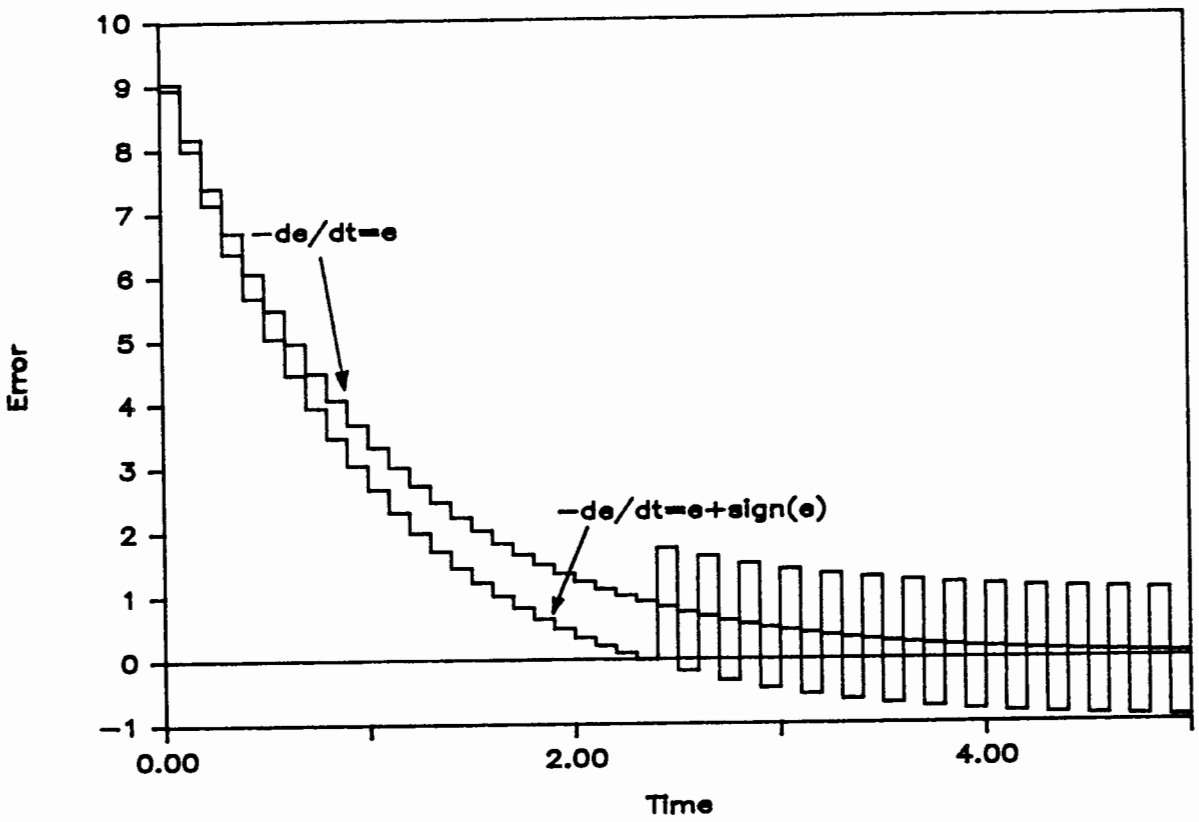

Figure 3.3 The effect of the sign(e) term on the closed loop behaviour

Hypothetical plots that clarify the differences between Eq 3.44 and Eq 3.46 are given in Fig 3.3 above. In the figure the initial error is assumed to be 10 units and a sampling period of 0.1 time units is used. As expected, the error of the closed loop system of Eq 3.43, dy/dt=-e, tends to zero exponentially. The closed loop equation containing the sign(e) term, Eq 3.46, tends to zero at a faster rate than Eq 3.44. The sign(e) term ensures that the decrease in the error is not exponential. On the first occurrence of a negative error, the error begins to oscillate between an upper and lower value at each successive sampling point. The amplitude of the oscillations gradually increases to one unit as the average between the peaks and troughs tends to zero. Thus the closed loop system error finally settles down to oscillations of amplitude 1 between +1 and -1. The amplitude of these oscillations is termed the limit cycle amplitude. By introducing extra parameters into the control scheme it is possible to choose the limit cycle amplitude $|\Delta y/2|$. The desired limit cycle amplitude is termed e_{SP}.

Thus the following controller

$$u = \frac{\hat{R} + a_c.e + d.\text{sign}(e)}{\hat{\alpha}\cdot(C^s - y)} \qquad \ldots\ldots\ldots(3.47)$$

gives the closed loop system

$$\frac{dy}{dt} = \frac{-de}{dt} = a_c\cdot e + d\cdot\text{sign}(e) \qquad \ldots\ldots\ldots(3.48)$$

when $\hat{\alpha} = \alpha$ and $\hat{R} = R$. The parameter a_c specifies the closed loop pole, i.e. the rate of a step response. The greater the value of a_c, the more sensitive the system and the more rapid the decrease in the error. The parameter d should be tuned itself during the limit cycle such that $e = \pm e_{SP}$. As an approximate test for limit cycle we can take

$$|e_t + e_{t-1}| < e_{SP}.$$

Thus the tuning for d becomes

$$d_{t+1} = d_t + k_d\cdot(e_{SP} - |e|) \qquad \ldots\ldots\ldots(3.49)$$

where

$$k_d = \begin{cases} k_d^0 \text{ when } |e_t + e_{t-1}| < e_{SP} \\ 0 \quad \text{otherwise} \end{cases} \qquad \ldots\ldots\ldots(3.50)$$

The choice of constants should be such that a reasonable compromise between control and identification is reached.

CHAPTER FOUR

METHOD FOR EVALUATING HOLMBERG'S SIMULTANEOUS PARAMETER ESTIMATION AND DISSOLVED OXYGEN CONTROL TECHNIQUE

4.1 INTRODUCTION

The theory behind Holmberg's simultaneous oxygen utilisation rate (OUR) parameter estimation and dissolved oxygen (DO) control technique has been presented in Chapter 3. Chapter 4 now explains how Holmberg's technique was evaluated. In essence Holmberg's method was tested through computer simulations of the controlled behaviour a completely mixed aeration basin. The simulation program was written in Turbo Pascal for the IBM Personal Computer. The program simulated two facets of system operation:

(1) the real plant: and
(2) Holmberg's controller/parameter estimator interfaced with the real plant.

The chapter describes the methods by which the real plant and Holmberg's controller/parameter estimator were simulated. This is followed by an explanation of the simulation program operation. Finally the program is tested by simulating an example used by Holmberg.

4.2 SIMULATION OF THE REAL PLANT

The process to be simulated is the controlled response of an aerated reactor in a diffused air activated sludge system. This reactor will be referred to as the "aerator". The controller cum estimator requires only measurements of the dissolved oxygen concentration and a knowledge of the air flow rate. Therefore a complex dynamic model for the activated sludge process was not required. Rather a simple model for DO response in the real plant was used. It was assumed:

(i) The DO concentration in the aerator could be measured at any time.
(ii) The air flow rate to the aerator could be manipulated.

(iii) The relation between air flow rate and oxygen mass transfer coefficient is known.

(iv) The time-varying oxygen requirement in the reactor, reflected by the OUR, was specified.

(v) Changes in DO concentration could be tracked by specifying an initial DO concentration and thereafter solving the DO mass balance differential equation.

Modelling the DO response in the aerator requires a knowledge of the flow regime. Ekama and Marais (1984) report that the mixing (or hydraulic) regimes of aerators vary between two extremes: completely mixed and plug flow. In completely mixed regimes the influent is instantaneously and thoroughly mixed (theoretically) with the reactor contents. Hence the effluent flow from the CFSTR reactor has the same constitution as the reactor contents. Also, the concentration of any compound will be uniform throughout the reactor, as will parameters such as the OUR. In practice the response of a well-mixed reactor often closely approximates the ideal continuous flow stirred tank reactors (CFSTR). In a plug flow regime, the reactor is usually of the long channel type basin. The influent is introduced at one end of the channel, flows along the channel axis and is mixed by air spargers set along the base of the channel. In ideal plug flow each volume element along the axis is assumed to remain unmixed with the elements leading and following. That is, a single plug flow reactor ideally is comprised of an infinite number of CFSTR's in series. In practice ideal plug flow behaviour is difficult to achieve. Rather the behaviour usually lies between the extremes of true plug flow and completely mixed. Common practice is to approximate the intermediate flow regime by a finite number of CFSTR's in series. Figure 4.1, taken from Dold and Marais (1987), illustrates how a channel type aerator may be modelled as a train of CFSTR's in series.

This study considered the behaviour in a single completely mixed aerator. Such a reactor will be characterized by a single DO concentration and a single OUR value. Changes in DO in the reactor are described by a mass balance for oxygen over the reactor:

$$\frac{dC_{OUT}}{dt} = \frac{Q}{V}\cdot(C_{IN}-C_{OUT}) + K_La\cdot(C^S-C_{OUT}) - R \qquad \ldots\ldots\ldots (4.1)$$

where

C_{OUT}	=	dissolved oxygen concentration in the reactor and the stream leaving the completely mixed reactor
C_{IN}	=	dissolved oxygen concentration in stream entering the reactor
C^S	=	dissolved oxygen saturation concentration
Q	=	flow rate of stream entering/leaving reactor
V	=	CFSTR volume
R	=	oxygen utilisation rate (= Respiration rate)
K_La	=	oxygen transfer coefficient
t	=	time

The $Q/V(C_{IN}-C_{OUT})$ term is called the hydraulic term. Generally this term is relatively small compared to the other two terms of Eq 3.1. However, occasions do arise in reactors in which both C_{IN} is close to zero (and thus not close to C_{OUT}) and the Q/V ratio is high; for example in a selector reactor incorporated in a system configuration for sludge bulking control. In such cases the hydraulic term may be of importance.

The oxygen mass transfer coefficient, K_La, is a function of several variables including airflow rate, temperature, wastewater characteristics and aerator geometry. Of these variables, the air flow rate is the most important. Goto (1984) gives estimates of K, a plant specific oxygen transfer coefficient, as a function of air flow rate. Figure 4.2 shows such a set of estimates. Goto fitted a straight line and a power curve to the estimates. He concluded that the straight line fit of the form

$$K_La = \alpha\cdot F_{AIR} + a_2 \qquad \ldots\ldots\ldots(4.2)$$

where

α	= slope of line
a_2	= K axis intercept
F_{AIR}	= air flow rate

produced better correlations, and thus recommended the use of the linear correlation over that of the power fit. A disadvantage of the linear fit

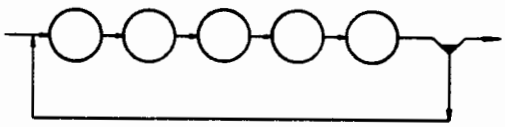

Fig 4.1 The modelling of a channel-type aerator by 5 CFSTR's in series.

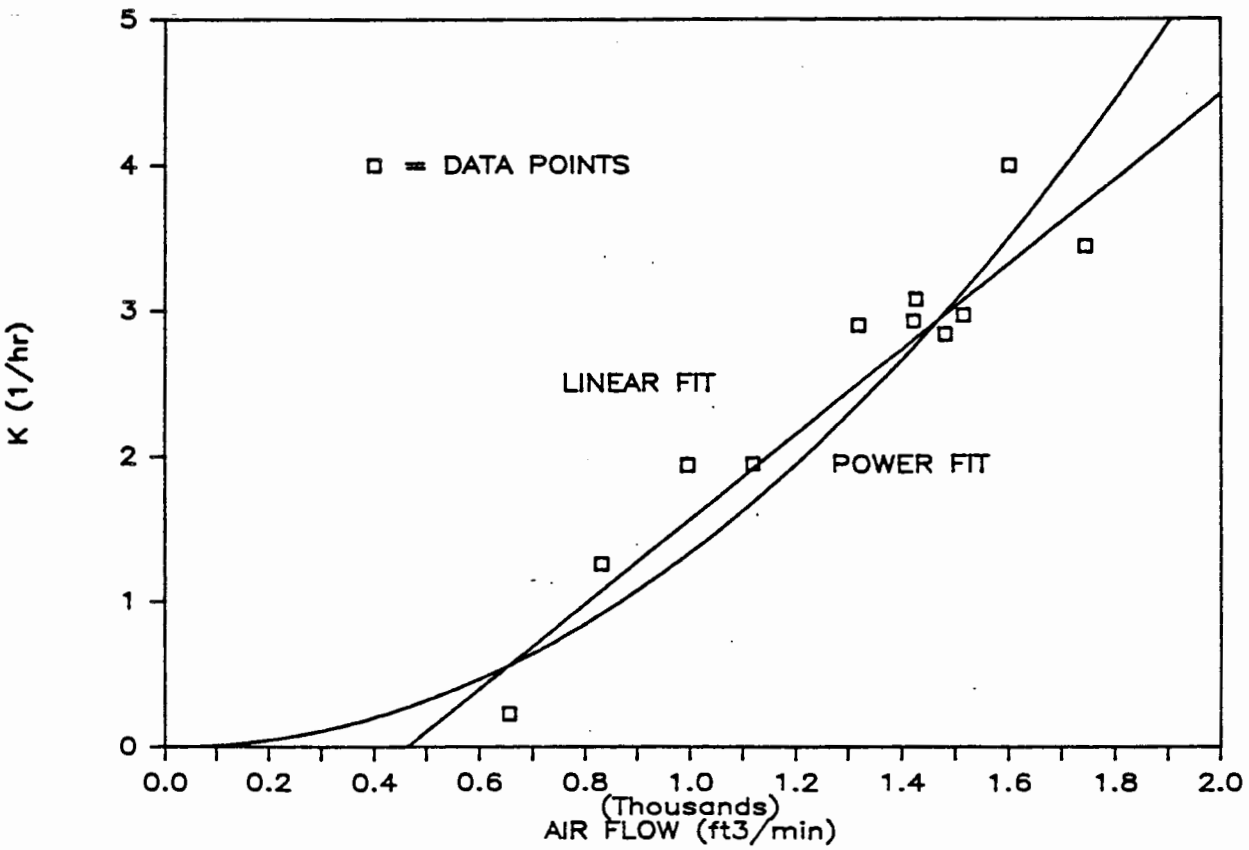

Fig 4.2 Goto's curve-fits to the K-airflow relationship.

is that negative oxygen transfer coefficients, a meaningless concept, are predicted at air flow rates less than $-a_2/\alpha$. The simulation program assumed the oxygen transfer coefficient in the real plant to be a linear function of air flow rate, as in Eq 4.2, but ensured that negative values of K_La were not generated by setting all negative K_La's to zero. The air flow rate settings were provided by the controller.

The maximum dissolved oxygen concentration or saturated dissolved oxygen concentration, C^s, is also a function of several variables. Of these the most important are wastewater temperature and pressure. As C^s is a function of pressure its value changes with depth in the aerator. An range of C^s's thus exist between the surface of the aerator liquid and the bottom of the aerator. However, for simplicity, the C^s value is usually taken at mid-depth (Schmidt and Redmon, 1975). In the simulations the C^s was assumed to be primarily a function of temperature and the dependence of C^s on depth was ignored. The validity of this assumption will be analyzed in the following chapter.

The oxygen utilisation rate, R, is the primary variable in the hydraulic model equation. For simulation purposes it was assumed that the OUR varied sinusoidally, with a 24 hour period.

Equation 4.1 was forward-integrated using the fourth order Runge-Kutta method. A fixed specific step length was utilised. The step length was always less than or equal to 1 minute. The relatively slow moving dynamics and the global error of $O(h^4)$ due to the Runge-Kutta technique ensured accurate integration.

To provide realistic simulations as well as a fuller evaluation of the Holmberg technique the option of adding dead time to the process was included.

4.3 SIMULATION OF THE CONTROLLER/ESTIMATOR

The role of the controller/estimator is two-fold. Firstly the estimator is to estimate the OUR and K_La using only measurements of dissolved oxygen concentration and a knowledge of the air flow rate. Secondly,

suitable control action is to be determined with these estimates to keep the dissolved oxygen concentration close to its set point.

4.3.1 OUR and K_La estimation

The parameter estimator proposed by Holmberg makes estimates of R, the respiration rate or oxygen utilisation rate, and α, the slope of the assumed straight line relationship between K_La and air flow rate[1]. Thus OUR is estimated directly while K_La can be calculated from:

$$K_La = \alpha * F_{AIR} \qquad \text{.....(4.3)}$$

It will be recalled from Chapter 3 that two methods of parameter estimation exist : A zero order method in which the parameters of the real process were assumed constant over the sampling interval, and a first order method in which these parameters were assumed to vary linearly over the sampling interval.

(i) Zero order method

The method for estimating R (respiration rate) and α in the zero order approach is set out in Fig 4.3. The symbols used are the same as those in Chapter 3: i.e.

u = airflow rate
y = DO measurement, etc

All carets(^) indicate estimated values. For example, $\hat{y}$ is the estimated value of y. Certain variables are followed by an integer within parentheses - eg $\hat{y}(2)$, u(1), y(0). These parentheses are used for all variables in which the values at successive sampling intervals are required for estimation purposes. A number, k, within parentheses denotes that the variable value k sampling intervals prior to the current time is to be utilised. Thus $\hat{y}(2)$ is the value of $\hat{y}$ two sampling intervals prior to the current time.

---

[1] Holmberg assumed that the parameter a_2 in the K_La/F_{AIR} relation of Eq 4.2 was zero. The validity of this assumption will be considered later.

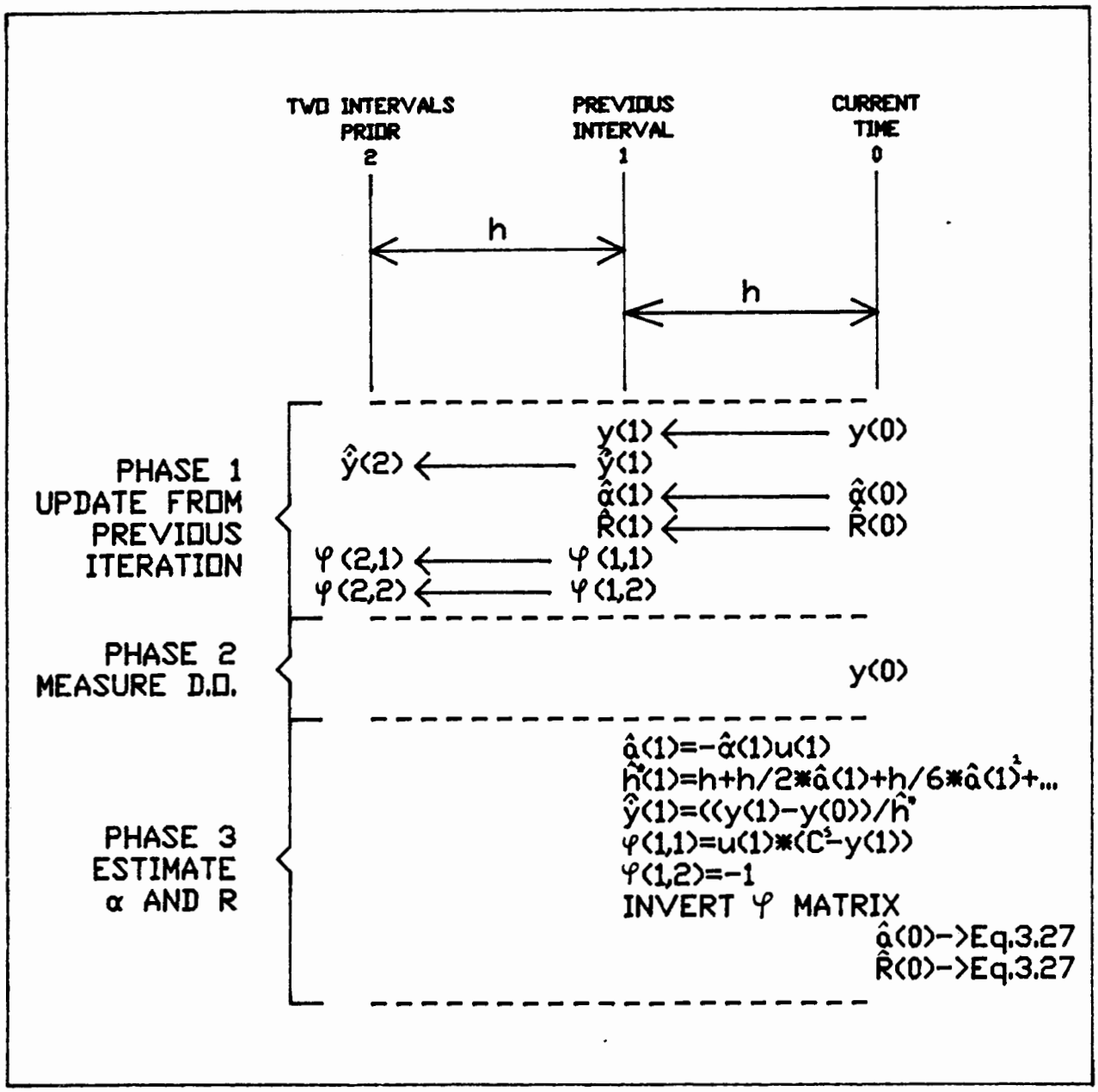

Fig 4.3 The zero order method of estimating α and R.

Figure 4.3 shows that the estimation of α and R is comprised of three phases. In the first phase, values that were measured or estimated in the previous iteration but which are still required in the current iteration are assigned new variable names so as to make place for the current values of those variables. Thus y(1) becomes the previous iteration's y(0), $\hat{\alpha}(1)$ becomes the previous iteration's $\hat{\alpha}(0)$, etc. The second phase consists of the measurement of the current dissolved oxygen concentration, y(0). The third phase consists of the steps required to estimate α and R. These are :

(i) estimate a through Eq 3.7.
(ii) estimate h^* through Eq 3.22.
(iii) estimate $\dot{y}$ through Eq 3.21.
(iv) update the φ matrix through Eq 3.24.
(v) invert the φ matrix.
(vi) estimate α, R through Eq 3.27.

(ii) First order method

The first order method is more complex than the zero order method, although the overall structure of the two methods are similar. The major difference between the two methods lies in the fact that the slopes of the parameters α and R, $\dot{\alpha}$ and $\dot{R}$, are estimated in the first order method, whereas the first order method assumes $\dot{\alpha}$ and $\dot{R}$ to be zero. Figure 4.4 illustrates schematically the steps involved in estimating α and R through the first order method. As in the zero order case, the first phase consists of updating those values that were measured or used in the previous iteration and which are required in the current iteration. Here it includes all those variables that are updated in the corresponding phase of the zero order method plus previous $\hat{R}$ and $\hat{\alpha}$ values and the variables used to estimate the current values of $\dot{R}$ and $\dot{\alpha}$.

The second phase of the first and zero order methods are identical - measurement of the current dissolved oxygen concentration. In the third phase, the steps required to estimate α and R are carried out. These steps are more complex than the zero order method. The steps are:

(i) estimate $\dot{\alpha}$ and $\dot{R}$ by using the least squares approach of Eq 3.40 and Eq 3.41.

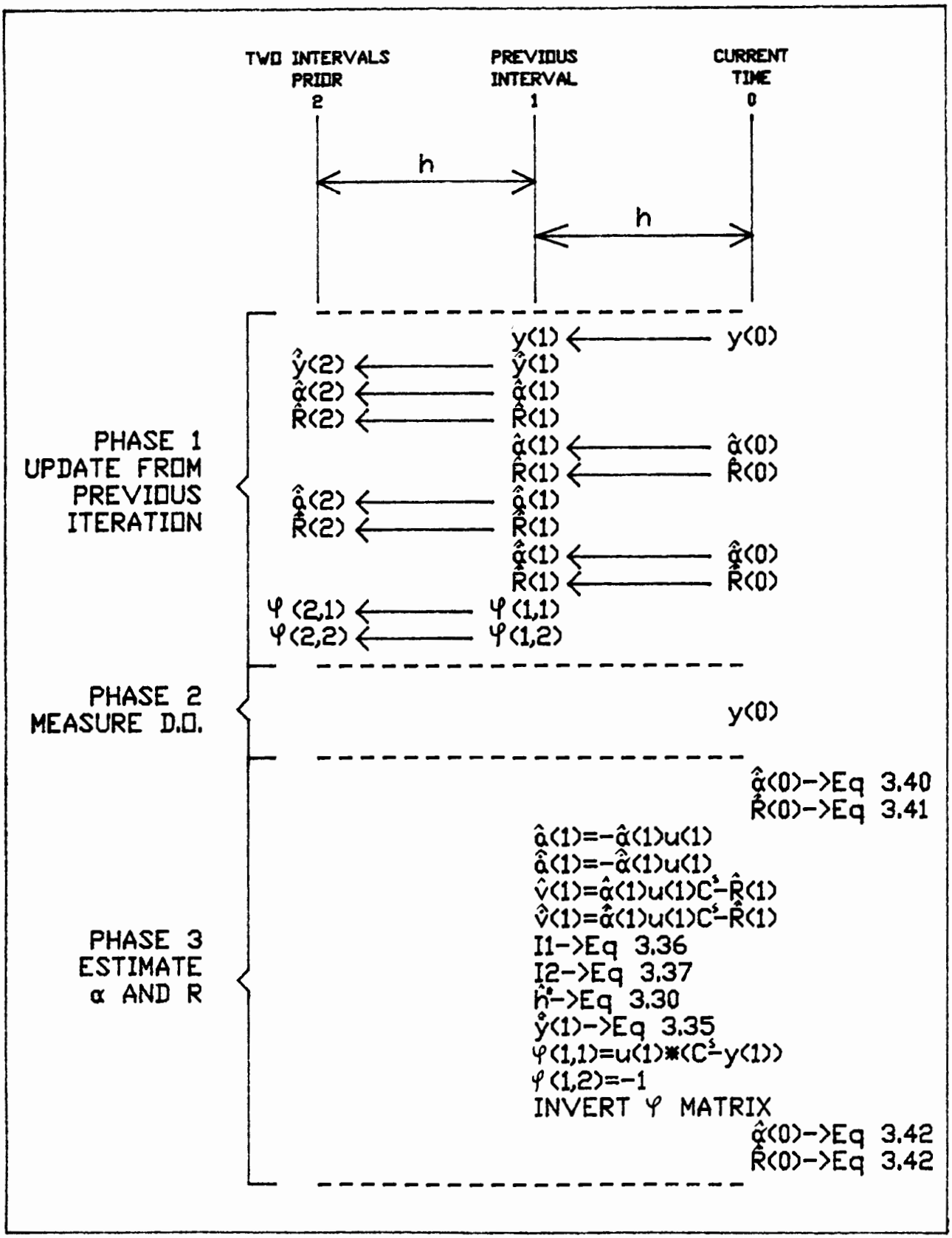

Fig 4.4 The first order method of estimating OUR.

(ii) estimate the values of the terms required to estimate $\dot{y}(1)$ i.e.:

$$\hat{a} = -\alpha(1)\cdot u(1) \qquad \text{Eq 3.7}$$

$$\hat{\hat{a}} = -\hat{\alpha}(1)\cdot u(1) \qquad \text{Eq 3.38}$$

$$\hat{v} = \hat{\alpha}(1)\cdot u(1)\cdot C^s - R \qquad \text{Eq 3.8}$$

$$\hat{\hat{v}} = \hat{\alpha}(1)\cdot u(1)\cdot C^s - \hat{R} \qquad \text{Eq 3.39}$$

$$I_1 = f(\hat{a}(1),\hat{\hat{a}}(1),h) \qquad \text{Eq 3.36}$$

$$I_2 = f(\hat{a}(1),\hat{\hat{a}}(1),h) \qquad \text{Eq 3.37}$$

$$h^* = f(\hat{a}(1),\hat{\hat{a}}(1),h) \qquad \text{Eq 3.30}$$

(iii) estimate $\dot{y}(1)$ from Eq 3.35

(iv) estimate new values of the Ψ matrix

(v) invert Ψ matrix

(vi) estimate α, R through Eq 3.42 .

4.3.2 Controller simulation

The controller uses the estimates of α and R to calculate the required controller response. The controller mechanism is independent of the identification procedure used. Thus, whether zero or first order identification is used, the controller response is given by Eq 3.47:

$$u = \frac{\hat{R} + a_c.e + d.\mathrm{sign}(e)}{\hat{\alpha}\cdot(C^s - y)} \qquad \text{.....(4.4)}$$

There are two controller constants in Eq 3 47. The first, a_c, specifies the closed loop pole. The greater the value of a_c the more sensitive the controller and the more rapid the decrease in the error. Whereas a_c is not tuned by the tuning mechanism, the second controller constant, d, can be self-adjusted by the controller. The greater the magnitude of d, the greater the limit cycle amplitude. The value of d is modified ('tuned') so as to allow a suitable compromise between the contradictory demands of identification and control. The tuning for d is:

$$d_{t+1} = d_t + k_d\cdot(e_{SP} - |e|) \qquad \text{.....(4.5)}$$

where e_{SP} and k_d are specified as 'tuning' constants. The tuning constant e_{SP} is the magnitude of the desired limit cycle amplitude. The value of k_d is given by:

$$k_d = \begin{cases} k_d^0 \text{ when } |e_t + e_{t-1}| < es_p \\ 0 \text{ otherwise} \end{cases} \quad \ldots\ldots\ldots(4.6)$$

4.4 PROGRAM OPERATION

The Turbo Pascal simulation program was compiled into a file called AERATOR.COM. In order to execute the simulation program the user types 'aerator' followed by a carriage return*. On execution the user is presented with a menu. The user may then select one of the options:

1) enter parameters defining the simulation conditions;
2) display the current values of the parameters defining the simulation conditions;
3) change one or more of the parameters defining the simulation conditions;
4) simulate the process using the current parameter values; or
5) exit the program.

The menu of choices above has arisen as a result of a desire to adhere to modern programming techniques of modularizing and structuring programs as much as possible.

The modular nature of the simulation program is illustrated in Fig 4.5. Each of the four modules consists of its individual separately compiled code. The four modules are :

- INPUT.CHN : The module used to enter the parameters defining the simulation conditions.

- DISPLAY.CHN : Displays the simulation parameters.

- CHANGE.CHN : Changes one or more of the simulation parameters.

---

* If the user wishes to take advantage of the graphics options available, then INT10.COM and HARDCOPY.COM must be executed before AERATOR.COM.

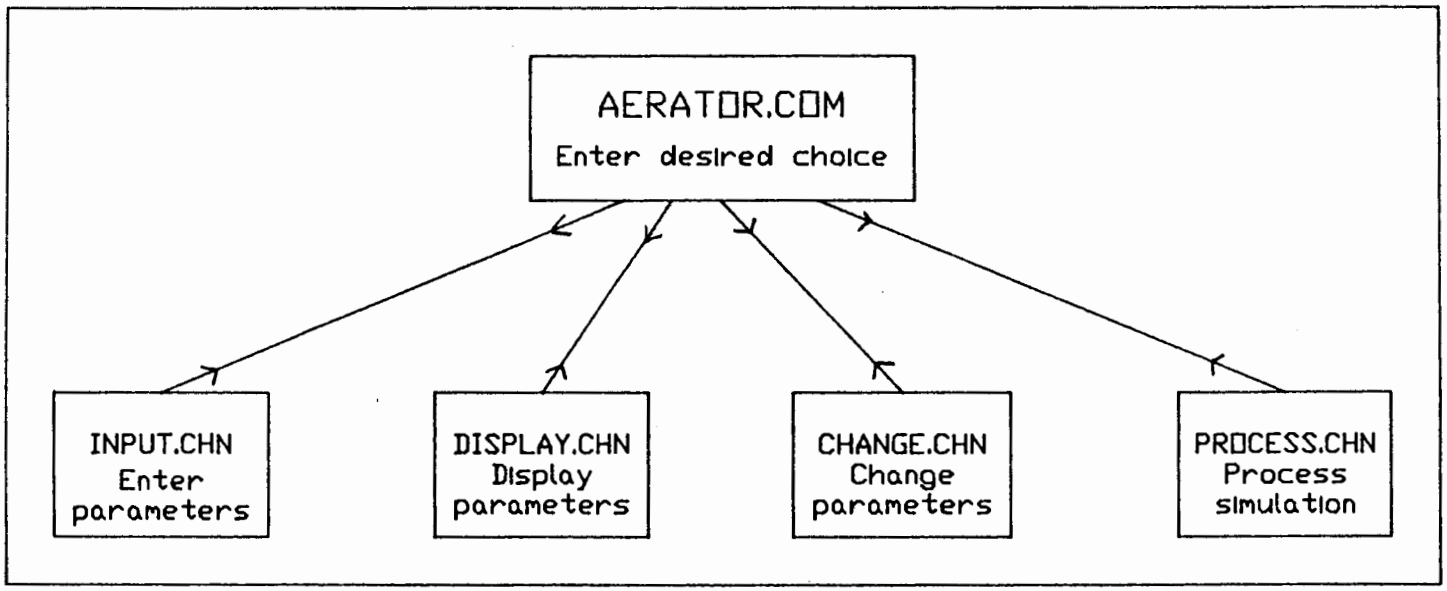

Fig 4.5 The modular nature of the simulation program.

- PROCESS.CHN : The core of the simulation program.

Only one of the four modules may be executed at a time. To pass from one of the four modules to another, one must pass through the central menu in AERATOR.COM. Thus, for example, to display the values of the current parameters, and then change the value of one these parameters, requires the following sequence:

a) call the 'display parameters' option in the main menu of AERATOR.COM;
b) display the variables according to the choices available in DISPLAY.CHN;
c) leave DISPLAY.CHN and return to the main menu of AERATOR.COM;
d) choose the 'change parameters' option in AERATOR.COM;
e) change the desired parameters.

The core of the simulation program, PROCESS.CHN, may not be executed until all the parameters defining the simulation conditions have been entered. The simulation parameters are entered by calling INPUT.CHN.

4.4.1 The operation of INPUT.CHN

There are two methods for entering the simulation parameters. Either the entire set of variables are entered one variable at a time from the keyboard, or alternately a set of variables may be recalled from a data file stored on disk. Data files may be stored to disk in CHANGE.CHN.

The parameters that are required for the simulation fall into the following categories:

- Process parameters
- Controller parameters
- Time parameters
- Identification parameters
- Results output parameters

4.4.1.1 Description of the process parameters

Process parameters consist of all those parameters that define the conditions under which the real process, as specified by Eq 3.1, operates. The process parameters are:

i) Q

Q, the wastewater flowrate entering and leaving the reactor, may be made to vary sinusoidally with time by specifying:

- mean Q
- amplitude of Q sine wave
- Q sine wave period
- offset in degrees from the origin (eg an offset of 90° converts the sine-wave into a cosine-wave).

ii) V

V is the reactor volume. The volume is assumed constant.

iii) C_{IN}

The influent dissolved oxygen concentration, C_{IN}, is assumed constant.

iv) $C_{OUT(initial)}$

$C_{OUT(initial)}$ is the dissolved oxygen concentration in the reactor at the beginning of the simulation.

v) α and a_2

The parameters α and a_2 define the relationship between K_La and the air flow rate to be used in simulation of real plant; i.e. :

$$K_La = \alpha \cdot airflow + a_2$$

Whereas the specified value of a_2 remains unchanged throughout the simulation, it is possible to vary α sinusoidally with time. Thus in the same manner that the flowrate Q is defined in terms of a sine-wave, the following parameters define the exact nature of the sinusoidal variation in α:

- mean α
- amplitude of α sine wave
- period of α sine wave
- offset of sine wave in degrees.

vi) OUR

In most activated sludge plants, the oxygen utilisation rate varies approximately sinusoidally over the day and thus, as for the simulation parameters Q and α, the value of OUR at each point in time is defined by:

- the mean OUR
- the amplitude of the OUR sine wave
- the wavelength of the OUR sine wave
- the OUR sine wave offset in degrees.

vii) Wastewater temperature

The DO saturation concentration, C^s, was assumed to be solely a function of temperature through the relation given by Bratby(1987):

$$C^s = \frac{51,6}{31,6 + T} * 9.07 \qquad .....(4.7)$$

where

T = temperature in °C

To specify a C^s, a wastewater temperature is required. Even though in practice the wastewater temperature does not vary greatly with time, the temperature of the wastewater can be specified by the previously used sine-wave characteristics; viz.

- the mean temperature
- the amplitude of the temperature sine-wave
- the period of the temperature sine-wave
- the temperature sine wave offset

ix) Initial air flow rate

If the process is uncontrolled the air flow rate remains constant at the initial air flow rate throughout the simulation.

x) DO noise band.

In practice any measurement value will include some measurement error. The measurement of the dissolved oxygen concentration is no exception. The error present in all DO measurements is simulated by being able to

specify the magnitude of the noise level. The value of the DO concentration made available to the controller is given by :

$$\text{Measured DO} = \text{True DO} * (1 + \text{DO\_Noise}) \quad .....(4.8)$$

where DO_Noise is a random number between zero and DO_band.

xi) Q band

Q band is a parameter identical in function and operation to DO_band, but instead applied to the flow rate measurement.

xii) Process lag

In order to render the simulations more realistic, it is possible to specify the magnitude of a dead time in the process. This process lag may be thought of as a method of accounting for a process that does not fully conform to the hydraulic model used, or as a method of specifying a dead time inherent to measurement of the DO.

4.4.1.2 Description of the controller parameters

The following controller parameters must be specified :

- The type of controller. The user has the choice of the following controllers:
  - i) One of the traditional P, PI, PD, PID controllers;
  - ii) Holmberg's dual mode controller;
  - iii) One of the proposed extensions to Holmberg's controller;
  - iv) No controller at all, in which case the air flow rate remains constant at the initial air flow rate throughout the simulation.
- If a controller is chosen then the DO setpoint must be specified. Furthermore, the controller's tuning constants must also be specified. Holmberg's controller requires the specification of the following constants:

  a_c, d, e_{SP}, k_d.

  The traditional PID-type controllers require:

  K, the gain.

  τ_i, the integral time constant

τ_d, the derivative time constant

4.4.1.3 Description of time parameters

The time parameters consist of:

i) The Runge-Kutta time interval step used in integrating the real process equation, Eq 4.1.

ii) The sampling interval used by the controller/estimator.
The sampling interval must be greater than or equal to the Runge-Kutta time step.

4.4.1.4 Description of the identification parameters

The user is required to specify whether first or zero order identification is used. If first order identification is used, the user must specify the number of points utilised in the least squares fit for estimating $\dot{\alpha}$ and $\dot{R}$ (Eq 3.40 and Eq 3.41).

4.4.1.5 Description of the output parameters

To facilitate the analysis of the simulation runs, specific attention was paid to output of simulation results. The program output allows most variables and parameters that are calculated to be displayed. The list of variables that may be displayed is given in Table 4.1.

The program is able to display the simulation results in various formats. The number of variables that may be output simultaneously varies according to which output mode is chosen. The user must choose between one of the following output modes:

a) Numeric output
b) Graphical output
c) Numeric and disk output
d) Graphical and disk output

a) Numeric output

The numeric output mode allows for eight variables to be displayed simultaneously on a standard text screen. The program always chooses the simulation time elapsed as the first of the eight variables, leaving the

TABLE 4.1 List of variables that may be output either graphically, numerically or to disk

C_{OUT}, DO Measurement	True and measured DO
Air flow	air flow rate = control Action
R, $\hat{R}$	True and estimated Oxygen Utilisation Rate
α, $\hat{\alpha}$	True and estimated α. See Eq 3.2
a2, a2(est)	True and estimated a2 (a2 used in Eq 3.2)
$K_L a$, $K_L a$(est)	True and estimated $K_L a$ (See Eq 3.2)
$\hat{a}$, $\hat{\hat{a}}$	Intermediate values used to estimate $\dot{y}$
$\hat{v}$, $\hat{\hat{v}}$	Intermediate values used to estimate $\dot{y}$
h^*	Pseudo sampling interval. See Eq 3.22
I_1, I_2	Intermediate values used to calculate $\dot{y}$ via the first order method.
$\hat{\dot{y}}$	Estimated rate of change in C_{OUT}
Temperature	Wastewater temperature - used to calculate C^s of Eq 4.2
Q, Q[0]	True and measured wastewater flow rate.
Control Action	Control action calculated from Eq 3.47
S	sensitivity of $\dot{y}$ to rates of parameter change

user to choose the remaining seven from the list in Table 4.1. The values of the eight variables are updated at intervals equal to the Runge-Kutta step size used to integrate the process model equation, Eq 4.1. A disadvantage with the numeric output mode lies in the fact that broad trends are not always clearly discernible when displayed in numeric form.

b) Graphical Output

The graphical output mode is useful for displaying the broad trends of the simulation. In order to take advantage of the graphical output mode, the IBM Personal Computer executing the program must be equipped with

additional hardware in the form of a Hercules graphics card. Also, a procedure called INT10.COM must be executed before AERATOR.COM is run.

The graphical output allows for any four variables found in Table 4.1 to be displayed simultaneously on the screen. The y-axis scales (ie. the lowest and highest values envisaged) must be individually specified for each of the four chosen variables. The X-axis is the simulation time, and its units and range must be specified. Once the simulation time exceeds the X-axis range, the graphical output re-commences on the left hand axis and simultaneously clears and over-draws the previously drawn lines as the simulation continues from the left to right. The X-axis time units must be chosen from the following :

- minutes
- hours
- days
- weeks

The four Y-axes are always hashed and divided into ten divisions. However, there is no default number of divisions for the X-axis, and so the number of X-axis divisions desired must be specified. No default number of X-axis divisions is chosen by the program as the large differences in time-scales and units demand different numbers of divisions. For example, a simulation period of 24 hours would most suitably require 12 or 24 X-axis divisions, whereas a simulation period of a week would be suited to 7 axis divisions.

It is possible to dump the contents of the graphics screen at any moment of the simulation to a dot matrix printer. To be able to send a copy of the graphic screen to the printer a file called HARDCOPY.COM must be executed after INT10.COM but before AERATOR.COM is executed. The graphics screen is dumped to the printer by depressing the 'Print screen' and '1' keys in succession. The user must also specify whether a copy of the graph is to be sent to the printer automatically each time the lines being drawn reach the right hand side axis.(The user need not depress the 'Print screen' key, but must still depress the '1' key)

c) and d) Disk Output

To allow statistical analysis and numerical comparison of simulations runs, an option has been included in the program to allow output of the simulation runs to be written to disk in a text file format compatible with the well known Lotus 1-2-3 spreadsheet package. The disk output is always written concurrently with either numeric or graphical output. No limit is placed on the number of variables that may be written to disk, but Lotus 1-2-3 will not load files that have had 18 or more variables written to disk simultaneously.

4.4.2 The operation of DISPLAY.CHN

The entire set of variables may be displayed by choosing the 'display variables' option in AERATOR.COM. AERATOR.COM will then execute DISPLAY.CHN which displays the current values of the variables either on the screen or, if desired, will send a copy to the printer for permanent record.

4.4.3 The operation of CHANGE.CHN

Once a set of variables has been loaded by executing INPUT.CHN, it is possible to change any of these parameters defining the existing simulation environment by calling the 'change parameters' option in AERATOR.COM. When this option is chosen, CHANGE.CHN is executed. CHANGE.CHN is particularly helpful when a number of simulations are completed one after another. In this situation most sets of simulation parameters differ only slightly from one another. CHANGE.CHN was written so as to speed up the setting up of new, slightly different conditions as it is far quicker to change one or two conditions of a previous simulation environment than to re-enter an entire set of new conditions. There is also an option within CHANGE.CHN to save a set of parameters to disk for later use in INPUT.CHN.

4.4.4 The operation of PROCESS.CHN

PROCESS.CHN is the core of the simulation program, and may only be executed once a set of parameters defining the simulation conditions has been entered by executing INPUT.CHN. The operation of PROCESS.CHN is displayed in block-diagram format in Fig 4.6. Figure 4.6 shows that

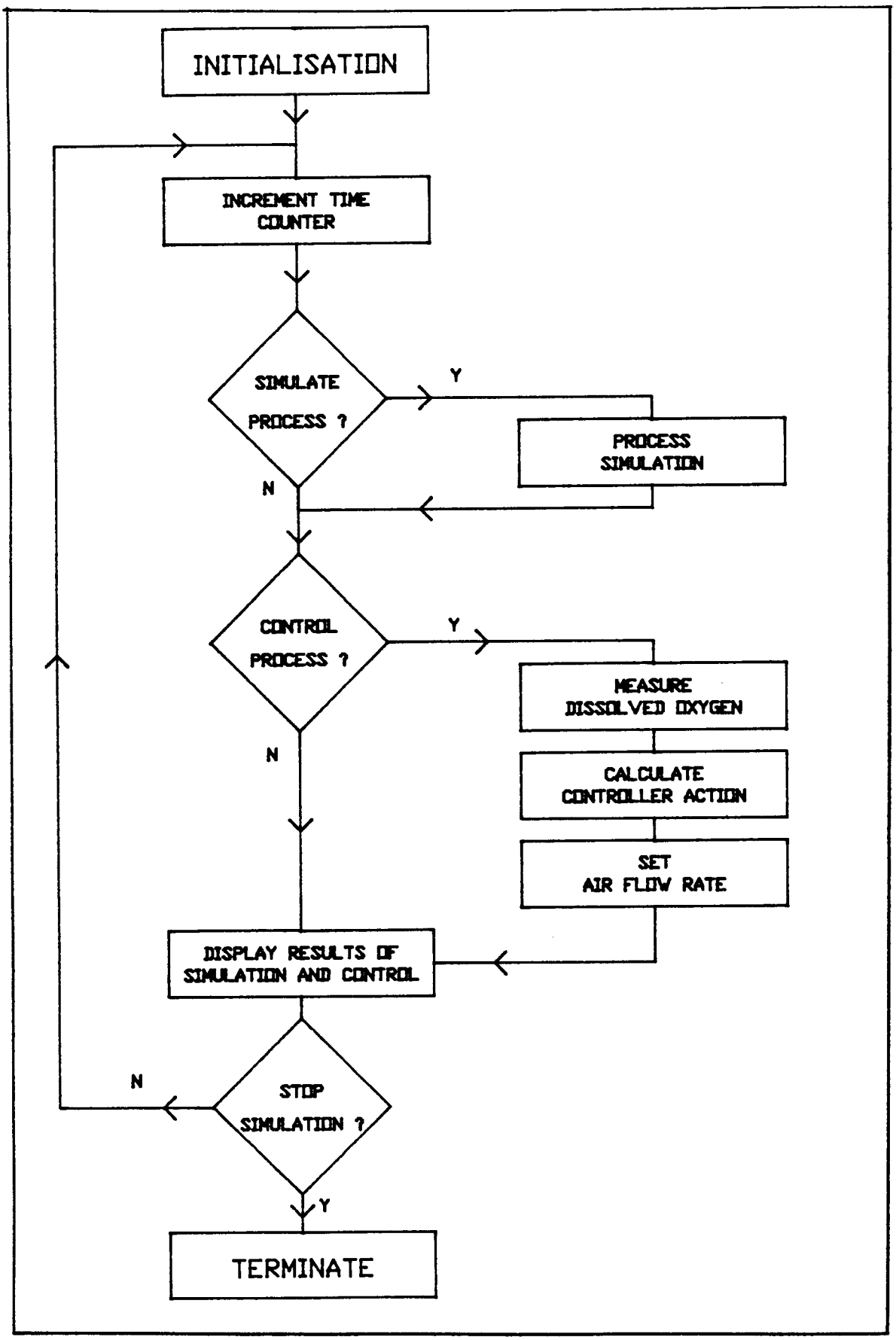

Fig 4.6 Flow diagram of PROCESS.CHN, the core of the simulation program.

PROCESS.CHN is first initialized before entering an infinite loop. The following instructions are carried out within the loop:

i) The time counter is incremented.
ii) The process response is simulated at the specified intervals.
iii) If it is time to take control action then:
    a) the dissolved oxygen concentration is measured:
    b) the controller action is calculated:
    c) the air flow rate is set according to the controller action.
iv) The results of the iteration are displayed.
v) If the user hits any key then the simulation is terminated and program execution is returned to AERATOR.COM.

4.5 CONFIRMATORY SIMULATION RUN

The simulation program was checked by simulating one of the runs undertaken by Holmberg (1986). Conditions for the simulation were:

i) $Q/V = 0$
ii) $C_{OUT(Initial)} = 0$
iii) Mean $\alpha = 3*10^{-7}/1 = 0.018$ min/hr/m^3
    α sine wave amplitude = $3.3*10^{-8}/1 = 0.002$ min/hr/m^3
    α sine wave period = 10 hours (estimated)
    α sine wave offset = 90°
iv) Mean OUR = 10mgO/l/hr
    OUR sine wave amplitude = 1 mgO/l/hr
    OUR sine wave period = 10 hours (estimated)
    OUR sine wave offset = 90°
v) C^s. The value of C^s used in Holmberg's simulation is not given, and thus this value had to be guessed. C^s is a function of temperature as given by Eq 4.7. Holmberg is Swedish, and thus a relatively cold wastewater temperature of 10°C was utilised to estimate C^s.
vi) The process was assumed ideal i.e. no process lag, and no noise in the measurement of either the DO concentration or Q.
vii) Holmberg's dual mode controller was used with the following parameters :

$$a_c = 0.16666 \text{ /min} = 10\text{/hour}$$

e_{SP} = 0.01 mgO/l

k_d^o = 0.01667 /min = 1/hour

d = 0.01666 mgO/l.min = 1 mgO/l.hr

viii) Setpoint = 2mgO/l

ix) Sampling interval = 6 minutes

x) First order identification, with 5 points used to estimate $\dot{R}$ and $\dot{\alpha}$.

The results of the two simulations are displayed in Fig 4.7 and Fig 4.8. Figure 4.7a shows the true values of α and R and their respective estimated values, as simulated by the program used in this study . Figure 4.7b displays the α and R values and their respective estimates, as simulated by Holmberg. In both simulations the estimated values of α and R follow the true values of α and R very closely. The two simulations have produced almost identical results. There are however, minor differences. It will be noticed that in Fig 4.7a, the first two values of $\hat{\alpha}$ and $\hat{R}$ show major oscillations, whereas in Fig 4.7b (Holmberg's simulation) oscillations of the same magnitude are not observed. This phenomena is ascribed to the fact that in Holmberg's simulation the values or α and R are held constant for three hours before commencing the sinusoidal variation in α and R. In the simulation program used in this thesis, the sinusoidal variation in α and R is commenced immediately. This difference in operating conditions is important. It will be shown in Chapter 5 that the greater the variation in a parameter, the worse its estimate. It may appear as if the estimates of both α and R in Fig 4.7a are consistently worse than those of Fig 4.7b. However, closer examination of the figures reveals that the apparent greater inaccuracy of Fig 4.7a is due to the greater resolution in both the X and Y axes of Fig 4.7a.

Figures 4.8a and 4.8b display the air flow rate and DO concentration changes corresponding to Figures 4.7a and 4.7b, respectively. It will be noticed that in both this study's and in Holmberg's simulations, the DO is well-controlled. Moreover, the DO concentration time profiles in Fig 4.8a and Fig 4.8b are very similar. The air flow rates also follow similar trends. The slight differences between the air flow rates of Fig 4.8a and 4.8b is ascribed to the initial differences in R and α, as well as the uncertainty in the value of C^s used by Holmberg.

The simulation run above included all the more difficult aspects of Holmberg's method: first order identification and the Holmberg controller. As the results obtained under these conditions by Holmberg were confirmed by this study's simulation, it would appear that the simulation program results may be accepted.

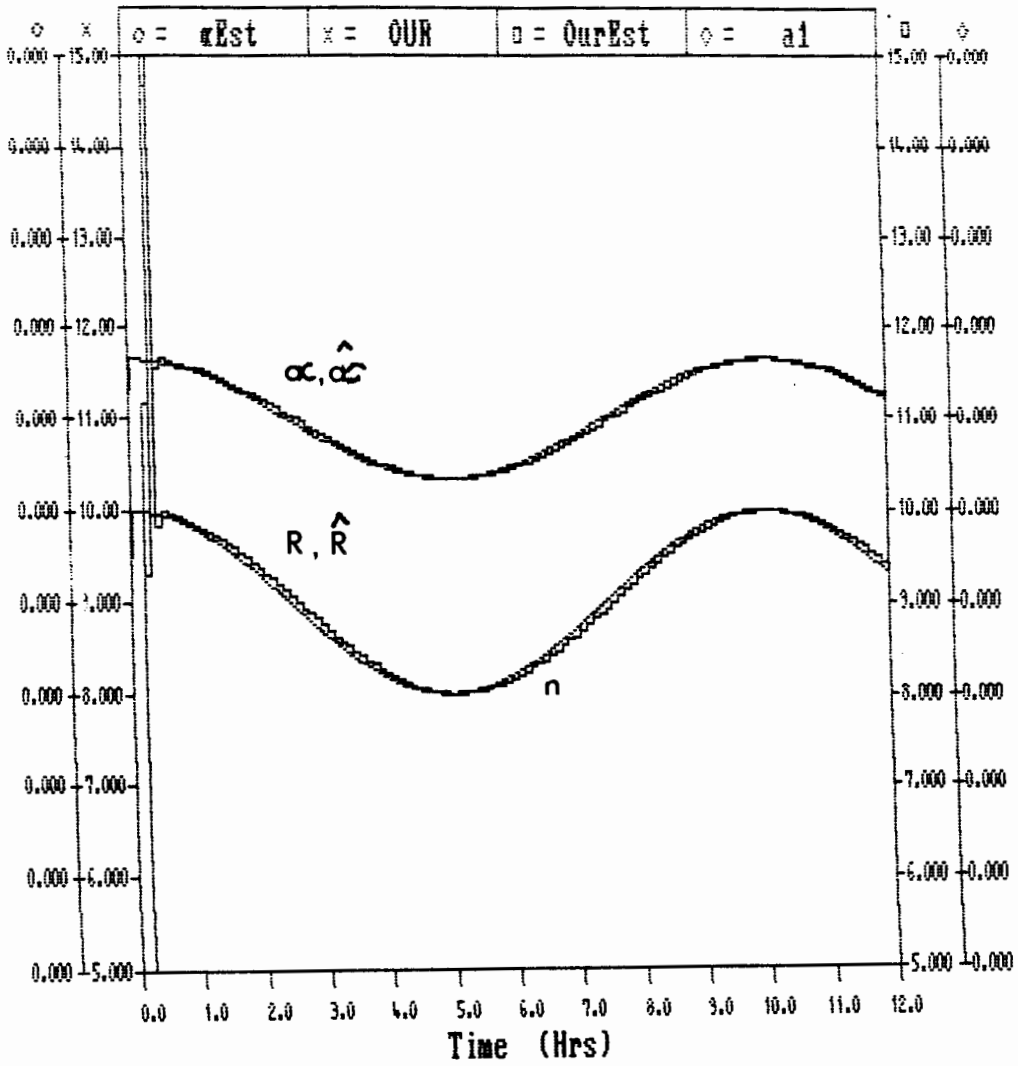

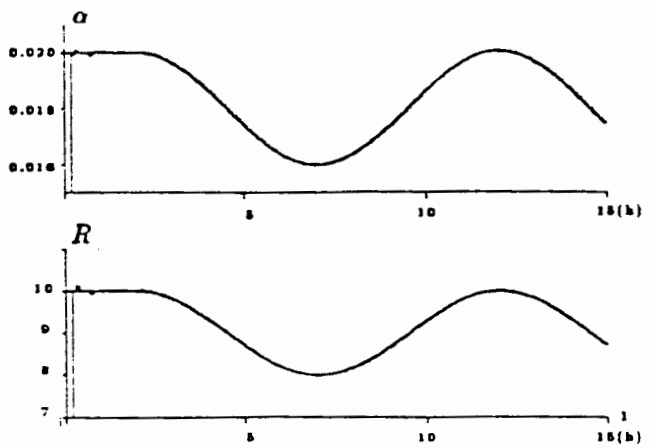

Fig 4.7 The values of α and R and their estimates as estimated by
a) this thesis's simulation program
b) Holmberg

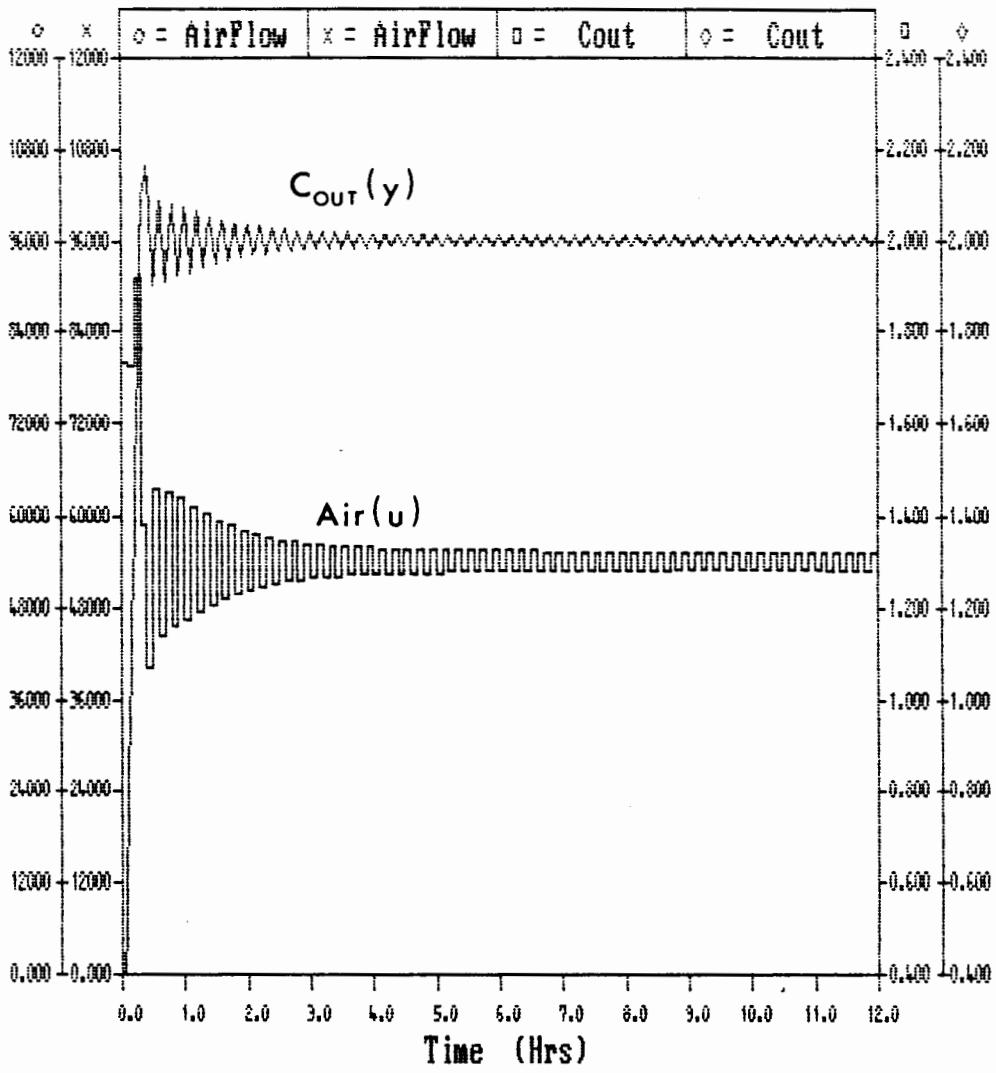

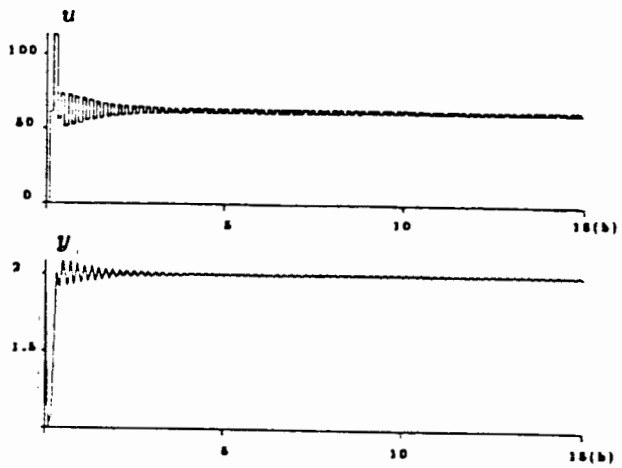

Fig 4.8a and Fig 4.8b The values of y (C_{OUT}) and u (airflow) corresponding to the simulations of Fig 4.7a and 4.7b.

CHAPTER FIVE

EVALUATION AND MODIFICATIONS TO HOLMBERG'S METHOD

5.1 INTRODUCTION

This chapter evaluates Holmberg's method for simultaneous parameter estimation and dissolved oxygen control. The evaluation was carried out entirely through simulation runs using the program described in Chapter 4. The evaluation is a multi-faceted problem, as it involves analyzing the effect of a number of variables. The factors that are considered are, the effect of:

(i) the rates of change in OUR and α
(ii) identification technique
(iii) the flow terms
(iv) the assumed K_La/F_{AIR} relationship
(v) inaccuracies in C^s
(vi) the controller parameters

Once the effect of the above six factors have been considered, various modifications that overcome some of the shortcomings of Holmberg's method will be presented. Finally, the problem of dead-time will be discussed.

5.2 EVALUATION OF HOLMBERG'S METHOD

The results of the simulations used to evaluate both Holmberg's method and the proposed extensions to the method are usually presented in graphical form. As more than 50 parameters are required to define each simulation run, it is impossible to mention magnitudes of all parameters used for every simulation run in the text without sacrificing clarity. Therefore only the important parameters that quantify the exact differences between simulation runs are mentioned within the discussion. For purposes of completeness, Appendix C lists the entire parameter sets of all the simulation runs in this chapter.

5.2.1 The effect of the rates of change in the parameters α and OUR

In a full-scale activated sludge system consisting of a number of zones in series the OUR is not constant, but decreases through the plant. Dold and Marais (1987) have explained the reasons for a decreasing OUR along an aerobic reactor train such as that considered in Fig 4.1. The reasons for the "tapered" oxygen demand are two-fold :

(i) Approximately 20 percent of the influent COD is in a readily biodegrable (soluble) form and is utilized rapidly on entering the system: this manifests itself as a high OUR at the head of the system.

(ii) In long sludge age plants, the nitrification rate often is sufficiently high that nitrification is completed close to the head of the plant. Again this manifests itself as a high OUR at the head of the system.

In the final passes of the system the OUR is principally due to oxidation of substrate from hydrolysis of slowly degradable COD and nitrification of ammonia made available by organism death, and thus the OUR is low compared to that in the first passes.

In addition to the OUR being highest in the aerated zones closest to the head of the system, the largest OUR fluctuations are found in these zones (see Fig. 5.1). Again the fluctuations are linked to the varying utilization rates of readily biodegrable influent COD and ammonia nitrogen that arise as a result of the cyclic COD and TKN loads on the plant over a 24 hour period. At the head of the reactor train daily variations of approximately 50 percent above and below the mean daily OUR can be expected. On the other hand, reactors at the end of the train are subject to very small daily variations in the OUR, to the extent that the OUR in these final reactors may be considered constant.

The first run simulates the type of behaviour encountered in an aeration reactor at the end of a plant. The OUR and α are assumed constant. In the simulation the OUR was the average obtained by Dold and Marais

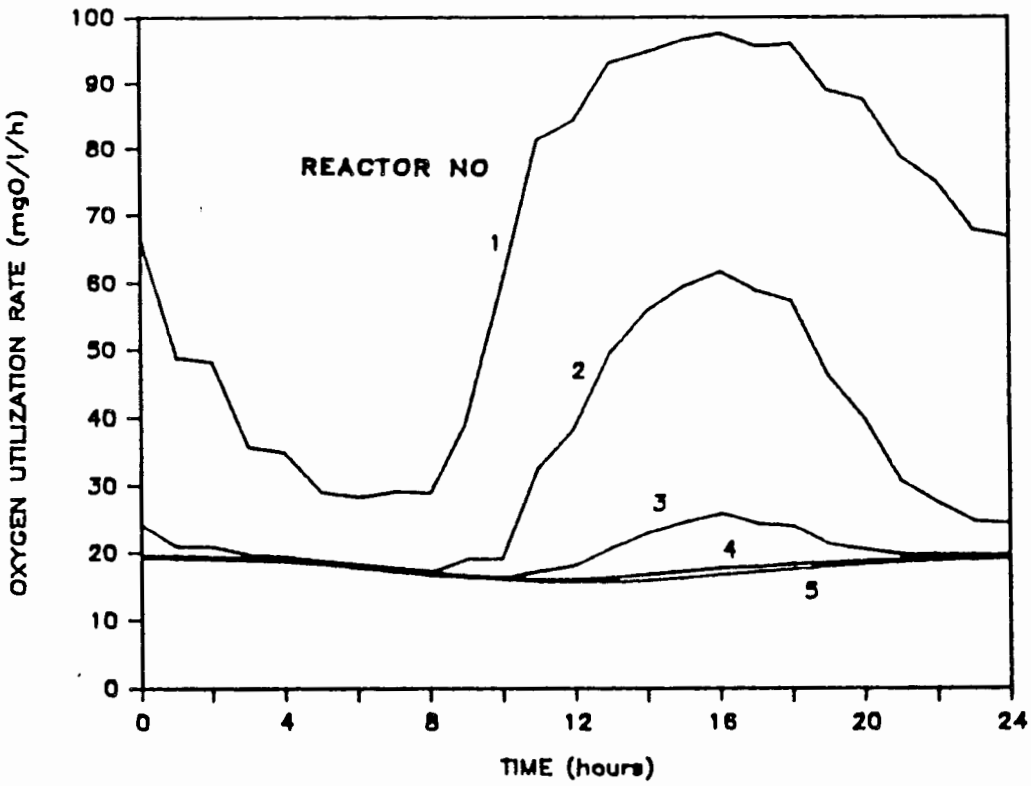

Fig 5.1 Typical variation of the oxygen utilisation down the aeration train [reactor 1 = head of aeration train, reactor 5 = end of aeration train], from Dold and Marais (1987).

(1987) in the fifth and last aeration reactor of a five-in-series aeration train : OUR = 20 mgO/l/hr. The K_La was assumed to be directly proportional to the air flow rate (i.e. $K_La = \alpha * F_{AIR}$). The proportionality constant was obtained by fitting a straight line to Goto's (1986) data given in Fig 4.2 : $\alpha = 1.2*10^{-6}$/l. The flow terms of the real process model, Eq 3.1 , were set to zero. A full list of the parameters used for this simulation run is provided in Appendix C and is labeled EXP2.DAT.

The results of the simulation are given in Figs 5.2a and 5.2b. Figure 5.2a shows that the estimates of α and OUR converge very rapidly (within 5 sampling intervals) to the true values of α and OUR. No offset is observed in either estimate after the values of $\hat{\alpha}$ and $\hat{R}$ converge. Figure 5.2b illustrates that the dissolved oxygen concentration, C_{OUT}, settles very rapidly to the setpoint of 2.0 mgO/l. The air flow rate also settles down rapidly to its final value. The magnitude of the oscillations in air flow rate, reflected in corresponding oscillations in C_{OUT}, decrease from the start of the simulation until a simulation time of 5 hours, after which time the magnitude of the oscillations, termed the limit cycle amplitude, remains constant. The decrease in the amplitude of the oscillations indicates that the controller parameters have been tuned.

The second run simulates an aeration reactor at the head of an aeration train. Here, the OUR is higher than at the end of the aeration train. Furthermore, the OUR is not constant, but is assumed to vary sinusoidally over the day. The OUR used was that obtained by Dold and Marais (1987) in their first aeration reactor. The OUR has a mean value of 65 mgO/l/hr with a sinusoidal amplitude of 15 mgO/l/hr. The wavelength of the OUR sine wave is 24 hours. The parameter α was set to vary sinusoidally by 10 percent around the value used in the previous run, Experiment 2. The full set of simulation parameters for this run, Experiment 3, are listed in Appendix C. The results of the simulation are given in Fig. 5.3a and 5.3b. Figure 5.3a illustrates that the dissolved oxygen concentration is suitably controlled. The air flow rate stabilizes rapidly to the required value and subsequently gradually decreases over the 12 hour period simulated, following the decreasing OUR with time. The amplitude of the dissolved oxygen concentration is

FILE USED TO GENERATE THIS DATA : exp2.DAT

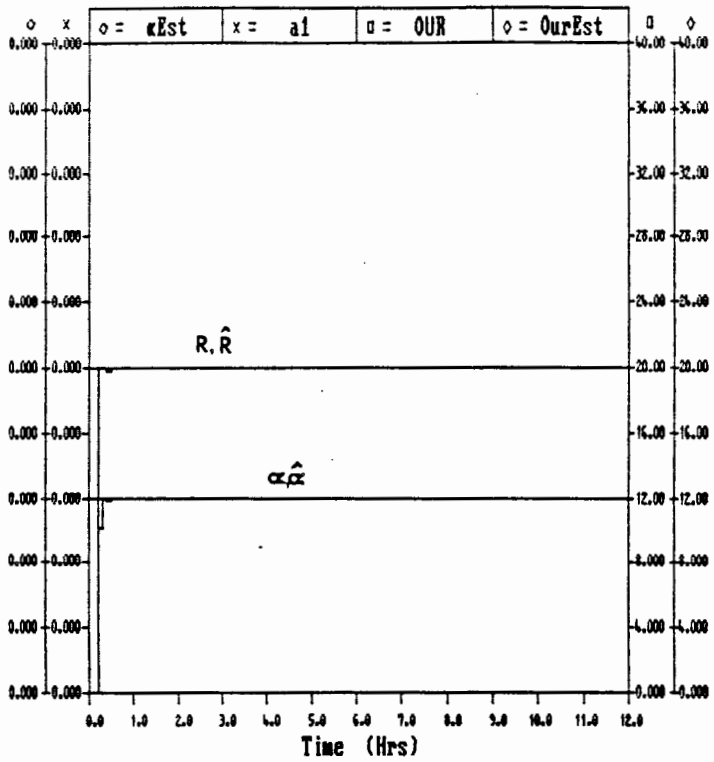

Fig 5.2a (Experiment 2) The true and estimated α and R values in a simulation run in which α and R are constant.

FILE USED TO GENERATE THIS DATA : exp2a.DAT

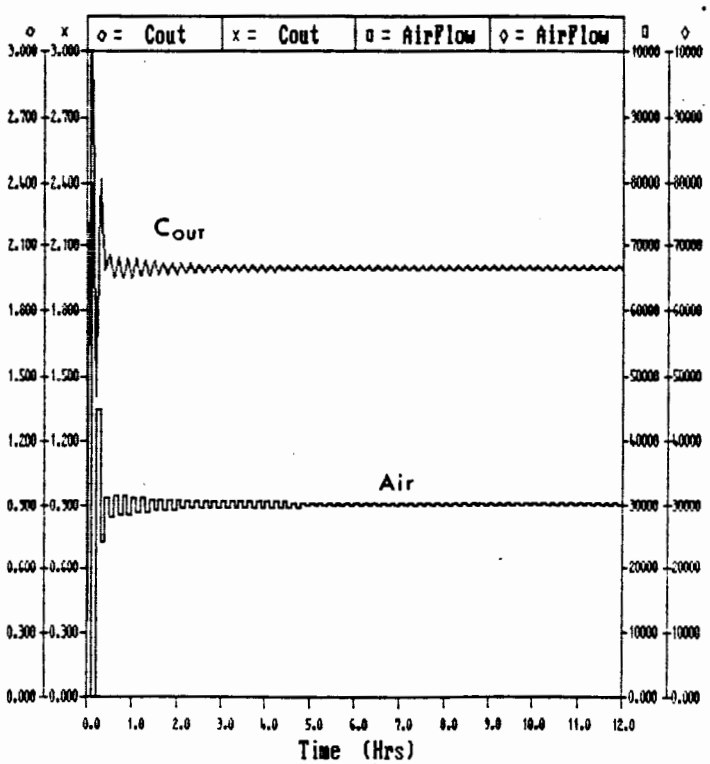

Fig 5.2b (Experiment 2) The airflow rate and dissolved oxygen control over the first 12 hours of a run in which α and R are constant.

FILE USED TO GENERATE THIS DATA : exp3.DAT

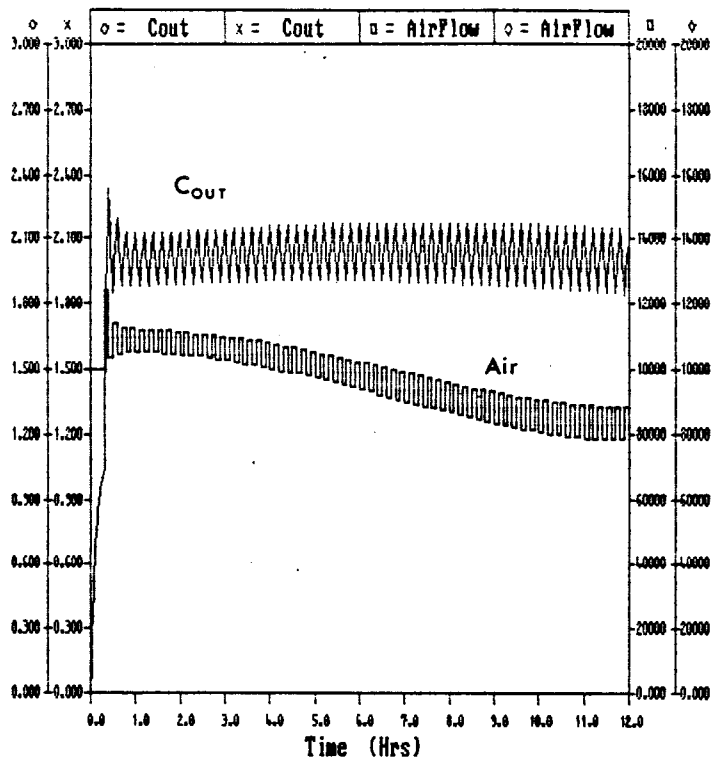

Fig 5.3a (Experiment 3) Airflow rate and dissolved oxygen control over the first 12 hours of a run in which OUR and α vary.

FILE USED TO GENERATE THIS DATA : exp3a.DAT

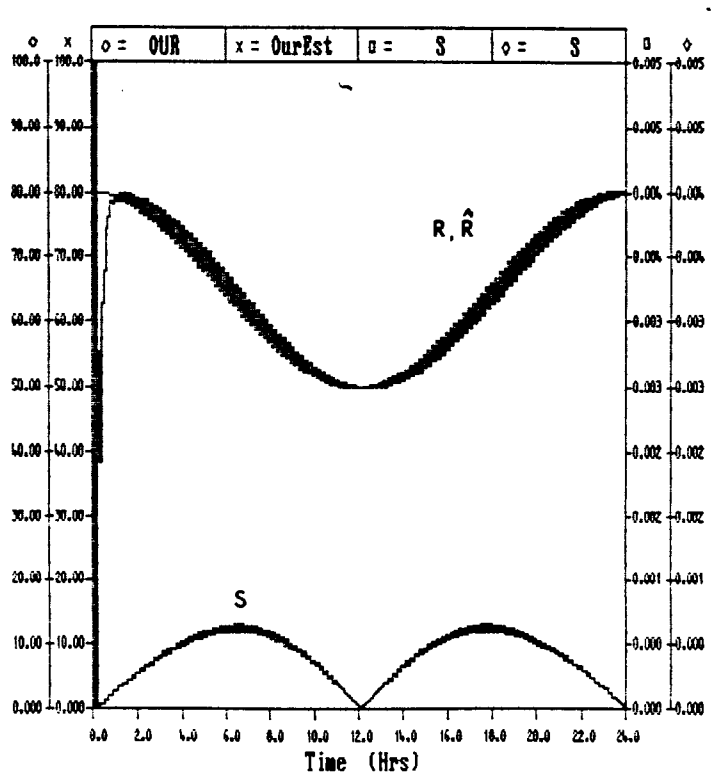

Fig 5.3b (Experiment 3) The dependence of the magnitude of the oscillations of $\hat{R}$ on S.

greater than that of the previous run (see Fig 5.2a.). The reason for this will be explained later in Section 5.2.6. Figure 5.3b shows that $\hat{R}$, the OUR estimate, closely follows the true value of the OUR. However, unlike the constant OUR case of Experiment 2 (Fig 5.2b), $\hat{R}$ oscillates around the true value of the OUR. The magnitude of the oscillations in $\hat{R}$ varies with time. Thus at time = 6.0 hours, the OUR estimate oscillations are approximately 3 mg O/l/hr whereas at time = 12 hours this oscillation has decreased to zero.

Holmberg was able to explain the reasons for the varying magnitude of oscillations in $\hat{R}$. He defined a variable, S, equal to the error in $\hat{\dot{y}}$ due to parameter (i.e. α and R) variation. Mathematically S is expressed as:

$$S = \left| \frac{d}{dt} \dot{y} \right| = \left| \frac{d\dot{y}}{d\theta} \frac{d\theta}{dt} \right| = \left| \varphi^T \dot{\theta} \right|$$

$$= \left| \dot{\alpha} u(C^s - y) - \dot{\hat{R}} \right| \quad .....(5.1)$$

From the development of Eq 5.1 it is apparent that S is also a measure of the sensitivity in $\dot{y}$ with respect to the variations in θ (θ is the matrix $|\alpha \; R|^T$ and φ is the matrix $|u(C^s - y) \; -1|$). The values of S are plotted together with the OUR estimates in Fig. 5.3b. It can be seen that there is a direct relationship between S and the magnitude in the oscillations of $\hat{R}$. Thus at time = 12 hours, $S \approx 0$ and the corresponding oscillation in $\hat{R}$ is also zero. In the previous run (Experiment 2) the value of $\dot{\theta}$ is zero at all times, as α and R are constant. Thus, through Eq 5.1, S is zero at all times and no oscillation in $\hat{R}$ or $\hat{\alpha}$ are observed.

It should be noted that S is a function of both $\dot{\alpha}$ and $\dot{R}$. If α and R vary in phase with one another; that is if $\dot{\alpha}$ and $\dot{R}$ are of the same sign, then the magnitude of S will be small as the terms $\dot{\alpha} \cdot u \cdot (C^s - y)$ and $-\dot{R}$ tend to cancel each other out. If on the other hand, α and R vary out of phase with one another (i.e. $\dot{\alpha}$ and $\dot{R}$ of opposite sign) then S will tend to be large as the terms $\dot{\alpha} u(C^s - y)$ and $-\dot{R}$ will tend to augment one another. The next simulation run (Experiment 4) demonstrates this effect. The simulation conditions of this run are identical to those of the previous

run, Experiment 3, except that the OUR is now 90° out of phase with α. The results are displayed in Fig 5.4. The S wave observed in Fig 5.4 differs from the S wave generated by the previous run (see Fig 5.3b) in several respects :

(i) The values of S are higher in Fig 5.4 than those in Fig 5.3b. The maximum S values are 0.0013 mgO/l/min^2 in Experiment 4 as opposed to 0.0006 mg O/l/min^2 in Experiment 3. The reasons for this have already been outlined. The greater S values have resulted in greater oscillations in $\hat{R}$.

(ii) Although the wavelength of the two S-waves are identical, the times at which the zero values occur are not the same. This is a result of the 90° offset in the OUR variation implemented in Experiment 4. Note that in Experiment 4, unlike Experiment 3, zero values in S do not correspond to either a maximum or minimum value in either the OUR or α.

5.2.2 First order versus Zero order identification

Holmberg (1986) has described two methods for parameter estimation. The first method, termed the 'zero order' method, assumes the parameters α and R to be constant over each sampling interval. The second method, termed the 'first order' method, assumes these parameters to vary linearly over the sampling interval. In order to highlight the differences in the two methods, simulations were carried out at conditions in which the parameters α and R varied; these conditions satisfy the first order method assumptions, but do not satisfy zero order method assumptions. It would be pointless attempting to highlight the differences between the two methods with simulation runs at constant OUR and α values as at these conditions the assumptions of both the zero order and first order identification methods would be satisfied.

An important parameter in either identification technique is the sampling interval. The sampling interval affects the validity of the assumptions made in each technique. For example, the zero order method

FILE USED TO GENERATE THIS DATA : exp4.DAT

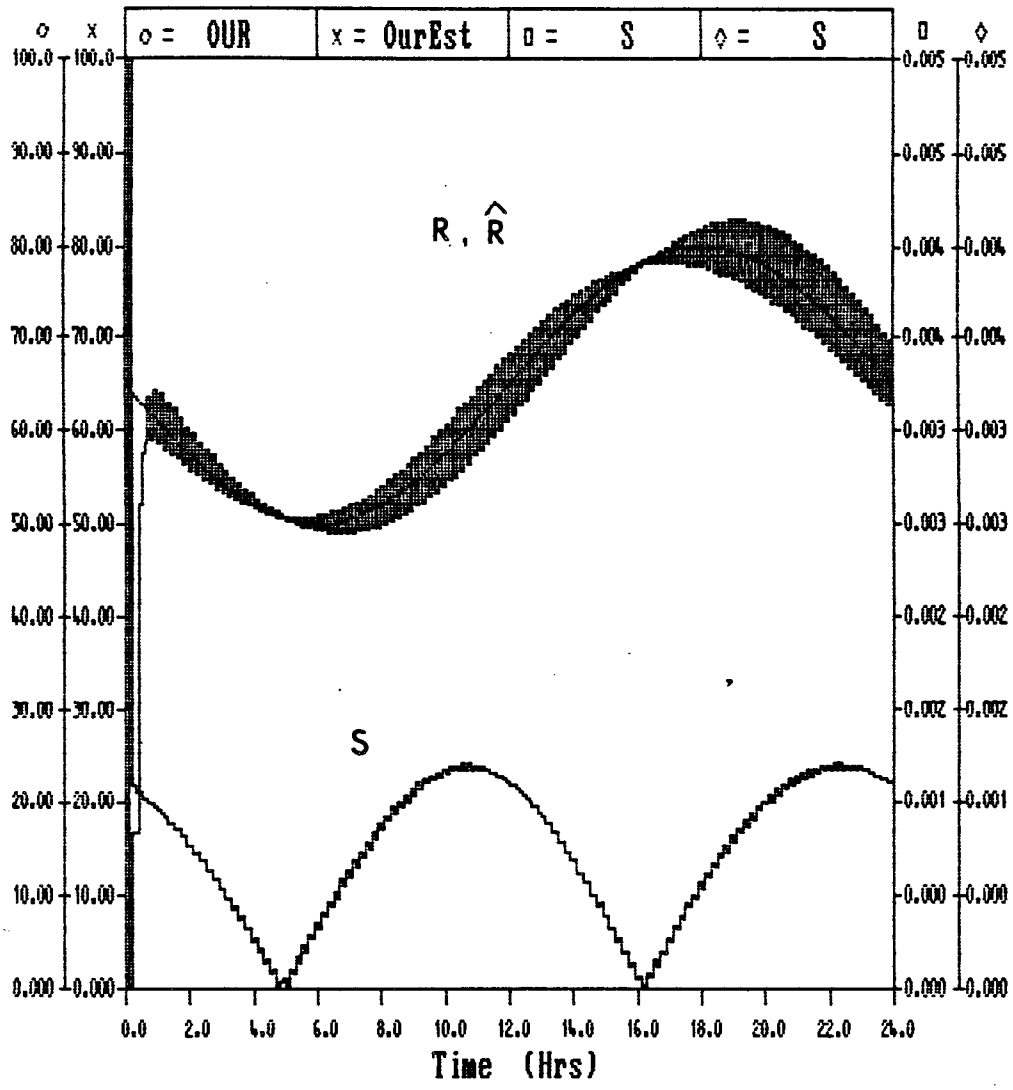

Fig 5.4 (Experiment 4) A simulation demonstrating how an out of phase α and R generate larger S values (compare to Fig 5.3b).

assumption that the parameters are constant over the sampling interval is more valid at small intervals than at large sampling intervals.

The differences between the zero and first order methods was demonstrated through a set of 20 simulation runs. In all 20 runs the parameters α and R vary as in Experiment 3, the simulation run of an aeration reactor at the head of Dold and Marais' (1987) aeration train. The 20 simulation runs differ from one another in only two respects :

(i) Identification technique. Ten simulations used the zero order identification technique, and ten used the first order technique.

(ii) Sampling interval. Ten different sampling intervals are used, varying from one to ten minutes. Although sampling intervals of up to 15 minutes have been used in the DO control of activated sludge processes (Rundqwist, 1986), sampling intervals of this magnitude were not used in the comparison, as no single set of controller parameters could be found to give rise to stable identification and control for the entire 1 to 15 minute sampling interval range.

The results of the simulations are shown in Figs 5.5 and 5.6. Figures 5.5 and 5.6 illustrate the effect of sampling time on the precision of $\hat{R}$ and operation of the DO controller, respectively. The points generated in both graphs are the average values at every sampling point generated over a full 24 hour simulation period.

Figure 5.5 illustrates that, for both zero and first order identification techniques, increasing the sampling interval will decrease the accuracy of the R estimates. This is to be expected because, as the sampling interval increases, less information is obtained from the process as measurements are being made less often. Perhaps what is more suprising is the similarity between the errors in $\hat{R}$ for the first and zero order methods. The zero order method has obtained almost identical results to the first order case at all the sampling intervals examined. In fact it is impossible to distinguish between the accuracies of the two methods from Fig 5.5. Careful scrutinity of the values used to plot Fig 5.5 (Appendix D, Table E.1) reveals that the first order method generates slightly better estimates of $\hat{R}$. The

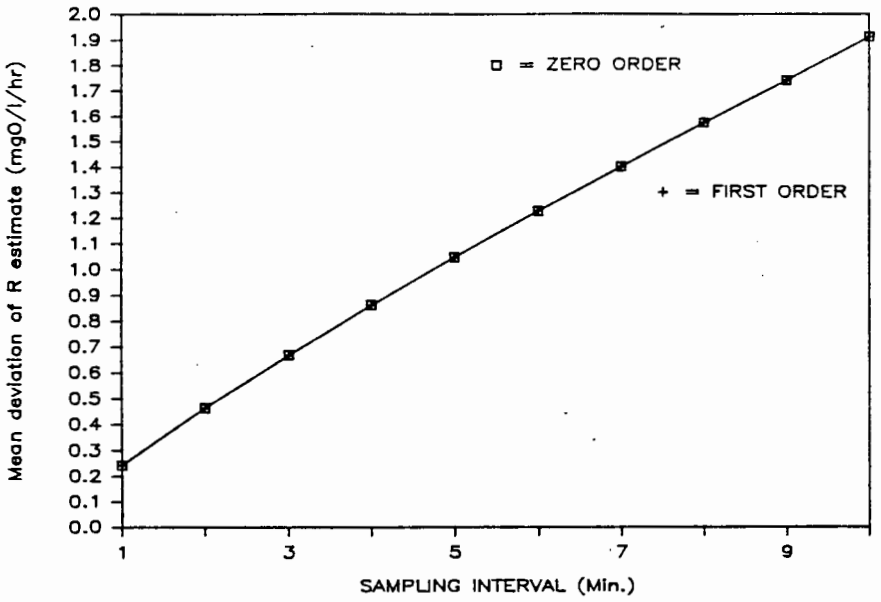

Fig 5.5 (Experiments 5) The effect of the sampling interval on the accuracy of R estimates for a set of runs using first order and zero order identification.

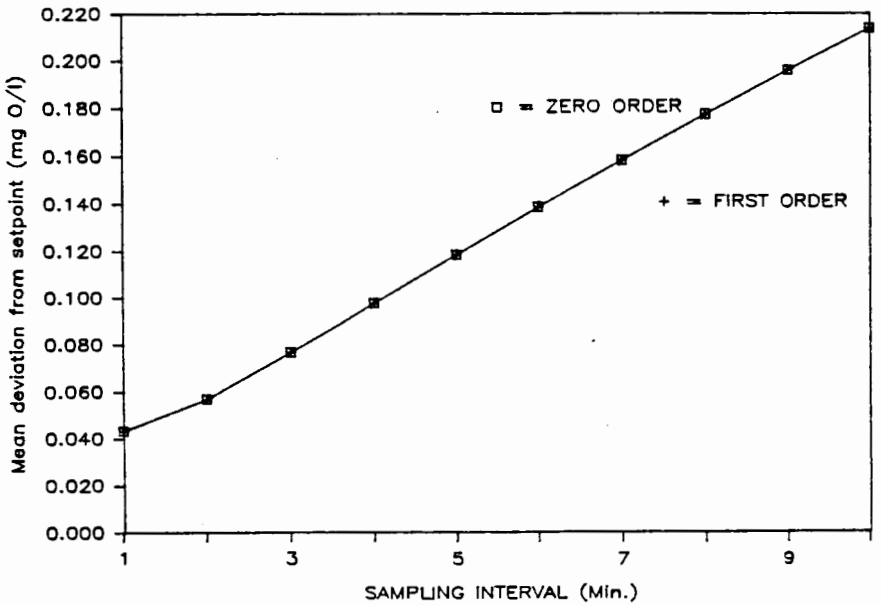

Fig 5.6 (Experiments 5) The effect of the sampling interval on the operation of the DO controller for a set of runs using first order and zero order identification.

difference between the estimates of the first and zero order method increases with increasing sampling interval. However these differences are extremely small, such that at a sampling interval of 10 minutes the difference between the estimates of the two methods is only 0.01 percent. To understand this phenomenon consider the 10 minute sampling interval run. The average rate of change in R is approximately:

$$\hat{R} \approx (\text{max. value of R} - \text{min. value of R})/12 \text{ hours}$$
$$= (80-50)/12 \text{ mgO/l/hr}^2$$
$$= 0.04 \text{ (mgO/l/hr)/min}$$
$$= 0.427 \text{ (mgO/l/hr)/ten minute sampling interval}$$

The average OUR in the above runs was 65 mgO/l/hr and thus the average change in OUR over the sampling interval is approximately :

$$\text{Percent change in OUR over 10-min. interval} = 0.427/65*100\ \%$$
$$= 0.64\%$$

The fact that the OUR changes only by, on average, 0.64% per 10-minute sampling interval means that the zero order assumption that the parameters are constant over the sampling interval is acceptable even when a sampling interval as long as 10 minutes is used. For smaller sampling intervals, the OUR changes by smaller percentages per sampling interval and thus the zero order assumption even more acceptable. This accounts for the apparently identical operation of the two methods. It should be noted that these simulations were carried out at conditions of rapidly varying parameters; conditions that would accentuate the differences between the operation of the first and zero order methods. If these simulations were carried at conditions found at the end of the aeration train, that is at almost constant OUR, the differences between the first and zero order methods would be even smaller. This finding clearly questions Holmberg's (1986) claim that the first order method yields "greatly improved estimates" over the first order method.

Figure 5.6 displays the effect of the sampling interval on the operation of the DO controller for the set of 20 runs. Two conclusions can be drawn from Fig 5.6:

(i) As the sampling interval increases, so the mean deviation in DO concentration from the setpoint increases.

(ii) The operation of the controllers that make use of first order and zero order parameter estimates are indistinguishable from each other. This is due to the fact that the two identification techniques generate, as discussed previously, almost identical parameter estimates.

5.2.3 The effect of the flow term on identification and control

In Holmberg's method it is proposed that the flow term in the DO mass balance (Eq 3.1) usually is very small. For this reason the term was excluded in the parameter estimator model. In all of Holmberg's (1986) simulations, and in all the simulations discussed so far in this chapter, the flow term was also excluded in simulating the response of the real process. Therefore, any problem arising from the assumption that the flow term is negligible would not be apparent. To test the validity of this assumption, Experiment 3 is now repeated, but with the flow term included in the real process model. The flow term is :

$$\text{Flow terms} = \frac{Q \cdot (C_{IN} - C_{OUT})}{V}$$

The values of Q and V used were values obtained from Dold and Marais (1987). An incoming dissolved oxygen concentration of 0.1 mg O/l was assumed. See EXP6.DAT in Appendix C for a full list of all the parameters used in this run.

The results of the run, displayed in Fig 5.7, show that an offset in the OUR estimate results when the Q/V term is included in simulation of the real process (see Fig 5.3b). The offset, however, under normal operation is only of the order of 1 or 2 mg O/l/h.

To quantify the offset, consider the DO mass balance equation:

$$\frac{dC_{OUT}}{dt} = \frac{Q}{V} \cdot (C_{IN} - C_{OUT}) + K_L a \cdot (C^s - C_{OUT}) - R \qquad \ldots\ldots\ldots (4.1)$$

If the process flow terms $Q/V \cdot (C_{IN} - C_{OUT})$ are ignored by the identifier, Eq 4.1 can be rewritten as

FILE USED TO GENERATE THIS DATA : exp6.DAT

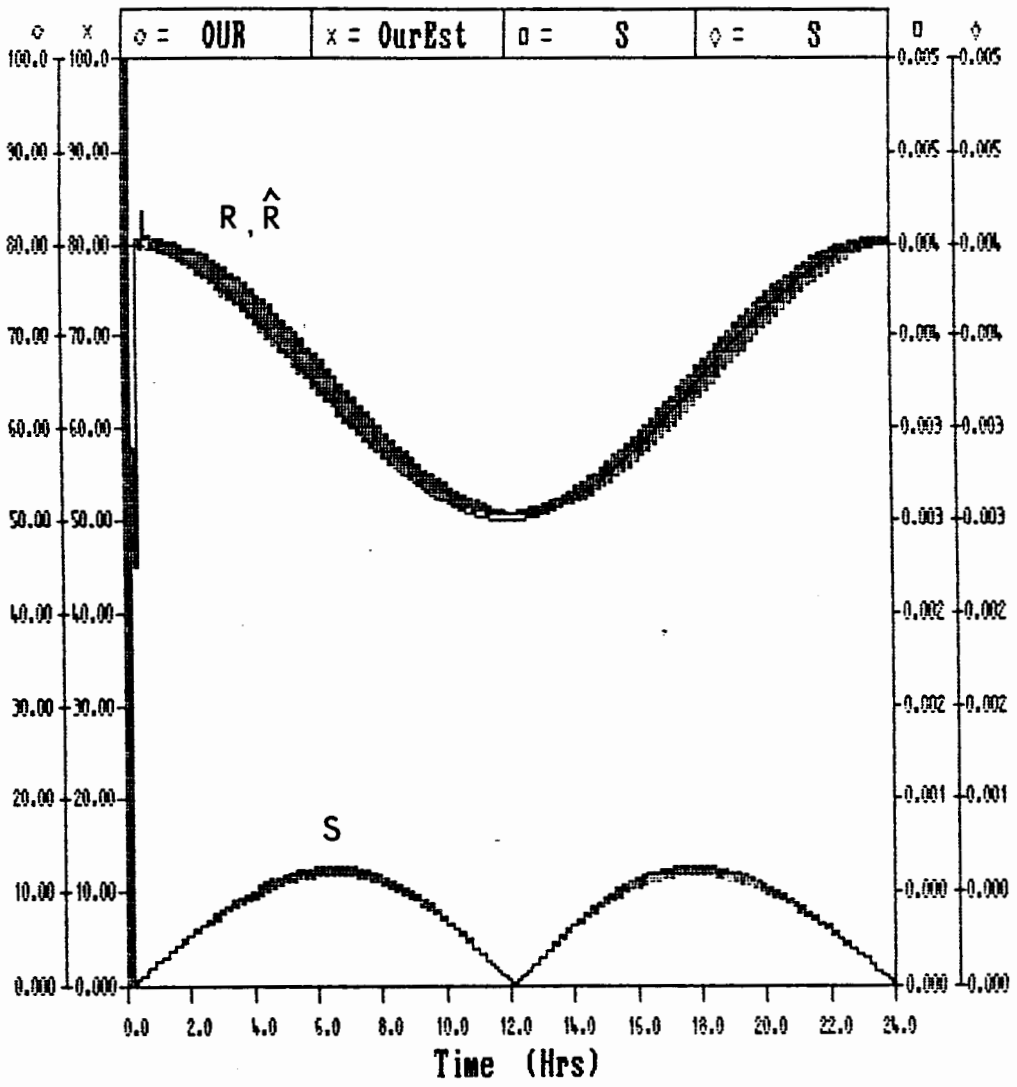

Fig 5.7 (Experiment 6) Effect of flow terms on the simulation of the OUR (Compare to Fig 5.3b).

$$\frac{dC_{OUT}}{dt} = K_L a \cdot (C^S - C_{OUT}) - R' \qquad \ldots\ldots\ldots (5.2)$$

where:

$$R' = R - \frac{Q}{V} \cdot (C_{IN} - C_{OUT}) \qquad \ldots\ldots\ldots (5.3)$$

The offset in the R estimate would therefore equal $Q/V \cdot (C_{IN} - C_{OUT})$. As $C_{OUT} > C_{IN}$, the term is negative, thus making $R' > R$. Therefore the R estimate should be greater than the true R by $Q/V \cdot (C_{IN} - C_{OUT})$. This is confirmed in Fig 5.7 which shows that the estimated R is greater than the true R, and that the offset is:

$$\begin{aligned} \text{Offset due to flow terms} &= Q/V\ (C_{IN} - C_{OUT}) \\ &= \frac{200*10^6\ \text{l/day}}{15*10^6\ \text{l}}\ (0.1 - 2.0) \\ &= -25.3\ \text{mg/l/day} \\ &= -1.1\ \text{mg O/l/hr} \end{aligned}$$

5.2.4 The effect of the assumed $K_L a/F_{AIR}$ relationship

In all of Holmberg's simulations, and in all the simulations discussed so far in this chapter, it has been assumed that the oxygen transfer coefficient, $K_L a$, in the real process is directly proportional to the air flow rate i.e.

$$K_L a = \alpha \cdot F_{AIR} \qquad \ldots\ldots\ldots (5.4)$$

This corresponds to the simplification in the estimator model. However it is likely, especially at high F_{AIR}, that the $K_L a/F_{AIR}$ relation is more accurately described by:

$$K_L a = \alpha \cdot F_{air} + a_2 \qquad \ldots\ldots\ldots (5.5)$$

This is clear from Fig 4.2 which illustrates the $K_L a/F_{AIR}$ curve fits obtained by Goto (1985).

Experiment 7 was run to test the parameter identification and DO control at conditions in which the process $K_L a/F_{AIR}$ was of the form of Eq 5.5 as opposed to the earlier runs when the true process $K_L a$ was directly proportional to the airflow rate as in Eq 5.4.

Values of α and a_2 were obtained from Goto (1985). All other conditions were identical to those of Experiment 3 (Fig 5.3). Figure 5.8a shows that the controller is still able to provide satisfactory DO control. Figure 5.8b shows the true and estimated values of the parameters R and α. The estimated R exhibits a wide offset from the true R value. The estimated α values also exhibits an offset, but which is small.

In the DO mass balance equation:

$$\frac{dC_{OUT}}{dt} = K_L a \cdot (C^S - C_{OUT}) - R \qquad \ldots\ldots\ldots (5.6)$$

If $K_L a = \alpha \cdot u + a_2$ then

$$\frac{dC_{OUT}}{dt} = \alpha \cdot u \cdot (C^S - C_{OUT}) + a_2 \cdot (C^S - C_{OUT}) - R \qquad \ldots\ldots(5.7)$$

$$= \alpha \cdot u \cdot (C^S - C_{OUT}) - R'$$

where

$$R' = R - a_2 \cdot (C^S - C_{OUT})$$

The identifier model equation is

$$\frac{dC_{OUT}}{dt} = \alpha \cdot u \cdot (C^S - C_{OUT}) - R \qquad \ldots\ldots\ldots(5.8)$$

Thus an offset between the true and estimated R values would be anticipated:

$$\text{Offset in } \hat{R} = a_2 \cdot (C^S - C_{OUT})$$

Checking this hypothesis with the values generated in Experiment 7 gives:

$$\text{Offset in } \hat{R} = \left| a_2 \ (C^S - C_{OUT}) \right|$$

FILE USED TO GENERATE THIS DATA : exp7.DAT

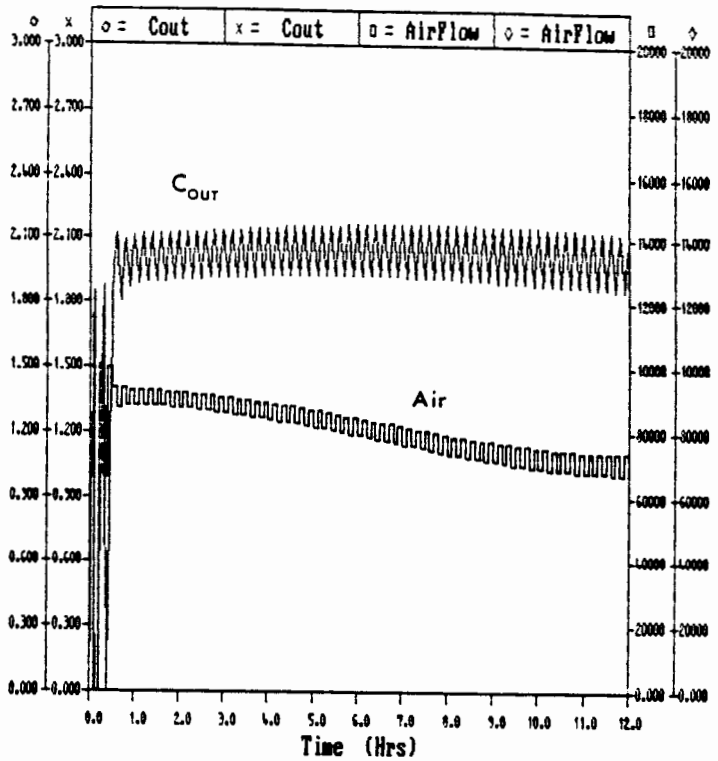

Fig 5.8a (Experiment 7) The DO and airflow rate values for a run in which the real process K_La/F_{AIR} relationship is of the form $K_La = \alpha \cdot F_{AIR} + a_2$.

FILE USED TO GENERATE THIS DATA : exp7.DAT

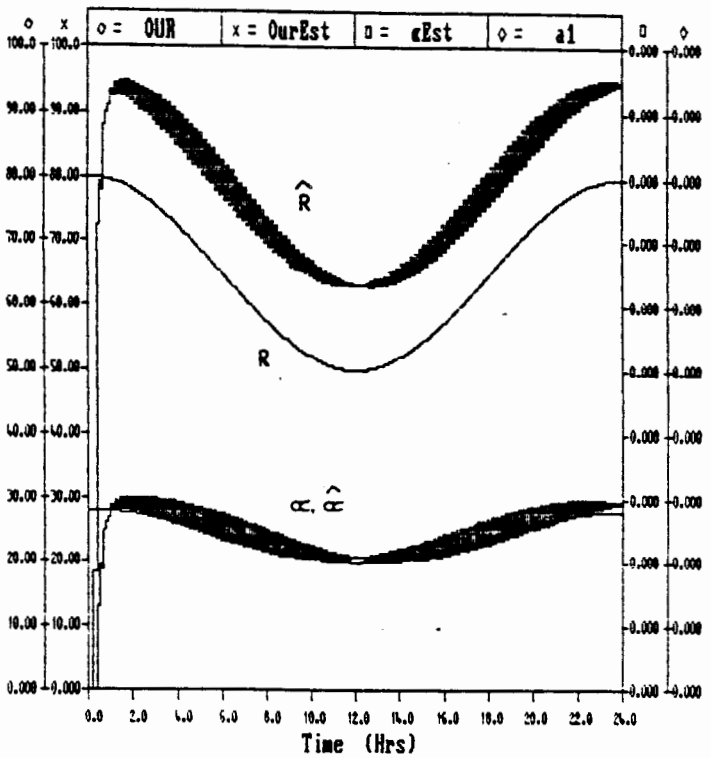

Fig 5.8b (Experiment 7) The true and estimated R and α parameter values for a run in which the real process K_La/F_{AIR} relationship is of the form $K_La = \alpha \cdot F_{AIR} + \alpha 2$.

$$= 0.02256(11.25 - 2.0)$$
$$= 0.208 \text{ mg O/l/min}$$
$$= 12.5 \text{ mg O/l/hr}$$

The calculated $\hat{R}$ offset of 12.5 mg O/l/hr is very close to the observed $\hat{R}$ offset of approximately 14 mg O/l/hr. It should be noted, however, that this explanation does not account for the small offset in $\hat{\alpha}$.

5.2.5 The effect of inaccuracies in C^s

It has been mentioned in Chapter 4 that C^s is a function of pressure and temperature. As C^s is a function of pressure its value changes with depth in an aerator. A range of C^s values thus exist between the surface of the aerator liquid and the base of the aerator. These variations may be compounded by differences in temperature.

Whatever the true average value of C^s, the question was raised as to the effect of an incorrectly assumed average C^s. Experiment 8 was completed by using the same conditions as Experiment 3 (Fig 5.3), expect that 1 mg O/l was added to the true C^s value used by the estimator/controller. The results of the simulations are displayed in Figs 5.9a and 5.9b. Figure 5.9b illustrates the effect of the incorrectly assumed average C^s values on the parameters estimates. It can be concluded from Fig 5.9b that an incorrectly assumed Cs will create an offset in both $\hat{\alpha}$ and $\hat{R}$. For a discrepancy of 1 mg O/l/in C^s, $\hat{\alpha}$ values contain offsets of up to 50% whereas the $\hat{R}$ estimates are very small, in the order of less than 1 mg O/l/hr.

In explaining the offset in R as before, consider

$$\frac{dC}{dt} = K_L a \cdot ((C^s + x) - C_{OUT}) - R \quad \ldots\ldots\ldots (5.9)$$
$$= K_L a \cdot (C^s - C_{OUT}) - R + K_L a \cdot x$$
$$= K_L a \cdot (C^s - C_{OUT}) - R'$$

where x = inaccuracy in C^s estimates

$R' = R - K_L a \cdot x$

$= R - \alpha \cdot u \cdot x$

FILE USED TO GENERATE THIS DATA : exp8.DAT

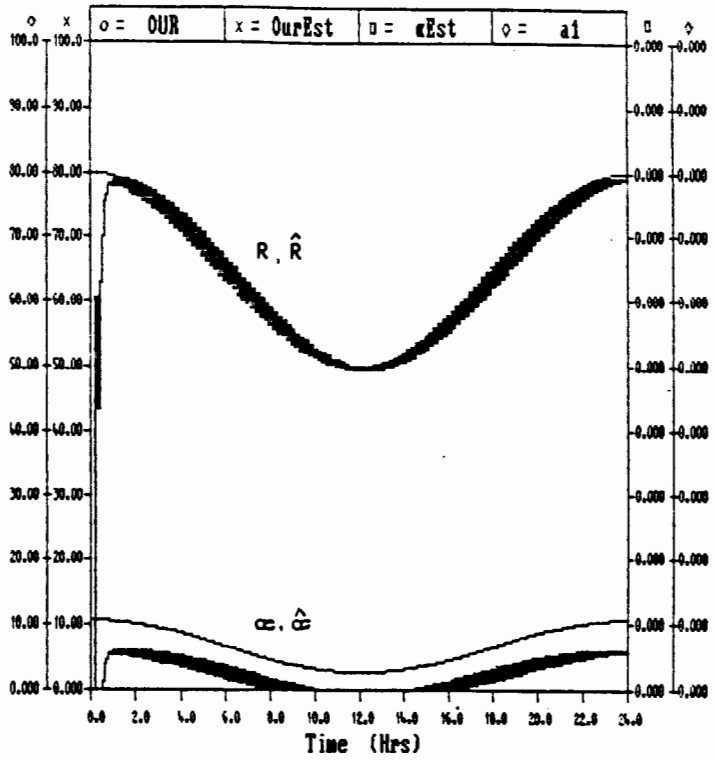

Fig 5.9a (Experiment 8) Dissolved oxygen and airflow rate profiles of runs in which a C^s offset of 1 mg O/l was utilised by controller/estimator.

FILE USED TO GENERATE THIS DATA : exp8.DAT

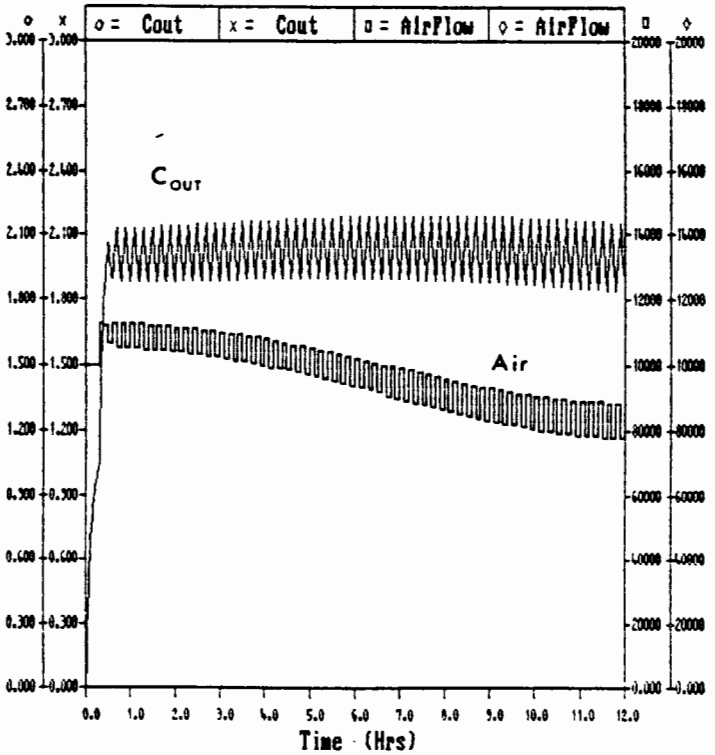

Fig 5.9b (Experiment 8) The true and estimated R and α parameter values for a run in which a C^s offset of 1 mg O/l was utilised by controller/estimator.

The offset in R is $\alpha \cdot u \cdot x$. Substituting values for Experiment 8 gives

$$\text{offset in } R \approx |\alpha \cdot u \cdot x|$$
$$= 1.2*10^{-6}*100000*1$$
$$= 0.12 \text{ mg } O/l/hr$$

which is approximately what is observed in Fig 5.9b. Again as in the flow terms section and K_La/F_{AIR} section no similar explanation for the offset in α can be proposed.

5.2.6 The effect of controller parameters on parameter identification and control

A case study was used to illustrate the effect of the controller parameters on identification and DO control. The case study was carried out at conditions similar to Experiment 3: that is, a high and fluctuating OUR, no flow terms and a proportional relationship between α and F_{AIR}. The results of this case study, Experiment 9, are given in Fig 5.10 which displays the values of the following four variables :

(i) d - the tuned controller constant
(ii) S - the error in $\hat{y}$ due to α and R variation.
(ii) C_{OUT}
(iv) $\hat{R}$ - the estimated value of R.

At the start of the simulation the oscillations in C_{OUT} are large as a result of the large initial value of the d controller parameter (see Eq 3.47). Concomitant with the large variations in in C_{OUT} are very small oscillations in the estimated R values. The magnitude of oscillations in $\hat{R}$ vary in phase with the magnitude of S (as discussed in Section 5.2.1). However at low values of S, such as at t = 11 to 12 hours, conditions are reached in which the conditions for tuning d are satisfied, and thus the value of d is decreased accordingly. The decreased d value causes smaller oscillations in the C_{OUT} values and larger oscillations in $\hat{R}$. Thus at t = 13 hours C_{OUT} oscillates between 1.85 and 2.1 mgO/l, whereas before the tuning of d, C_{OUT} oscillates between 1.8 and 2.15 mgO/l. The oscillations in $\hat{R}$ increase with the

FILE USED TO GENERATE THIS DATA : exp9.DAT

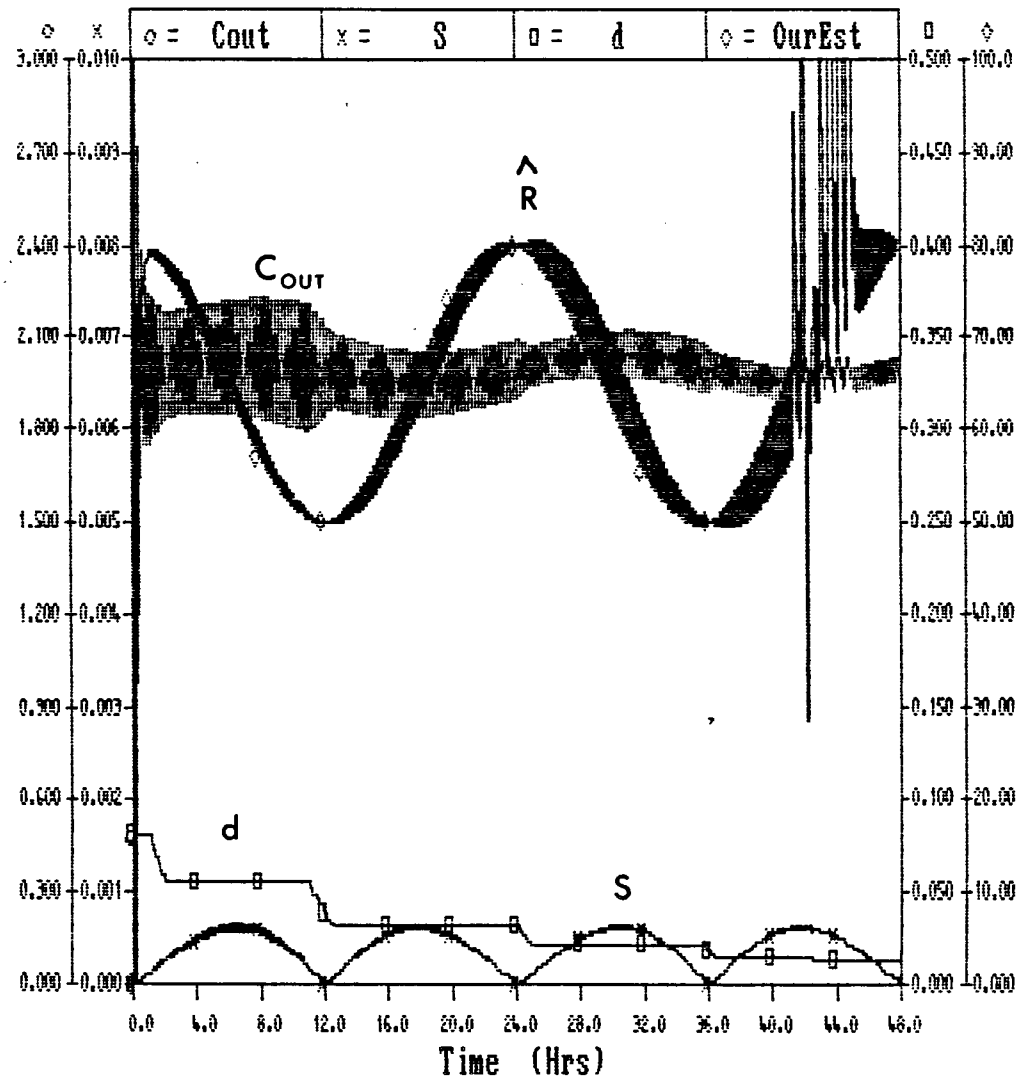

Fig 5.10 (Experiment 9) Results of the case study showing the interaction between the tuned controller constant and the
(i) estimates of R, $\hat{R}$
(ii) control of the DO.

decreasing oscillations in C_{OUT}. This dependence of the $\hat{R}$ and C_{OUT} oscillations on the d controller parameter value clearly demonstrates the contradictory demands of the identifier and the controller.

The d controller parameter is tuned whenever the S value is low. The d controller parameter thus decreases with time, resulting in smaller and smaller oscillations in C_{OUT} and larger and larger oscillations in $\hat{R}$. Eventually at t = 45 hours the oscillations in C_{OUT} have decreased to such an extent that the estimator becomes unstable, resulting in wild oscillations in $\hat{R}$. The controller is formulated in such a manner that it is unable to increase the d-parameter to counter these wild oscillations. The abating of the oscillations at t=46 to t = 48 hours is due to the low value of S at that time, and therefore as soon as the value of S increases the wild oscillations will re-commence. The tuning ability of the self tuning controller is thus limited, as the tuner only tunes one of four controller constants, and as illustrated above, only does so with limited success.

5.3 MODIFICATIONS TO HOLMBERG'S METHOD

Certain shortcomings have been identified in the estimator as proposed by Holmberg. In this section extensions to Holmberg's method are proposed to overcome some of these problems.

5.3.1 Accounting for flow terms

Experiment 6 in Section 5.2.3 demonstrated that Holmberg's method was unable to account for the flow terms, and thus an offset in the estimation of $\hat{R}$ occurred. In order to account for the flow terms, extensions to the theory are required. Also, knowledge of the flow rate, Q, a reactor volume, V, will be required.

Consider the controller model of the process to be

$$\frac{dC_{OUT}}{dt} = \frac{Q}{V}\cdot(C_{IN}-y) + \alpha\cdot u(C^{S}-y) - R \qquad \text{.....(5.10)}$$

where $y = C_{OUT}$ (process output)

$u = F_{AIR}$ (process input)

Putting $a = -\alpha \cdot u - Q/V$ .....(5.11)

and $v = \alpha \cdot u \cdot C^S - R + Q/V * C_{IN}$ .....(5.12)

transforms the nonlinear equation to the linear equation:

$$\frac{dy}{dt} = a \cdot y + v \qquad .....(3.9)$$

Equations 5.11 and 5.12 differ from Holmberg's method in only one aspect: the final flow term is not included in Eqs 3.7 and 3.8.

As before it is possible to re-write Eq 5.10 in matrix format :

$$\dot{y} = \left[\varphi^T\right] \cdot \left[\theta\right] + \left[K\right] \qquad .....(5.13)$$

where as before

$$\varphi = \begin{bmatrix} u \cdot (C^S - y) \\ -1 \end{bmatrix} \qquad .....(3.24)$$

and

$$\theta = \begin{bmatrix} \alpha \\ R \end{bmatrix} \qquad .....(3.25)$$

but

$$K = \left[Q/V * (C_{IN} - C_{OUT})\right] \qquad .....(5.14)$$

Equation 5.13 differs from that used by Holmberg by the last K - matrix term (see Eq 3.23).

The controller response can also be modified to account for the flow terms. The controller response becomes :

$$u = \frac{\hat{R} - Q/V\cdot(C_{IN}-y) + a_c.e + d.sign(e)}{\hat{\alpha}\cdot(C^S - y)} \quad .....(5.15)$$

Compare this form of the controller response to Eq 3.47.

The theory behind the inclusion of the flow terms is implemented by making the following changes to Holmberg's method:

Changes to zero order method

- estimate a through Eq 5.11 instead of Eq 3.7
- estimate $\dot{y}$ through

$$\hat{\dot{y}}(kh) = \frac{y(kh+h) - y(kh)}{h^*} + Q/V.(C_{IN} - y(kh)) \quad .....(5.16)$$

instead of Eq 3.21.

Changes to first order method

- estimate a through Eq 5.11 instead of Eq 3.7
- estimate $\dot{Q} = (Q[0]-Q[1])/h$
- estimate $\dot{a}$ through

$$\dot{a} = -\dot{\alpha}\cdot u - Q/V \quad .....(5.17)$$

instead of through Eq 3.8.

- estimate $\dot{v}$ through

$$\dot{v} = \dot{\alpha}\cdot u\cdot C^S - \dot{R} + Q/V \quad .....(5.18)$$

instead of through Eq 3.39

- estimate $\dot{y}$ through

$$\hat{\dot{y}}(kh) = \frac{y(kh+h) - y(kh) - (\hat{a}\cdot I_1\cdot y(kh) + \hat{v}\cdot I_2)}{h^*} + Q/V\cdot(C_{IN}-C_{OUT})$$

instead of through Eq 3.35.

The experiment that brought the effect of the flow terms on parameter estimation to the fore, Experiment 6, is now re-run using the new identification method. Figure 5.11 clearly shows that the offset in $\hat{R}$, clearly apparent in Fig 5.7, had been eliminated through the use of this extended method.

5.3.2 Accounting for the assumed $K_L a/F_{AIR}$ relationship

Experiment 7 in Section 5.2.4 demonstrated that if the real process $K_L a/F_{AIR}$ relation was of the form

$$K_L a = \alpha * F_{AIR} + a_2 \qquad \text{.....(5.5)}$$

with a_2 non-zero, while the parameter estimator assumed $a_2=0$, then large offsets in $\hat{R}$ occurred. In order to account for these offsets, extensions to the theory are required. The theoretical extensions proposed in this section will not include, for reasons of clarity, the flow term extensions proposed in Section 5.3.1, although the two extensions are readily combined (and have been in the simulation program). Consider the controller model of the process to be

$$\frac{dC_{OUT}}{dt} = (\alpha \cdot u + a_2) \cdot (C^s - y) - R \qquad \text{.....(5.19)}$$

where $y = C_{OUT}$ (process output)

$u = F_{AIR}$ (process input)

Putting $a = -\alpha \cdot u - a_2$ .....(5.20)

and $v = \alpha \cdot u \cdot C^s - R + a_2 . C^s$ .....(5.21)

transforms the nonlinear equation to the linear equation:

$$\frac{dy}{dt} = a \cdot y + v \qquad \text{.....(3.9)}$$

Equations 5.20 and 5.21 differ from Holmberg's method in only one aspect: the final term containing the a_2 variable is not included in Eqs 3.7 and 3.8.

FILE USED TO GENERATE THIS DATA : exp10.DAT

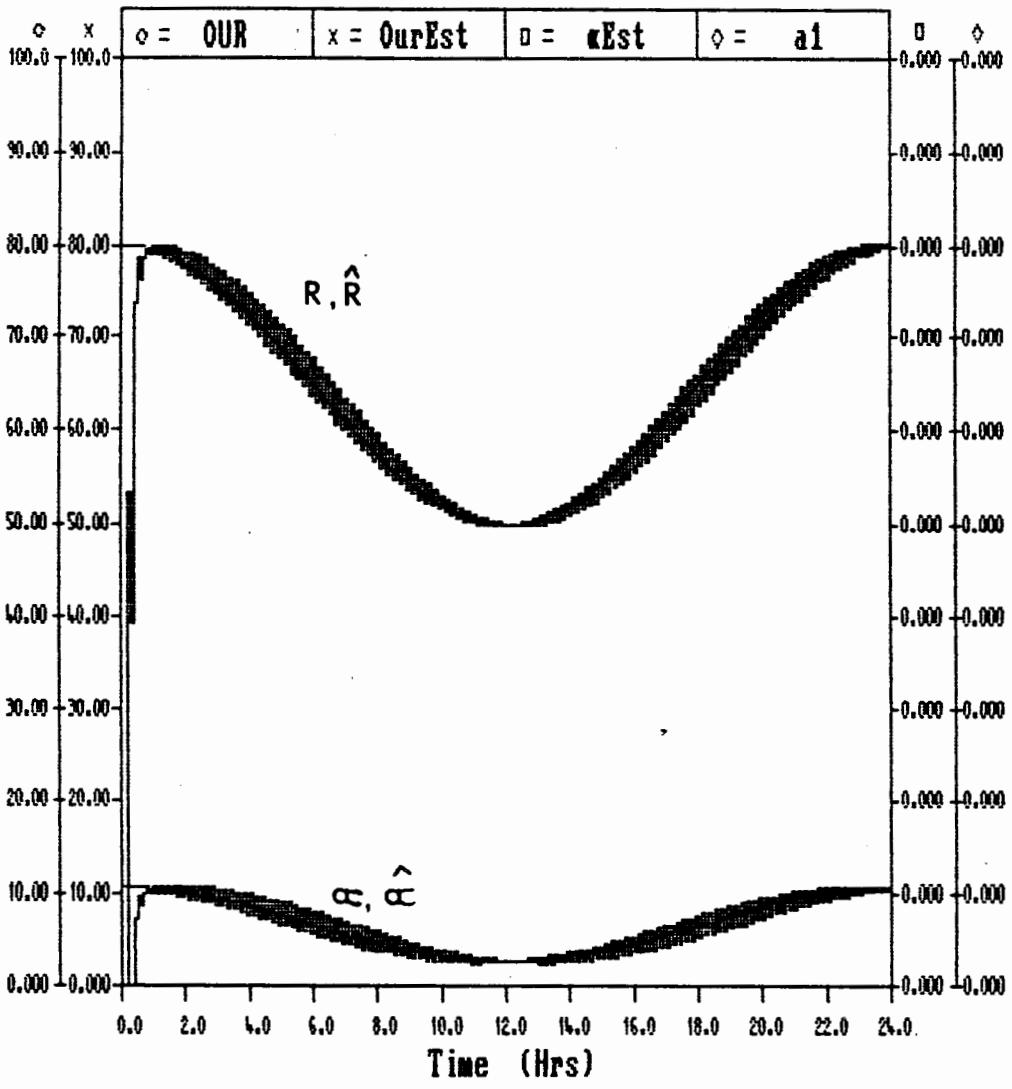

Fig 5.11 (Experiment 10) Experiment demonstrating how the parameter estimate offset caused by the flow terms can be eliminated using the proposed modified identifier. Compare this figure to Fig 5.7.

As before it is possible to re-write Eq 5.10 in matrix format :

$$\dot{y} = \left[\varphi^T\right] \cdot \left[\theta\right] \qquad \text{.....(5.22)}$$

where the φ^T and θ matrices now have an extra term :

$$\varphi = \begin{bmatrix} u\cdot(C^s - y) \\ -1 \\ C^s - y \end{bmatrix} \qquad \text{.....(5.23)}$$

and

$$\theta = \begin{bmatrix} \alpha \\ R \\ a_2 \end{bmatrix} \qquad \text{.....(5.24)}$$

The controller response is also modified to :

$$u = \frac{\hat{R} + a_2\cdot(C^s - y) + a_c.e + d.wave\_function}{\hat{\alpha}\cdot(C^s - y)} \qquad \text{.....(5.25)}$$

so as to account for the extra a_2 parameter and ensure the closed loop system is of the form :

$$\frac{dy}{dt} = \frac{-de}{dt} = e + wave\_function \qquad \text{.....(5.26)}$$

The deadbeat estimator solves for the parameters by solving a set linear of linear algebraic equations. In order to ensure a solution to the set of equations, that is, in order to ensure that a non-singular solution to the set of equations was available, Holmberg introduced the sign(e) function that ensured that the airflow u oscillated and changed at every sampling interval. However, now that there are three process parameters to identify, (α, R and a_2), the sign(e) wave-function term must be

modified so that the air flow rate is different at three successive sampling instants. The new wave -function term used is

$$\text{wave\_function} = \begin{cases} -1 & \text{for first sampling interval} \\ -1/3 & \text{for second sampling interval} \\ -1 & \text{for third sampling interval} \\ 1/3 & \text{for fourth sampling interval} \end{cases}$$

Figure 5.12 illustrates the closed loop behaviour in which the new wave function is utilised. This can be compared to Fig 3.3 which gives the closed loop response, under identical conditions, using Holmberg's sign(e) wave function term.

The following changes to the implementation of Holmberg's zero and first order methods are required:

Changes to zero order method

- estimate a through Eq 5.20 instead of Eq 3.7
- the φ matrix contains an extra row. Update φ through Eq 5.23 instead of Eq 3.24.
- The estimation of the parameters is now :

$$\begin{bmatrix} \\ \theta \\ \\ \end{bmatrix} = \begin{bmatrix} \varphi_1^T \\ \varphi_2^T \\ \varphi_3^T \end{bmatrix}^{-1} \cdot \begin{bmatrix} \dot{y}_1 \\ \dot{y}_2 \\ \dot{y}_3 \end{bmatrix} \qquad \text{.....(5.27)}$$

instead of Eq 3.27.

Changes to first order method

- estimate $\dot{a}$ as well as $\dot{R}$ and $\dot{\alpha}$ in the same way that $\dot{R}$ and $\dot{\alpha}$ are estimated in previous methods.
- estimate a from Eq 5.20 instead of Eq 3.7

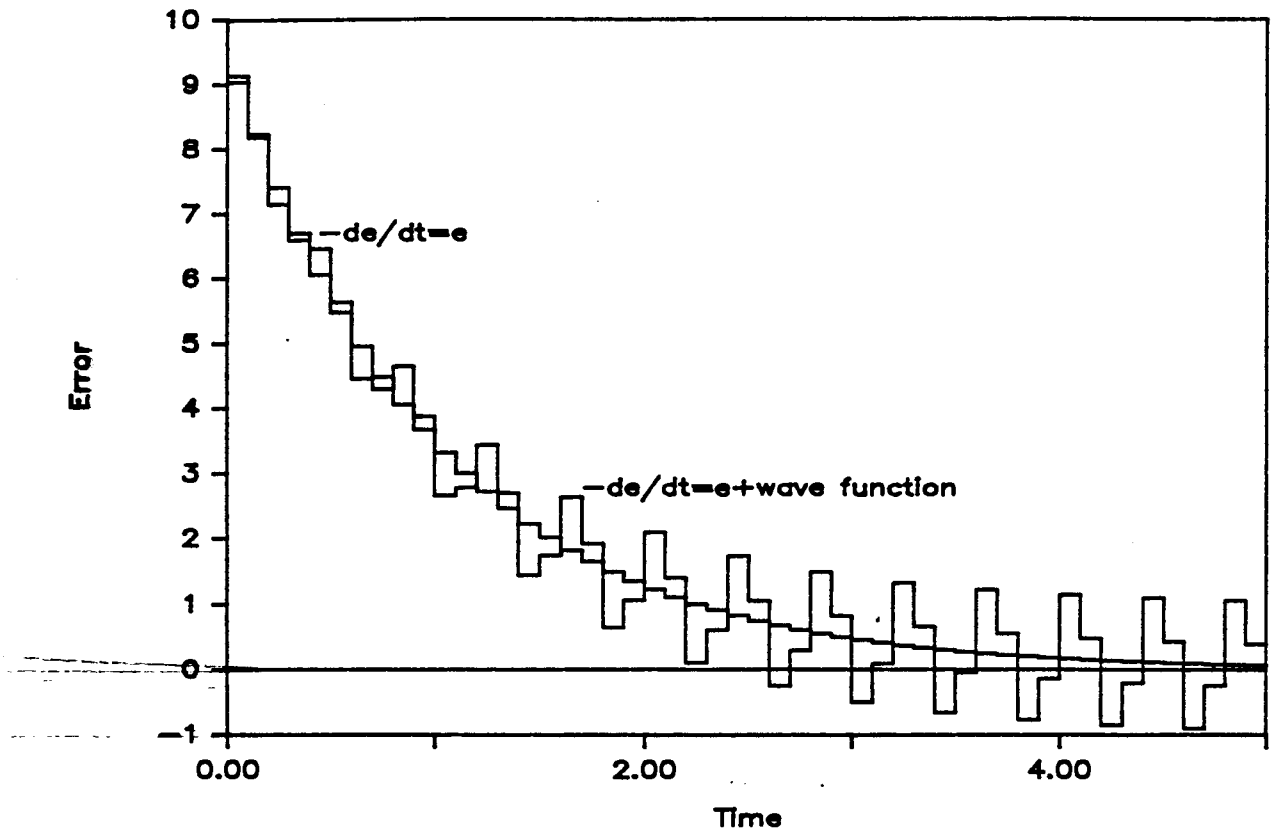

Fig 5.12 The effect of the new wave function term on the closed loop behaviour.

- estimate $\dot{a}$ from

$$\dot{a} = -\dot{\alpha} \cdot u - \dot{a}_2 \qquad \text{.....(5.28)}$$

instead of through Eq 3.8.

- estimate $\dot{v}$ through

$$\dot{v} = \dot{\alpha} \cdot u \cdot C^S - \dot{R} + \dot{a}_2 \cdot C^S \qquad \text{.....(5.29)}$$

instead of through Eq 3.39

- estimation of the parameters is through :

$$\begin{bmatrix} \varphi_1^T \\ \varphi_2^T \\ \\ \varphi_3^T \end{bmatrix} \cdot \hat{\theta} = \begin{bmatrix} \hat{y}_1 + \varphi_1^T \cdot \hat{\theta}_1 \cdot h \\ \hat{y}_2 + \varphi_2^T \cdot \hat{\theta}_2 . 2h \\ \\ \hat{y}_3 + \varphi_3^T \cdot \hat{\theta}_3 . 3h \end{bmatrix} \qquad \text{.....(5.30)}$$

instead of through Eq 3.42

The experiment that brought the effect of the an incorrectly assumed $K_L a/F_{AIR}$ relationship to the fore, Experiment 7, is now re-run using the new adopted identification method. Figure 5.13 clearly shows that the offset in $\hat{R}$, clearly apparent in Fig 5.8, has been eliminated through the use of this extended method that takes the modified $K_L a/F_{AIR}$ relationship into account. Although the offset has been eliminated through this method, the amplitude of the oscillations in the parameter estimates has increased. Furthermore the method initially generates unstable estimates of OUR and a_2. It should be remembered however that the controller parameters used in the simulation of Experiment 11 are not ideal, as they were merely chosen to be identical to those of Experiment 7 so as to provide a meaningful comparison with Experiment 7. Performance can be improved by adjusting controller parameters.

5.4 THE PROBLEM OF DEAD-TIME

Systems such as the activated sludge process that involve the transportation of fluids often exhibit control problems due tothe dead-time inherently associated with these processes. To analyze the effect

FILE USED TO GENERATE THIS DATA : exp11.DAT

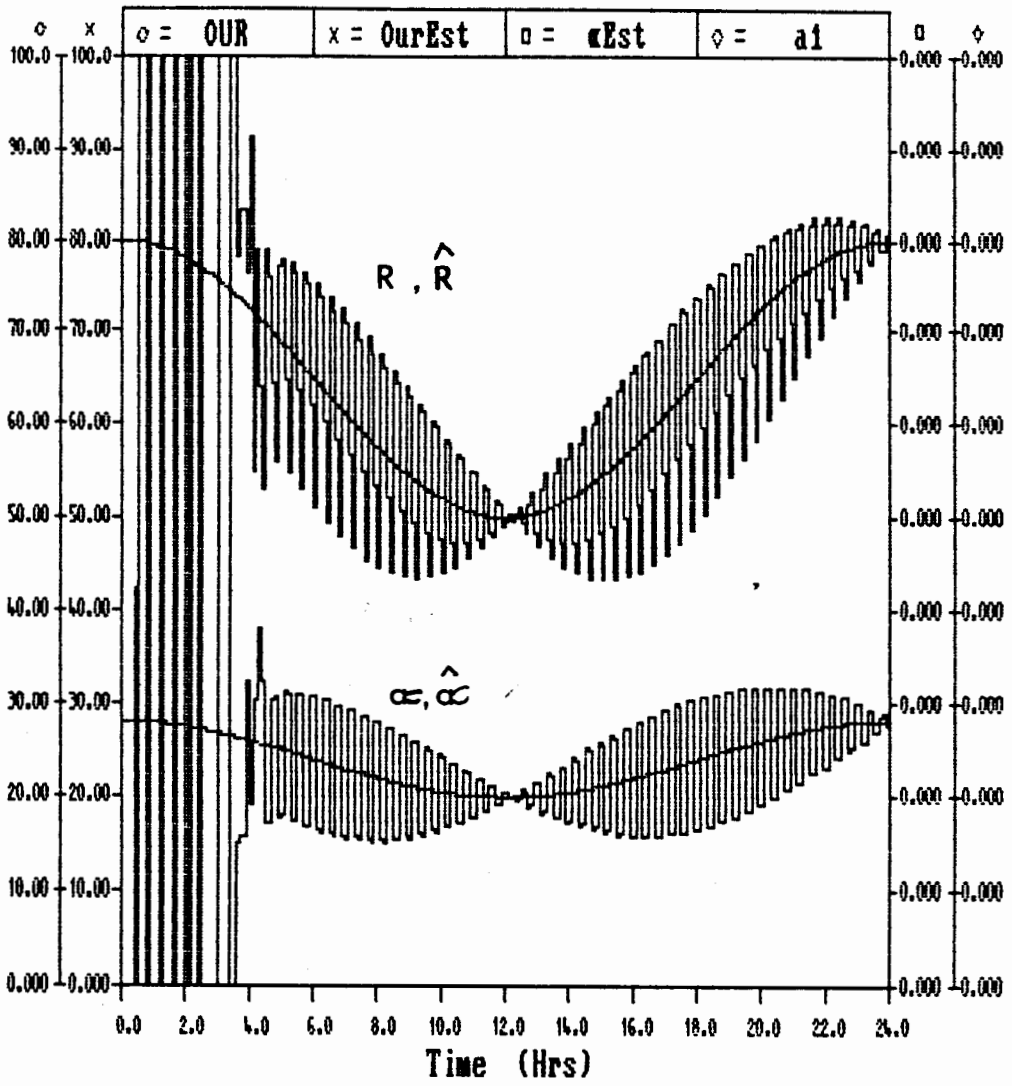

Fig 5.13 (Experiment 11) Experiment demonstrating how the parameter estimate offset caused by an incorrectly assumed proportional $K_L a/F_{AIR}$ relationship can be eliminated by changing the assumed $K_L a/F_{AIR}$ relationship.

of dead-time on parameter identification, a series of runs were completed at different sampling intervals, each with differing amounts of dead-time. The process conditions of Experiment 3 were used for all the runs. A parameter set of one of the runs is listed in Appendix C as EXP12.DAT. The results of the runs are displayed in Fig 5.14.

Figure 5.14 shows that the offset from the true R mean value of 65mgO/l/hr is dependent on both the dead-time and the sampling interval used. The first trend apparent from the graph is that for a given sampling interval, the greater the dead-time, the greater the offset in the estimate of R. The second trend is that the greater the sampling interval, the less the offset for a given dead-time.

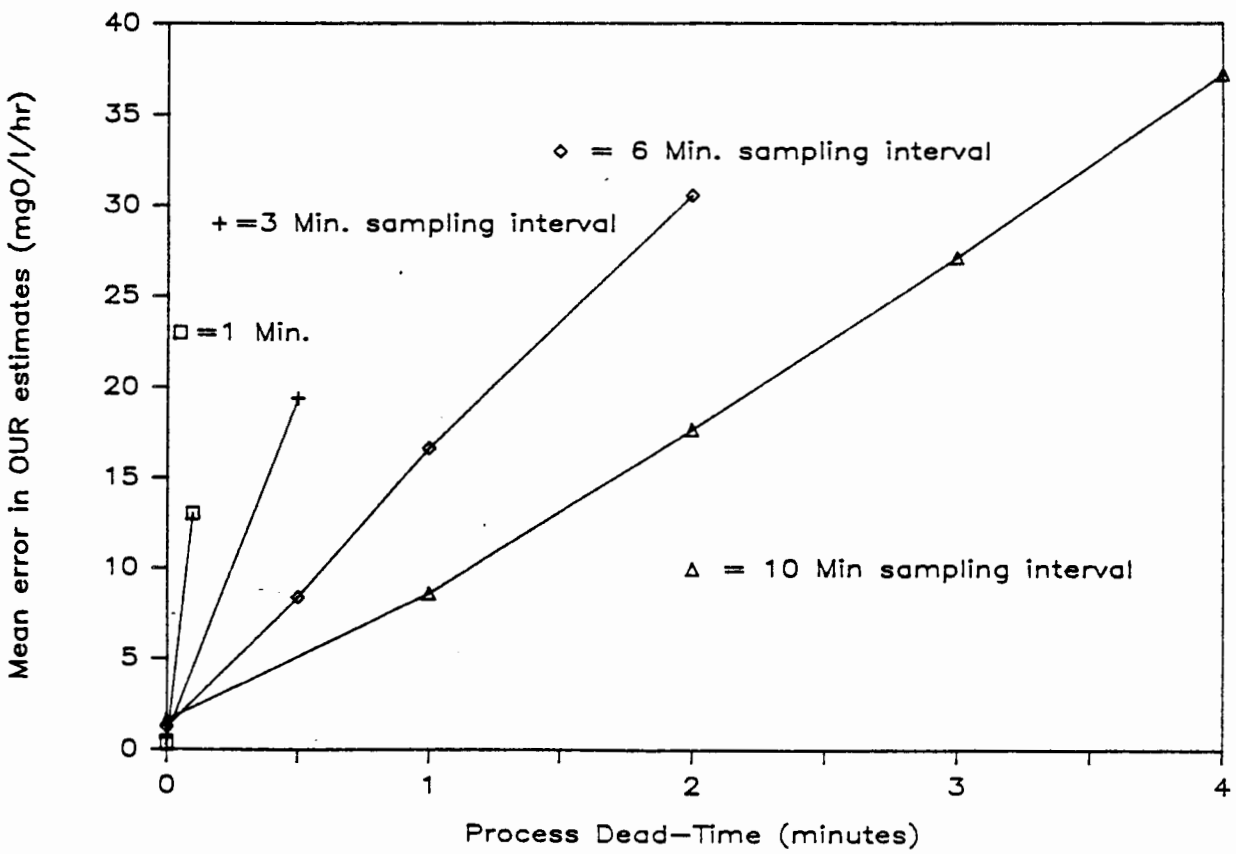

Fig 5.14 A sample run illustrating the effect of deadtime on the $\hat{R}$ estimates at various sampling intervals.

CHAPTER SIX

CONCLUSIONS

The objective of this investigation was to evaluate Holmberg's method for simultaneous dissolved oxygen control and parameter estimation. The method adopted for evaluating the system was through simulations of controlled process behaviour. The following conclusions may be drawn from the results :

(i) The simulation program was shown to predict the results presented by Holmberg (1986) very closely.

(ii) Simulations were conducted in which the α and OUR parameters of the real process were held constant. These conditions are encountered at the end of an aeration train. Results indicated that under such conditions Holmberg's estimator converged rapidly and without offset to the true parameter values. The dissolved oxygen (DO) control was also effective.

(iii) Simulations were conducted in which the α and OUR parameters of the real process were assumed to vary in a sinusoidal fashion; the amplitude of the OUR fluctuation was similar to that encountered in practice at the head of an aeration train. Under these circumstances the parameter estimates converged rapidly to the true values but the estimates now oscillated about the true values. The magnitude of the estimate oscillations were shown to be dependent on a parameter, S, that Holmberg had defined. The DO control was effective.

(iv) Holmberg (1986) proposed two methods for parameter estimation. The first method, termed the "zero order" method assumes the α and OUR parameters to be constant over each sampling interval. The second method, termed the "first order" method assumes the α and OUR parameters to vary linearly over the sampling interval. Simulations in which the sampling interval ranged from 1 to 10

minutes demonstrated that the two methods yield virtually indistinguishable parameter estimates and DO control. This is at variance with Holmberg's observation that the first order method yields "greatly improved" estimates.

(v) Holmberg's estimator assumes the flow terms of the real process DO mass balance to be negligible. If the flow terms are included in simulation of the real process, but excluded from the estimator model, offsets occur in the values of the parameter estimates. Nevertheless, the dissolved oxygen control is effective.

(vi) In Holmberg's simulations it was assumed that in the real process, the oxygen transfer coefficient, K_La, is directly proportional to the air flow rate and that the relation passes through the origin. However, Goto (1985) found that a linear relationship, but not passing through the origin, best described the K_La/air flow rate relationship. If the real process K_La/air flow rate relationship was modelled in the form proposed by Goto (1985), Holmberg's estimator was shown to yield large offsets in the estimated values of the parameters, especially the OUR. DO control was still satisfactory.

(vii) An incorrect saturation dissolved oxygen concentration, C^s, was shown to cause offsets in the estimates of the OUR and α. The offset in the OUR estimates was small whereas the offset in the α estimate was large.

(viii) Holmberg's observation that the objectives of the DO controller and the parameter estimator are contradictory was shown to be correct. At given conditions, improving the DO control resulted in worse parameter estimates. Similarly, improving the parameter estimates resulted in worse DO control.

(ix) An extension to Holmberg's method was proposed to overcome the small parameter estimate offsets resulting from excluding the flow terms in the estimator model of the real process.

(x) A further extension to Holmberg's method was proposed to overcome the significant offsets (particularly in OUR) resulting from an incorrectly assumed K_La/F_{AIR} relationship. This proposed extension was shown to eliminate the offsets in the parameter estimates.

(xi) The effect of dead-time on parameter esimation was investigated. It was found that:

- for a given dead-time, the greater the sampling interval, the smaller the parameter estimate offsets.
- for a given sampling interval, the greater the dead-time, the greater the parameter estimate offsets.

REFERENCES

Bratby J (1987). Aeration in the Activated sludge process. handout in Course CE541, Wasterwater Treatment I, Dept. of Civil Engineering, University of Cape Town.

Cook S, Marselli-Livelli S (1981). Estimation and control problems in activated sludge processes. Wat.Sci.Tech., 13, p737.

Clifft R C, Andrews J F (1981). Aeration control for reducing energy consumption in small activated sludge plants. Wat.Sci.Tech., 13, p371.

Dold P L, Ekama G A, Marais G v R (1981). A general model for the activated sludge process. Prog. Wat. Tech., 12,47-77.

Dold P L, Marais G v R (1986). Evaluation of the general activated sludge model proposed by the IAWPRC task group. Wat.Sci.Tech., 18, p63.

Dold P L, Marais G v R (1987). Benefits of including unaerated zones in nitrifying activated sludge plants. Wat.Sci.Tech., 19, p195.

Ekama G A, Dold P L, Marais G v R (1986). Procedures for determining influent COD fractions and the maximum specific growth rate of heterotrophs in Activated Sludge systems. Wat. Sci. Tech., 18, p91.

Ekama G A, Marais G v R (1984). Theory, design and operation of nutrient removal activated sludge processes. p4-2. Published by the Water Research Commission, P O Box 824 Pretoria 0001.

Flanagan M J, Bracken B D, Roesler J F (1977). Automatic dissolved oxygen control. ASCE Jnl. of Env. Eng. Div., 103, 4, p707.

Gerald C F, Wheatley P O, (1984). Applied Numerical Analysis. Third Ed. Addison-Wesley.

Goto M (1985). On-line estimation of oxygen uptake rate in the activated sludge process. Ph.D. Dissertation, Rice University, Houston, Texas.

Goto M, Andrews F J (1985). On-line estimation of oxygen uptake rate in the activated sludge process. **Advances in Water Pollution Control: Instrumentation and control of water and wastewater treatment and transport systems**, Editor :Drake R A R, 4th IAWPRC conference, p465.

Holmberg A (1981). Microprocessor-based estimation of oxygen utilization in the activated sludge process. **Int. J. Systems Sci.**, 12, 6, p703.

Holmberg A, Ranta J (1982). Procedures for parameter and state estimaton of microbial growth models. **Automatica**, 18, 2, p181.

Holmberg U, Olsson G (1985). Simultaneous on-line estimation of oxygen transfer rate and respiration rate. Paper presented at 1st IFAC Symposium on Modelling of Biotechnological Processes, Noordwijkerhout, The Netherlands.

Isermann R (1982). Parameter Adaptive Control Algorithms - A tutorial. **Automatica**, 18, 5, p513.

Kalman K E (1958). Design of a self-optimising control system. **ASME**, 80, p468.

Ko K Y-J, McInnis B C, Goodwin G C (1982). Adaptive control and identification of the dissolved oxygen process. **Automatica**, 18, 6, p727.

McInnis C, Lin C C-Y, Butler P B (1979). Adaptive microcomputer dissolved oxygen control for wastewater treatment. IEEE conference, p789.

Nicholls H A (1982). The development of a control system for nutrient removal plants based on respiration measurements. Report Doc4.2b/82, Department of Civil Engineering, University of Cape Town.

Olsson G, Andrews J F (1978). The dissolved oxygen profile - a valuable tool for control of the activated sludge process. Water Research, 12, p985.

Olsson G, Rundquist L, Eriksson L, Hall L (1985). Self-tuning control of the dissolved oxygen concentration in activated sludge systems. Advances in Water Pollution Control: Instrumentation and control of water and wastewater treatment and transport systems, Editor :Drake R A R, 4th IAWPRC conference, p473.

Rundqwist L (1986). Self-tuning control of the dissolved oxygen concentration in an activated sludge system. Thesis for degree of Teknisk Licentiat, Dept. of Automatic Control, Lund Institute of technology, Sweden.

Scmidt F L, Redmon D J (1975). Oxygen transfer efficiency in deep tanks. Jour. WPCF, 47, 11, 2586-2598.

Stephanopolous G. (1984). Chemical process control: An introduction to theory and practice. Prentice-Hall, New Jersey.

Wells C H (1979). Computer control of fully nitrifying activated sludge processes. Inst. Techn, 26, 4, p32.

Wittenmark B, Astrom K J (1984). Practical issues in the implementation of self-tuning control. Automatica, 20, 5, p595.

APPENDIX A

DERIVATIONS RELEVENT TO CHAPTER 3

Appendix A lists a set of derivations relevent to the development of Chapter 3. The derivations presented in this appendix are tabulated in TABLE A.1 below.

TABLE A.1
Derivations presented in Appendix A

DERIVATION	SECTION
Eq 3.10, 3.11 and 3.12	Part 1
Eq 3.29 and Eq 3.31	Part 2
Eq 3.35 and Eq 3.36	Part 3
Eq 3.39 and Eq 3.40	Part 4

Part 1 Derivation of Eq 3.10, Eq 3.11 and Eq 3.12

A general first order equation is of the form:

$$\frac{dy}{dt} = a \cdot y + v \qquad \text{.....(3.9)}$$

This is a linear differential equation of the form :

$$\frac{dy}{dx} + Py = Q$$

where

$$x = t$$
$$P = -a$$
$$Q = V$$

All linear equations of the above form are termed exact differential equations and can be solved by the use of integrating factors. The integrating factor is defined as :

$$I.F. = \exp\left[\int P\, dx\right]$$

$$= \exp\left[\int_0^h -a(kh + s)ds\right]$$

Defining

$$\xi \equiv \xi(h) \equiv \exp\left[\int_0^h a(kh + s)ds\right] \qquad \text{.....(3.11)}$$

puts

$$I.F = 1/\xi(h)$$
$$= 1/\xi$$

Thus multiplying both sides of Eq 3.9 by the integrating factor gives :

$$\frac{d[y/\xi]}{dt} = v/\xi$$

$$\Rightarrow \qquad \int_0^h d[y(kh+s)/\xi(s)] = \int_0^h [v(kh+t)/\xi(t)]\, dt$$

$$\Rightarrow \quad y(kh+h)/\xi(h) - y(kh)/\xi(0) = \int_0^h [v(kh+t)/\xi(t)]\,dt$$

$$\Rightarrow \quad y(kh+h) = \xi(h)*y(kh)/\xi(0) + \xi(h)*\int_0^h [v(kh+t)/\xi(t)]\,dt$$

$$\Rightarrow \quad y(kh+h) = \xi(h)*y(kh)/1 + \int_0^h [\xi(h-t)*v(kh+t)]\,dt$$

Putting $h-t = s$

gives: $-dt = ds$

and the new limits of integration become :

when $t=0,\ s=h$

$t=h,\ s=0$

$$\Rightarrow \quad y(kh+h) = \xi(h)*y(kh) - \int_h^0 [\xi(s)*v(kh+h-s)]\,ds$$

$$\Rightarrow \quad y(kh+h) = \xi(h)*y(kh) + \int_0^h [\xi(s)*v(kh+h-s)]\,ds$$

Which is of the form :

$$y(kh+h) = \xi \cdot y(kh) + \Gamma \qquad \text{.....(3.10)}$$

where

$$\xi \equiv \xi(h) \equiv \exp\left[\int_0^h a(kh+s)\,ds\right] \qquad \text{.....(3.11)}$$

$$\Gamma \equiv \Gamma(h) \equiv \int_0^h \xi(s) \cdot v(kh+h-s)\,ds \qquad \text{.....(3.12)}$$

Part 2 Derivation of Eq 3.29 and Eq 3.31

Derivation of Eq 3.29

It is convenient to define :

$$h^* = \int_0^h \xi(s)\,ds \qquad \text{.....(3.13)}$$

where

$$\xi \equiv \xi(h) \equiv \exp\left[\int_0^h a(kh + s)\,ds\right] \qquad \text{.....(3.11)}$$

and for first order extrapolation :

$$a(kh + t) = a + \dot{a}\cdot t \quad \text{where} \quad a = a(kh) \;\&\; \dot{a} = \dot{a}(kh)$$

Thus Eq 3.11 becomes :

$$\xi \equiv \xi(h) \equiv \exp\left[\int_0^h (a + \dot{a}s)\,ds\right]$$

$$= \exp\left[(ah + \frac{\dot{a}h^2}{2})\right]$$

$$= \exp[ah]\cdot\exp\left[\frac{\dot{a}h^2}{2}\right] \qquad \text{.....(A.1)}$$

Substituting Eq A.1 into Eq 3.13 gives :

$$h^* = \int_0^h \exp[as]*\exp[\dot{a}s^2/2]\,ds$$

Integrating by parts gives :

$$h^* = (\exp[ah]\cdot\exp[\dot{a}h^2/2])/a - 1/a + \dot{a}/a\int_0^h s*\exp[as]*\exp[\dot{a}s^2/2]\,ds$$

And making use of Eq A.1 gives:

$$h^* = \bar{\chi}/a \quad -1/a \quad + \dot{a}/a \int_0^h s*\bar{\chi}(s)ds$$

Which on rearranging gives :

$$\bar{\chi} = 1 + ah^* + \dot{a} \int_0^h s*\bar{\chi}(s)ds \qquad .....(3.29)$$

Derivation of Eq 3.31

We have :

$$\Gamma \equiv \Gamma(h) \equiv \int_0^h \bar{\chi}(S) \cdot v(kh+h-S)dS \qquad .....(3.12)$$

and putting s = h-S

gives: $-ds = dS$

and the new limits of integration become :

when S=0, s=h

S=h, s=0

ie.

$$\Gamma = -\int_h^0 \bar{\chi}(h-s) \cdot v(kh+s)ds$$

$$\Gamma = \int_0^h \bar{\chi}(h-s) \cdot v(kh+s)ds$$

and for first order extrapolation :

$$v(kh + t) = v + \dot{v} \cdot t \quad \text{where} \quad v = v(kh) \;\&\; \dot{v} = \dot{v}(kh)$$

$$r = \int_0^h \xi(h-s)*[v(kh)+ s*\dot{v}(kh)]ds$$

$$r = h^*.v + \dot{v}\int_0^h s.\xi(h-s)ds \qquad .....(3.31)$$

Part 3 Derivation of Eq 3.35 and Eq 3.36

The Runge-Kutta fourth order method is used to integrate

$$I_1 = \int_0^h s * \underline{\xi}(s)\,ds \qquad \text{.....(3.30)}$$

The Runge-Kutta method is desribed in Gerald and Wheatley[1984] and is used as follows :

For

$$I = \int_0^h f(x)\,dx$$

calculate :

$$K_1 = h.f(0)$$
$$K_2 = h.f(h/2)$$
$$K_3 = h.f(h/2)$$
$$K_4 = h.f(h)$$

The integral is then given by :

$$I \approx 1/6\ (\ K_1 + 2K_2 + 2K_3 + K_4\ ) \qquad \text{.....(A.2)}$$

Putting $f(x) = s \cdot \underline{\xi}(s)$ gives:

$$K_1 = h \cdot 0 \cdot \underline{\xi}(0) = 0$$
$$K_2 = h \cdot h/2 \cdot \underline{\xi}(h/2) = h^2/2 \cdot \underline{\xi}(h/2)$$
$$K_3 = h \cdot h/2 \cdot \underline{\xi}(h/2) = h^2/2 \cdot \underline{\xi}(h/2)$$
$$K_4 = h \cdot h \cdot \underline{\xi}(h) = h^2 \cdot \underline{\xi}(h)$$

Substitution of K_1, K_2, K_3 and K_4 into Eq A.2 gives :

$$I \approx 1/6\ (\ 0 + h^2/2 \cdot \underline{\xi}(h/2) + h^2/2 \cdot \underline{\xi}(h/2) + h^2 \cdot \underline{\xi}(h)\ )$$
$$= h^2/6 \cdot (2\underline{\xi}(h/2) + \underline{\xi}(h)) \qquad \text{.....(3.35)}$$

Similarly for

$$I_2 = \int_0^h s \cdot \underline{\xi}(h-s)\,ds \qquad \text{.....(3.32)}$$

Putting $f(x) = s \cdot \xi(h-s)$ gives:

$$K_1 = h \cdot 0 \cdot \xi(h-0) = 0$$
$$K_2 = h \cdot h/2 \cdot \xi(h-h/2) = h^2/2 \cdot \xi(h/2)$$
$$K_3 = h \cdot h/2 \cdot \xi(h-h/2) = h^2/2 \cdot \xi(h/2)$$
$$K_4 = h \cdot h \cdot \xi(h-h) = h^2 \cdot \xi(0)$$

and again substitution of K_1, K_2, K_3 and K_4 into Eq A.2 gives :

$$I \approx 1/6 \; (\; 0 + 2 \cdot h^2/2 \cdot \xi(h/2) + 2 \cdot h^2/2 \cdot \xi(h/2) + h^2 \;)$$
$$= h^2/6 \cdot (2\xi(h/2) + \xi(0)) \qquad \text{.....(3.36)}$$

Part 4 Derivation of Eq 3.39 and Eq 3.40

Consider Fig A.1 below representing a hypothetical change of $\hat{\alpha}$ with time.

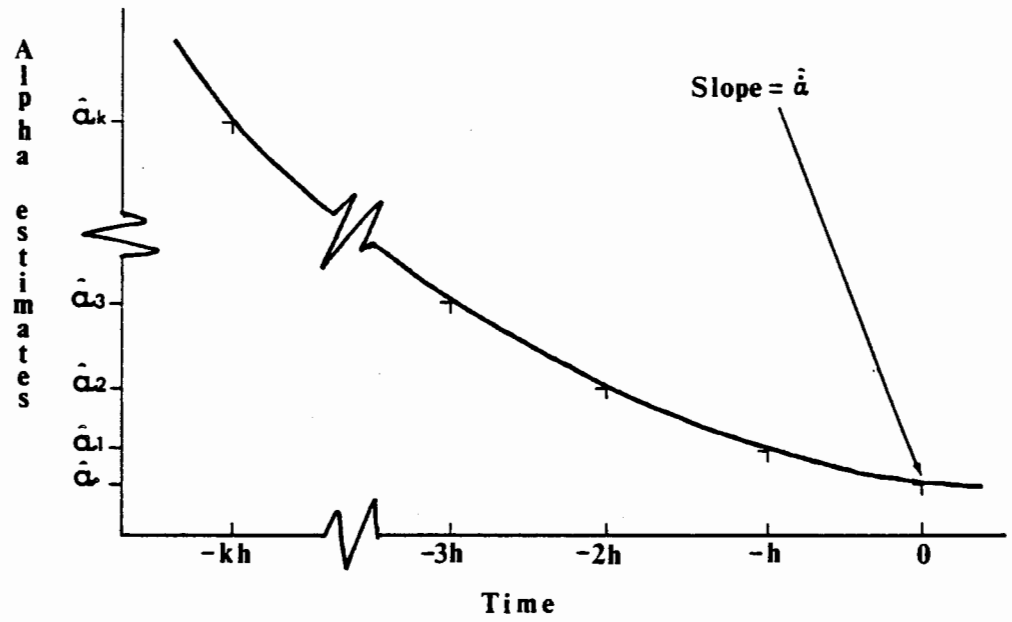

Figure A.1 Illustration of how $\dot{\alpha}$ is estimated

At each sampling interval (-kh,...,-3h,-2h,-h,...) estimates of α are made ($\hat{\alpha}_k$,...,$\hat{\alpha}_3$,$\hat{\alpha}_2$,$\hat{\alpha}_1$...). It is possible to estimate $\dot{\alpha}$ at time=0 by linear regression on the equation

$$\hat{\alpha}_k = \hat{\alpha} + \dot{\hat{\alpha}} \cdot kh \qquad \text{.....(A.3)}$$

Define $e_k = \hat{\alpha} + \dot{\hat{\alpha}} \cdot kh - \hat{\alpha}_k$

and put $S = \sum_{k=1}^{n} e_k^2$

S is to be minimised by choosing suitable $\hat{\alpha}$ and $\dot{\alpha}$. This is done by taking partial derivatives of S with respect to $\hat{\alpha}$ and $\hat{\dot{\alpha}}$:

$$\frac{\delta S}{\delta \hat{\alpha}} = \sum_{k=1}^{n} 2e_k \cdot \frac{\delta e_k}{\delta \hat{\alpha}} = 0$$

$$\Rightarrow \quad \sum_{k=1}^{n} (\hat{\alpha} + \hat{\dot{\alpha}} \cdot kh - \hat{\alpha}_k) * 1 = 0$$

$$\Rightarrow \quad \hat{\alpha} \sum_{k=1}^{n} 1 + \hat{\dot{\alpha}} . \sum_{k=1}^{n} kh = \sum_{k=1}^{n} \hat{\alpha}_k \qquad \text{.....(A.4)}$$

Also

$$\frac{\delta S}{\delta \hat{\dot{\alpha}}} = \sum_{k=1}^{n} 2e_k \cdot \frac{\delta e_k}{\delta \dot{\alpha}} = 0$$

$$\Rightarrow \quad \sum_{k=1}^{n} (\hat{\alpha} + \hat{\dot{\alpha}} \cdot kh - \hat{\alpha}_k) * kh = 0$$

$$\Rightarrow \quad \hat{\alpha} \sum_{k=1}^{n} kh + \hat{\dot{\alpha}} . \sum_{k=1}^{n} (kh)^2 = \sum_{k=1}^{n} (kh) \cdot \hat{\alpha}_k \qquad \text{.....(A.5)}$$

Using Kramer's rule to solve the pair of simultaneous equations in Eq A.4 and Eq A.5 for $\hat{\alpha}$ gives :

$$\hat{\alpha} = \frac{\begin{vmatrix} n & \sum_{k=1}^{n} \hat{\alpha}_k \\ \sum_{k=1}^{n} kh & \sum_{k=1}^{n} (kh) * \hat{\alpha}_k \end{vmatrix}}{\begin{vmatrix} n & \sum_{k=1}^{n} kh \\ \sum_{k=1}^{n} kh & \sum_{k=1}^{n} (kh)^2 \end{vmatrix}}$$

ie.

$$\hat{\alpha} = \frac{n \cdot \sum_{k=1}^{n} (kh) . \hat{\alpha}_k - \sum_{k=1}^{n} (kh) \cdot \sum_{k=1}^{n} \hat{\alpha}_k}{n \cdot \sum_{k=1}^{n} (kh)^2 - (\sum_{k=1}^{n} (kh))^2} \qquad \text{.....(3.39)}$$

Similarly by putting

$$\hat{R}_k = \hat{R} + \hat{R}' \cdot kh$$

It is possible to show that

$$\hat{R}' = \frac{n \cdot \sum_{k=1}^{n} (kh).\hat{R}_k - \sum_{k=1}^{n} (kh) \cdot \sum_{k=1}^{n} \hat{R}_k}{n \cdot \sum_{k=1}^{n} (kh)^2 - \left(\sum_{k=1}^{n} (kh) \right)^2} \qquad \text{.....(3.41)}$$

APPENDIX B

LISTINGS OF THE PROGRAMS USED IN THE SIMULATION RUNS

This appendix gives a listing of the files used to generate the results presented in Chapter 5. The files are :

(i) AERATOR.PAS
(ii) INPUT.PAS
(iii) DISPLAY.PAS
(iv) CHANGE.PAS
(v) PROCESS.PAS
(vi) VARIABLE.PAS
(vii) COMMON.PAS
(viii) GXINC.PAS
(ix) PRINTER.DEF

Figure 4.5 illustrates how the first five files, i.e. AERATOR.PAS to PROCESS.PAS, are linked. The sixth file, VARIABLE.PAS is 'included' at compilation time into these first five files as VARIABLE.PAS contains the definitions of all the global variables. The seventh file, COMMON.PAS, contains various rountines that are common to two or more of the first five files. The eighth file, GXINC.PAS contains a set of routines used in conjunction with INT10.COM. GXINC.PAS is used exclusively by PROCESS.PAS. The last file listed in this Appendix, PRINTER.DEF, is the printer file specification file that is required for HARDCOPY.COM. The source code for INT10.COM and HARDCOPY.COM is not given as these were not written by the author.

The program listings are presented in a separately bound document.

APPENDIX C

PARAMETER LISTS USED FOR THE SIMULATION RUNS OF CHAPTER 5

In the simulation program used in this thesis, more than 50 parameters are required to define each simulation run. In order not to bog the reader down by listing each set of 50 parameters for every simulation run of Chapter 5, only the salient parameters are mentioned within the text of that Chapter. For purposes of completeness, this Appendix lists the entire set of parameters for all the simulation runs of Chapter 5. Also included in this Appendix is the entire list of parameters used for the confirmatory run of Chapter 4, entitled Holmberg.dat.

File name : holmberg.DAT

SIMULATED PROCESS MODEL VALUES

mean Θ = 0.0000000 [1/day]
Θ wave amplitude = 0.0000000 [1/day]
Θ cosine wave offset = 0.000 [°]
Θ cosine wave period = 0.000 [min]
V = 15000000.000 l
Cin = 0.000 mgO2/l
CoutInitial = 0.000 mgO2/l
mean a1 = 0.000000300 [1/l]
a1 wave amplitude = 0.000000033 [1/l]
a1 cosine wave offset = 90.000 [°]
a1 cosine wave period = 600.000 [min]
Kla axis intercept = 0.0000000 [1/min]
mean OUR = 10.000 [mgO/l/hr]
OUR wave amplitude = 1.000 [mgO/l/hr]
OUR cosine wave offset = 90.000 [°]
OUR cosine wave period = 600.000 [min]
mean Temp = 10.000 [°C]
Temp wave amplitude = 0.000 [°C]
Temp cosine wave offset = 0.000 [°]
Temp cosine wave period = 0.000 [min]
Initial air flow = 80000[l/min]
DO noise band = 0.000
Θ noise band = 0.000
No process lag

CONTROLLER

The process is controlled by a :

Dual mode controller
ac = 0.1666000 /min
esp = 0.0100000 mgO/l
kdo = 0.016666 /min
d = 0.016660 mgO/l.min
SETPOINT = 2.000 mgO2/l

TIME DATA

Runge Kutte interval = 1.000 min
Controller interval = 6.000 min

IDENTIFICATION

First order identification is being used
5 points used in least squares estimation

OUTPUT MODE

GRAPHICAL OUTPUT

axis	variable	Low limit	High limit
1	AirFlow	0.000	120000.000
2	AirFlow	0.000	120000.000
3	Cout	0.400	2.400
4	Cout	0.400	2.400

Symbol Frequency per screen = 0
Number of X-axis divisions =12
X - axis units in hours
Time per screen = 12.0 hours
Hardcopy sent to printer at end of each screen

File name : exp2.DAT

SIMULATED PROCESS MODEL VALUES

mean Θ = 0.0000000 [1/day]
Θ wave amplitude = 0.0000000 [1/day]
Θ cosine wave offset = 0.000 [°]
Θ cosine wave period = 0.000 [min]
V = 150000000.000 l
Cin = 0.000 mgO2/l
CoutInitial = 0.000 mgO2/l
mean a1 = 0.000001200 [1/l]
a1 wave amplitude = 0.000000000 [1/l]
a1 cosine wave offset = 0.000 [°]
a1 cosine wave period = 0.000 [min]
Kla axis intercept = 0.0000000 [1/min]
mean OUR = 20.000 [mgO/l/hr]
OUR wave amplitude = 0.000 [mgO/l/hr]
OUR cosine wave offset = 0.000 [°]
OUR cosine wave period = 0.000 [min]
mean Temp = 10.000 [°C]
Temp wave amplitude = 0.000 [°C]
Temp cosine wave offset = 0.000 [°]
Temp cosine wave period = 0.000 [min]
Initial air flow = 80000[l/min]
DO noise band = 0.000
Θ noise band = 0.000
No process lag

CONTROLLER

The process is controlled by a :

Dual mode controller
ac = 0.1666000 /min
esp = 0.0100000 mgO/l
kdo = 0.016670 /min
d = 0.010467 mgO/l.min
SETPOINT = 2.000 mgO2/l

TIME DATA

Runge Kutte interval = 1.000 min
Controller interval = 6.000 min

IDENTIFICATION

First order identification is being used
5 points used in least squares estimation

OUTPUT MODE

GRAPHICAL OUTPUT

axis	variable	Low limit	High limit
1	aEst	0.000	0.000
2	a1	0.000	0.000
3	OUR	0.000	40.000
4	OurEst	0.000	40.000

Symbol Frequency per screen = 0
Number of X-axis divisions =12
X - axis units in hours
Time per screen = 12.0 hours
Hardcopy sent to printer at end of each screen

File name : exp3.DAT

SIMULATED PROCESS MODEL VALUES

mean Q = 0.0000000 [1/day]
Q wave amplitude = 0.0000000 [1/day]
Q cosine wave offset = 0.000 [°]
Q cosine wave period = 0.000 [min]
V = 1500000000.000 l
Cin = 0.000 mgO2/l
CoutInitial = 0.000 mgO2/l
mean a1 = 0.0000001200 [1/l]
a1 wave amplitude = 0.0000000120 [1/l]
a1 cosine wave offset = 0.000 [°]
a1 cosine wave period = 1440.000 [min]
Kla axis intercept = 0.0000000 [1/min]
mean OUR = 64.998 [mgO/l/hr]
OUR wave amplitude = 15.000 [mgO/l/hr]
OUR cosine wave offset = 0.000 [°]
OUR cosine wave period = 1440.000 [min]
mean Temp = 10.000 [°C]
Temp wave amplitude = 0.000 [°C]
Temp cosine wave offset = 0.000 [°]
Temp cosine wave period = 0.000 [min]
Initial air flow = 100000[l/min]
DO noise band = 0.000
Q noise band = 0.000
No process lag

CONTROLLER

The process is controlled by a :

Dual mode controller
ac = 0.1666000 /min
esp = 0.0100000 mgO/l
kdo = 0.000010 /min
d = 0.040000 mgO/l.min
SETPOINT = 2.000 mgO2/l

TIME DATA

Runge Kutte interval = 1.000 min
Controller interval = 6.000 min

IDENTIFICATION

First order identification is being used
5 points used in least squares estimation

OUTPUT MODE

GRAPHICAL OUTPUT

axis	variable	Low limit	High limit
1	Cout	0.000	3.000
2	Cout	0.000	3.000
3	AirFlow	0.000	200000.000
4	AirFlow	0.000	200000.000

Symbol Frequency per screen = 0
Number of X-axis divisions =12
X - axis units in hours
Time per screen = 12.0 hours
Hardcopy sent to printer at end of each screen

File name : exp4.DAT

SIMULATED PROCESS MODEL VALUES

mean Q = 0.0000000 [1/day]
Q wave amplitude = 0.0000000 [1/day]
Q cosine wave offset = 0.000 [°]
Q cosine wave period = 0.000 [min]
V = 1500000000.000 l
Cin = 0.000 mgO2/l
CoutInitial = 0.000 mgO2/l
mean a1 = 0.0000001200 [1/l]
a1 wave amplitude = 0.0000000120 [1/l]
a1 cosine wave offset = 0.000 [°]
a1 cosine wave period = 1440.000 [min]
Kla axis intercept = 0.0000000 [1/min]
mean OUR = 64.998 [mgO/l/hr]
OUR wave amplitude = 15.000 [mgO/l/hr]
OUR cosine wave offset = 90.000 [°]
OUR cosine wave period = 1440.000 [min]
mean Temp = 10.000 [°C]
Temp wave amplitude = 0.000 [°C]
Temp cosine wave offset = 0.000 [°]
Temp cosine wave period = 0.000 [min]
Initial air flow = 100000[l/min]
DO noise band = 0.000
Q noise band = 0.000
No process lag

CONTROLLER

The process is controlled by a :

Dual mode controller
ac = 0.1666000 /min
esp = 0.0100000 mgO/l
kdo = 0.000010 /min
d = 0.040000 mgO/l.min
SETPOINT = 2.000 mgO2/l

TIME DATA

Runge Kutte interval = 1.000 min
Controller interval = 6.000 min

IDENTIFICATION

First order identification is being used
5 points used in least squares estimation

OUTPUT MODE

GRAPHICAL OUTPUT

axis	variable	Low limit	High limit
1	OUR	0.000	100.000
2	OurEst	0.000	100.000
3	3	0.000	0.005
4	3	0.000	0.005

Symbol Frequency per screen = 0
Number of X-axis divisions =12
X - axis units in hours
Time per screen = 24.0 hours
Hardcopy sent to printer at end of each screen

File name : exp5.DAT

SIMULATED PROCESS MODEL VALUES

mean Q = 0.0000000 [1/day]
Q wave amplitude = 0.0000000 [1/day]
Q cosine wave offset = 0.000 [°]
Q cosine wave period = 0.000 [min]
V = 15000000.000 l
Cin = 0.100 mgO2/l
CoutInitial = 1.500 mgO2/l
mean ai = 0.000001200 [1/l]
ai wave amplitude = 0.000000000 [1/l]
ai cosine wave offset = 90.000 [°]
ai cosine wave period = 0.000 [min]
Kla axis intercept = 0.0000000 [1/min]
mean OUR = 64.998 [mgO/l/hr]
OUR wave amplitude = 15.000 [mgO/l/hr]
OUR cosine wave offset = 90.000 [°]
OUR cosine wave period = 1440.000 [min]
mean Temp = 20.000 [°C]
Temp wave amplitude = 0.000 [°C]
Temp cosine wave offset = 0.000 [°]
Temp cosine wave period = 0.000 [min]
Initial air flow = 150000[l/min]
DO noise band = 0.000
Q noise band = 0.000
No process lag

CONTROLLER

The process is controlled by a :

Dual mode controller
ac = 0.1000000 /min
esp = 0.0010000 mgO/l
kdo = 0.001000 /min
d = 0.089517 mgO/l.min
SETPOINT = 2.000 mgO2/l

TIME DATA

Runge Kutte interval = 1.000 min
Controller interval = 10.000 min

IDENTIFICATION

Zero order identification is being used

OUTPUT MODE

GRAPHIC AND FILE OUTPUT

GRAPHICAL OUTPUT

axis	variable	Low limit	High limit
1	Cout	0.000	3.000
2	OUR	45.000	90.000
3	OurEst	45.000	90.000
4	Cout	0.000	3.000

Symbol Frequency per screen = 12
Number of X-axis divisions =12
X - axis units in hours
Time per screen = 24.0 hours
NO Hardcopy ever sent to printer

File name : exp6.DAT

SIMULATED PROCESS MODEL VALUES

mean Q = 200001600.0000000 [1/day]
Q wave amplitude = 0.0000000 [1/day]
Q cosine wave offset = 0.000 [°]
Q cosine wave period = 0.000 [min]
V = 15000000.000 l
Cin = 0.100 mgO2/l
CoutInitial = 0.000 mgO2/l
mean ai = 0.000001200 [1/l]
ai wave amplitude = 0.000000120 [1/l]
ai cosine wave offset = 0.000 [°]
ai cosine wave period = 1440.000 [min]
Kla axis intercept = 0.0000000 [1/min]
mean OUR = 64.998 [mgO/l/hr]
OUR wave amplitude = 15.000 [mgO/l/hr]
OUR cosine wave offset = 0.000 [°]
OUR cosine wave period = 1440.000 [min]
mean Temp = 10.000 [°C]
Temp wave amplitude = 0.000 [°C]
Temp cosine wave offset = 0.000 [°]
Temp cosine wave period = 0.000 [min]
Initial air flow = 100000[l/min]
DO noise band = 0.000
Q noise band = 0.000
No process lag

CONTROLLER

The process is controlled by a :

Dual mode controller
ac = 0.1666000 /min
esp = 0.0100000 mgO/l
kdo = 0.000010 /min
d = 0.040000 mgO/l.min
SETPOINT = 2.000 mgO2/l

TIME DATA

Runge Kutte interval = 1.000 min
Controller interval = 6.000 min

IDENTIFICATION

First order identification is being used
5 points used in least squares estimation

OUTPUT MODE

GRAPHICAL OUTPUT

axis	variable	Low limit	High limit
1	OUR	0.000	100.000
2	OurEst	0.000	100.000
3	S	0.000	0.005
4	S	0.000	0.005

Symbol Frequency per screen = 0
Number of X-axis divisions =12
X - axis units in hours
Time per screen = 24.0 hours
Hardcopy sent to printer at end of each screen

File name : exp7.DAT

SIMULATED PROCESS MODEL VALUES

mean Q = 0.0000000 [1/day]
Q wave amplitude = 0.0000000 [1/day]
Q cosine wave offset = 0.000 [°]
Q cosine wave period = 0.000 [min]
V = 150000000.000 l
Cin = 0.000 mgO2/l
CoutInitial = 0.000 mgO2/l
mean a1 = 0.000001719 [1/l]
a1 wave amplitude = 0.000000120 [1/l]
a1 cosine wave offset = 0.000 [°]
a1 cosine wave period = 1440.000 [min]
Kla axis intercept = -0.0225600 [1/min]
mean OUR = 64.998 [mgO/l/hr]
OUR wave amplitude = 15.000 [mgO/l/hr]
OUR cosine wave offset = 0.000 [°]
OUR cosine wave period = 1440.000 [min]
mean Temp = 10.000 [°C]
Temp wave amplitude = 0.000 [°C]
Temp cosine wave offset = 0.000 [°]
Temp cosine wave period = 0.000 [min]
Initial air flow = 100000[l/min]
DO noise band = 0.000
Q noise band = 0.000
No process lag

CONTROLLER

The process is controlled by a :

Dual mode controller
ac = 0.1666000 /min
esp = 0.0100000 mgO/l
kdo = 0.000010 /min
d = 0.040000 mgO/l.min
SETPOINT = 2.000 mgO2/l

TIME DATA

Runge Kutte interval = 1.000 min
Controller interval = 6.000 min

IDENTIFICATION

First order identification is being used
5 points used in least squares estimation

OUTPUT MODE

GRAPHICAL OUTPUT

axis	variable	Low limit	High limit
1	Cout	0.000	3.000
2	Cout	0.000	3.000
3	AirFlow	0.000	200000.000
4	AirFlow	0.000	200000.000

Symbol Frequency per screen = 0
Number of X-axis divisions =12
X - axis units in hours
Time per screen = 12.0 hours
Hardcopy sent to printer at end of each screen

File name : exp8.DAT

SIMULATED PROCESS MODEL VALUES

mean Q = 0.0000000 [1/day]
Q wave amplitude = 0.0000000 [1/day]
Q cosine wave offset = 0.000 [°]
Q cosine wave period = 0.000 [min]
V = 150000000.000 l
Cin = 0.000 mgO2/l
CoutInitial = 0.000 mgO2/l
mean a1 = 0.000001200 [1/l]
a1 wave amplitude = 0.000000120 [1/l]
a1 cosine wave offset = 0.000 [°]
a1 cosine wave period = 1440.000 [min]
Kla axis intercept = 0.0000000 [1/min]
mean OUR = 64.998 [mgO/l/hr]
OUR wave amplitude = 15.000 [mgO/l/hr]
OUR cosine wave offset = 0.000 [°]
OUR cosine wave period = 1440.000 [min]
mean Temp = 10.000 [°C]
Temp wave amplitude = 0.000 [°C]
Temp cosine wave offset = 0.000 [°]
Temp cosine wave period = 0.000 [min]
Initial air flow = 100000[l/min]
DO noise band = 0.000
Q noise band = 0.000
No process lag

CONTROLLER

The process is controlled by a :

Dual mode controller
ac = 0.1666000 /min
esp = 0.0100000 mgO/l
kdo = 0.000010 /min
d = 0.040000 mgO/l.min
SETPOINT = 2.000 mgO2/l

TIME DATA

Runge Kutte interval = 1.000 min
Controller interval = 6.000 min

IDENTIFICATION

First order identification is being used
5 points used in least squares estimation

OUTPUT MODE

GRAPHICAL OUTPUT

axis	variable	Low limit	High limit
1	OUR	0.000	100.000
2	OurEst	0.000	100.000
3	αEst	0.000	0.000
4	a1	0.000	0.000

Symbol Frequency per screen = 0
Number of X-axis divisions =12
X - axis units in hours
Time per screen = 24.0 hours
Hardcopy sent to printer at end of each screen

File name : exp9.DAT

SIMULATED PROCESS MODEL VALUES

mean Q = 0.0000000 [1/day]
Q wave amplitude = 0.0000000 [1/day]
Q cosine wave offset = 0.000 [*]
Q cosine wave period = 0.000 [min]
V = 150000000.000 l
Cin = 0.000 mgO2/l
CoutInitial = 0.000 mgO2/l
mean a1 = 0.000001200 [1/l]
a1 wave amplitude = 0.000000120 [1/l]
a1 cosine wave offset = 0.000 [*]
a1 cosine wave period = 1440.000 [min]
Kla axis intercept = 0.0000000 [1/min]
mean OUR = 64.998 [mgO/l/hr]
OUR wave amplitude = 15.000 [mgO/l/hr]
OUR cosine wave offset = 0.000 [*]
OUR cosine wave period = 1440.000 [min]
mean Temp = 10.000 [*C]
Temp wave amplitude = 0.000 [*C]
Temp cosine wave offset = 0.000 [*]
Temp cosine wave period = 0.000 [min]
Initial air flow = 100000[l/min]
DO noise band = 0.000
Q noise band = 0.000
No process lag

CONTROLLER

The process is controlled by a :

Dual mode controller
ac = 0.1666000 /min
esp = 0.0100000 mgO/l
kdo = 0.016670 /min
d = 0.080000 mgO/l.min
SETPOINT = 2.000 mgO2/l

TIME DATA

Runge Kutte interval = 1.000 min
Controller interval = 6.000 min

IDENTIFICATION

First order identification is being used
5 points used in least squares estimation

OUTPUT MODE

GRAPHICAL OUTPUT

axis	variable	Low limit	High limit
1	Cout	0.000	3.000
2	S	0.000	0.010
3	d	0.000	0.500
4	OurEst	0.000	100.000

Symbol Frequency per screen = 12
Number of X-axis divisions =12
X - axis units in hours
Time per screen = 48.0 hours
Hardcopy sent to printer at end of each screen

File name : EXP10.DAT

SIMULATED PROCESS MODEL VALUES

mean Q = 200001600.0000000 [1/day]
Q wave amplitude = 0.0000000 [1/day]
Q cosine wave offset = 0.000 [*]
Q cosine wave period = 0.000 [min]
V = 15000000.000 l
Cin = 0.100 mgO2/l
CoutInitial = 0.000 mgO2/l
mean a1 = 0.000001200 [1/l]
a1 wave amplitude = 0.000000120 [1/l]
a1 cosine wave offset = 0.000 [*]
a1 cosine wave period = 1440.000 [min]
Kla axis intercept = 0.0000000 [1/min]
mean OUR = 64.998 [mgO/l/hr]
OUR wave amplitude = 15.000 [mgO/l/hr]
OUR cosine wave offset = 0.000 [*]
OUR cosine wave period = 1440.000 [min]
mean Temp = 10.000 [*C]
Temp wave amplitude = 0.000 [*C]
Temp cosine wave offset = 0.000 [*]
Temp cosine wave period = 0.000 [min]
Initial air flow = 100000[l/min]
DO noise band = 0.000
Q noise band = 0.000
No process lag

CONTROLLER

The process is controlled by a :

Dual mode controller with flow terms included
ac = 0.1666000 /min
esp = 0.0100000 mgO/l
kdo = 0.000010 /min
d = 0.040000 mgO/l.min
SETPOINT = 2.000 mgO2/l

TIME DATA

Runge Kutte interval = 1.000 min
Controller interval = 6.000 min

IDENTIFICATION

First order identification is being used
5 points used in least squares estimation

OUTPUT MODE

GRAPHICAL OUTPUT

axis	variable	Low limit	High limit
1	OUR	0.000	100.000
2	OurEst	0.000	100.000
3	aEst	0.000	0.000
4	a1	0.000	0.000

Symbol Frequency per screen = 0
Number of X-axis divisions =12
X - axis units in hours
Time per screen = 24.0 hours
Hardcopy sent to printer at end of each screen

File name : EXP11.DAT

SIMULATED PROCESS MODEL VALUES

mean Q = 0.0000000 [l/day]
Q wave amplitude = 0.0000000 [l/day]
Q cosine wave offset = 0.000 [°]
Q cosine wave period = 0.000 [min]
V = 150000000.000 l
Cin = 0.000 mgO2/l
CoutInitial = 0.000 mgO2/l
mean a1 = 0.000001719 [1/l]
a1 wave amplitude = 0.0000000120 [1/l]
a1 cosine wave offset = 0.000 [°]
a1 cosine wave period = 1440.000 [min]
Kla axis intercept = -0.0225600 [1/min]
mean OUR = 64.998 [mgO/l/hr]
OUR wave amplitude = 15.000 [mgO/l/hr]
OUR cosine wave offset = 0.000 [°]
OUR cosine wave period = 1440.000 [min]
mean Temp = 10.000 [°C]
Temp wave amplitude = 0.000 [°C]
Temp cosine wave offset = 0.000 [°]
Temp cosine wave period = 0.000 [min]
Initial air flow = 100000[l/min]
DO noise band = 0.000
Q noise band = 0.000
No process lag

CONTROLLER

The process is controlled by a :

Steph's dual mode controller
ac = 0.1666000 /min
esp = 0.0100000 mgO/l
kdo = 0.000010 /min
d = 0.040000 mgO/l.min
SETPOINT = 2.000 mgO2/l

TIME DATA

Runge Kutte interval = 1.000 min
Controller interval = 6.000 min

IDENTIFICATION

First order identification is being used
5 points used in least squares estimation

OUTPUT MODE

GRAPHICAL OUTPUT

axis	variable	Low limit	High limit
1	OUR	0.000	100.000
2	OurEst	0.000	100.000
3	aEst	0.000	0.000
4	a1	0.000	0.000

Symbol Frequency per screen = 0
Number of X-axis divisions =12
X - axis units in hours
Time per screen = 24.0 hours
Hardcopy sent to printer at end of each screen

File name : exp12.DAT

SIMULATED PROCESS MODEL VALUES

mean Q = 0.0000000 [l/day]
Q wave amplitude = 0.0000000 [l/day]
Q cosine wave offset = 0.000 [°]
Q cosine wave period = 0.000 [min]
V = 150000000.000 l
Cin = 0.000 mgO2/l
CoutInitial = 0.000 mgO2/l
mean a1 = 0.000001200 [1/l]
a1 wave amplitude = 0.0000000120 [1/l]
a1 cosine wave offset = 0.000 [°]
a1 cosine wave period = 1440.000 [min]
Kla axis intercept = 0.0000000 [1/min]
mean OUR = 64.998 [mgO/l/hr]
OUR wave amplitude = 15.000 [mgO/l/hr]
OUR cosine wave offset = 0.000 [°]
OUR cosine wave period = 1440.000 [min]
mean Temp = 10.000 [°C]
Temp wave amplitude = 0.000 [°C]
Temp cosine wave offset = 0.000 [°]
Temp cosine wave period = 0.000 [min]
Initial air flow = 100000[l/min]
DO noise band = 0.000
Q noise band = 0.000
No process lag

CONTROLLER

The process is controlled by a :

Dual mode controller
ac = 0.1666000 /min
esp = 0.0100000 mgO/l
kdo = 0.000010 /min
d = 0.040000 mgO/l.min
SETPOINT = 2.000 mgO2/l

TIME DATA

Runge Kutte interval = 1.000 min
Controller interval = 10.000 min

IDENTIFICATION

First order identification is being used
5 points used in least squares estimation

OUTPUT MODE

GRAPHIC AND FILE OUTPUT

GRAPHICAL OUTPUT

axis	variable	Low limit	High limit
1	Cout	0.000	3.000
2	OUR	0.000	100.000
3	AirFlow	0.000	200000.000
4	OurEst	0.000	100.000

Symbol Frequency per screen = 0
Number of X-axis divisions =12
X - axis units in hours
Time per screen = 12.0 hours
NO Hardcopy ever sent to printer

APPENDIX D

TABLE OF DATA USED TO PLOT FIGURE 5.5 AND FIGURE 5.6

Figures 5.5 and 5.6 illustrate the effect of sampling time on the estimates of R and on DO control using the first order and zero order methods. As no discernible difference between the zero order and first order method is apparent from these Figures, this Appendix lists the data used to plot Figures 5.5 and 5.6, so as to quantify the difference (albeit small) between the values generated by the two methods.

TABLE D.1

Values used to plot Figures 5.5 and 5.6

Sampling Interval (min)	ZERO ORDER		FIRST ORDER	
	Mean error in $\hat{R}$	Mean DO setpoint difference	Mean error in $\hat{R}$	Mean DO setpoint difference
1	0.242176	0.043284	0.242176	0.043284
2	0.463263	0.056819	0.463263	0.056819
3	0.668742	0.076599	0.668742	0.076599
4	0.862851	0.097422	0.862851	0.097472
5	1.046662	0.118056	1.046662	0.118056
6	1.226649	0.138176	1.226492	0.138176
7	1.399737	0.157687	1.399973	0.157687
8	1.571543	0.176898	1.571533	0.176899
9	1.739320	0.195115	1.739278	0.195116
10	1.9122265	0.213039	1.912003	0.213041